- MASTER OF SCIENCE THESIS -

Development of a design tool for offshore wind farm layout optimization

Consideration of wake effects and electrical infrastructure costs and losses

Fernando Borbón Guillén

06 August 2010

TU/e Technische Universiteit Eindhoven University of Technology

TU Delft Technische Universiteit Delft

Development of a design tool for offshore wind farm layout optimization

Consideration of wake effects and electrical infrastructure costs and losses

MASTER OF SCIENCE THESIS

For obtaining the degree of Master of Science in Sustainable Energy Technology at Eindhoven University of Technology

by Fernando Borbón Guillén

Supervised by:
ir. M.B. Zaaijer (Michiel)
Prof. dr. G.J.W. van Bussel (Gerard)

06 August 2010

Department of Aerospace Engineering - Delft University of Technology
Department of Mechanical Engineering - Eindhoven University of Technology

Development of a design tool for offshore wind farm layout optimization
Copyright © 2009 by Fernando Borbón Guillén
All rights reserved

Supervised by:
ir. M.B. Zaaijer (Michiel)
Prof. dr. G.J.W. van Bussel (Gerard)

Wind Energy Research Group
Delft University of Technology
Kluyverweg 1
2629 HS Delft
The Netherlands

Abstract

A design tool has been developed with the aim of helping in the wind farm design process. The tool is able to handle rectangular layouts with any number of turbines. Wind farm power, as well as wind and site conditions can be specified by the user. The main tool models are described and the developing steps have been detailed. Results of tool functionality are presented and compared with other tools or real case studies. The two modes of operation are explained: the separation distance sweep mode and the optimization function mode. Besides, the advantage and limitations of the optimization mode are indicated. The main lessons learnt during the developing of this tool are described for each developing stage. The most relevant is that the optimum layout dimensions should be found using the separation distance sweep mode rather than the optimization function. As a main conclusion, the implemented design tool can be helpful for the design process of offshore wind farms. The tool allows the user to define turbine, wind and site conditions and wind farm layout properties. Based on these properties, the tool delivers the optimum layout dimensions considering the effects of wake losses and electrical cable losses and costs. Additional conclusions and recommendations are summarized together with some future work possibilities.

Descriptors: wind farm optimization, levelized production cost optimization, wake models, design tool.

Acknowledgements

I am very grateful with all those people who helped me to pavement my way through this personal goal of studying abroad.

Firstly, thanks to Costa Rica, my lovely country which made me be what I am now. Also, thanks to Dutch people for opening Europe doors to me and sponsoring my studies with their taxes.

Thanks to professor ir. Michiel Zaaijer for offering me such motivating thesis topic, giving me close guidance throughout my work and incentivizing my critic sense. Your kind personal touch with students made researching an enjoyable experience.

Moreover, I would like acknowledge the support of professor Dr. ir. Veldkamp for sharing useful information about wake models. Besides, thanks to professor Dr. ir. Gerard Van Bussel for teaching such emotive lectures where his passion for wind energy was contagious and helped me to decide selecting my graduation specialization.

To all of my friends from Eindhoven, thanks for giving me one of the best years in my life. I will never forget you. The same way, thanks to my thesis room colleagues who shared with me not only coffee but also knowledge, worries, expectations and the joy of graduating at Aerospace Engineering Faculty.

For my girlfriend Monica, I have truly enjoyed the time we have shared together and my visits to Portugal were really battery charging sessions to keep me going in the execution of this thesis.

In special, thanks to my parents for their unconditional support, trust, prayers and for inculcating in me the progress and self-improvement spirit.

Most importantly, thanks God for life gift, for making my dreams come true and for carrying me during difficult times.

- *Fernando Borbón Guillén*

Delft, The Netherlands

6 August 2010

Table of contents

List of figures

List of tables

Nomenclature

A	rotor area
a	axial induction factor
a	annuity factor
A_{farm}	area of the farm
C	conductor cross section
c	wind speed ratio
C	cable capacitance
C'	capacitance per phase per unit length
c_1	non-dimensional mixing length
c_1 , c_2	constants
C_c	capital cost of the farm
c_d	drag coefficient
$ceil$	ceiling function that rounds up to the nearest integer
C_t	thrust coefficient
C_T	thrust coefficient
c_w	asymptotic non-zero wake flow speed
C_y	annual cost
dx	x-component of distance between two turbines
dy	y-component of distance between two turbines
E_y	annual energy production
f	frequency
$f(V)$	probability of occurrence of wind speed V
h	height
Hr/Yr	hours per year, 8760

I ……electric current
$I(V)$ ……total wind farm current for wind speed V
$I(V)$ ……current distribution per phase for wind speed V
I_{rated} ……rated current
k ……decay factor
L ……cable length
L_{cable} ……length of an individual collection cable
LP ……wind farm loss percentage at rated power due to interconnection cables
l_w ……suitable length
n ……number of…
N_{cables} ……number of collection cables used in farm
N_t ……number of turbines
P ……price of single or three phase cable
p ……pressure
P ……Ohmic power losses
P_{cable} ……power transmitted in a collection cable
$P_{c\text{-}loss}$ ……wind turbine interconnection cable losses
P_{farm} ……total power rating of farm
$P_{loss\ cable}$ ……total cable loss per cable system
P_{rated} ……rated power of the wind farm
r ……radial distance coordinate from the wake centerline
R ……cable resistance
$R_{total,\Omega}$ ……total AC or DC resistance at 20°C per unit length
s_r ……normalized wind turbine separation
$tan(\delta)$ ……dielectric loss factor
T_{total} ……total thermal resistance of a cable including its surroundings
u ……axial velocity
U ……voltage
U_∞ ……free stream velocity at hub height
U_a ……flow speed
U_m ……measured axial velocity
u_r ……mean radial velocity in the wake
U_w ……velocity scale
u_x ……velocity deficit
v ……radial velocity
V ……wind speed
V_L ……RMS line voltage

ν_θ ……temperature coefficient
W ……dielectric power losses
W_d ……total dielectric losses of the cable
$W_{total(V)}$ ……total cable losses at certain wind speed V
$W_{total,\Omega}$ ……total Ohmic losses of the cable at rated current
x ……distance coordinate from the turbine
x_0 ……axial rotor position
z_0 ……roughness length
α ……decay constant
α , β ……constants
α_θ ……temperature coefficient of conductor
Δx ……distance in the horizontal axis
$\Delta\theta_d$ ……temperature increase of conductor due to dielectric losses
$\Delta\theta_{max}$ ……maximum temperature difference
θ_{amb} ……ambient temperature of surrounding soil
θ_{max} ……maximum operating temperature of cable
ϵ_a ……Ambient turbulence contribution to the eddy viscosity

Acronyms

AC	.....	Alternating Current
D	.....	Diameter
DC	.....	Direct Current
DOWEC	.....	Dutch Offshore Wind Energy Converter
ECN	.....	Netherlands Energy Research Foundation
ENDOW	.....	Efficient Development of Offshore Wind Farms
GH	.....	Garrad Hassan
HVAC	.....	Hingh Voltage Alternating Current
KBE	.....	Knowledge Based Engineering
LPC	.....	Levelized Production Cost
MIUU	.....	Uppsala University
MVAC	.....	Medium Voltage Alternating Current
RGU	.....	Robert Gordon University
UO	.....	University of Oldenburg

Chapter 1

Introduction

1.1 Background

With the increase of wind turbine size and its integration in space limited farms, the effects of wakes has become an essential part to evaluate during the project planning. The wind speed deficit due to turbine wakes results in a reduction of the energy yield. For the case of offshore wind farms, the less air mixing by ambient turbulence results in longer wakes. Figure 1-1 illustrates the effect of wakes in wind velocity reduction. In this figure, blue and green colors indicate slower wind speed and yellow and orange colors indicate higher wind speed.

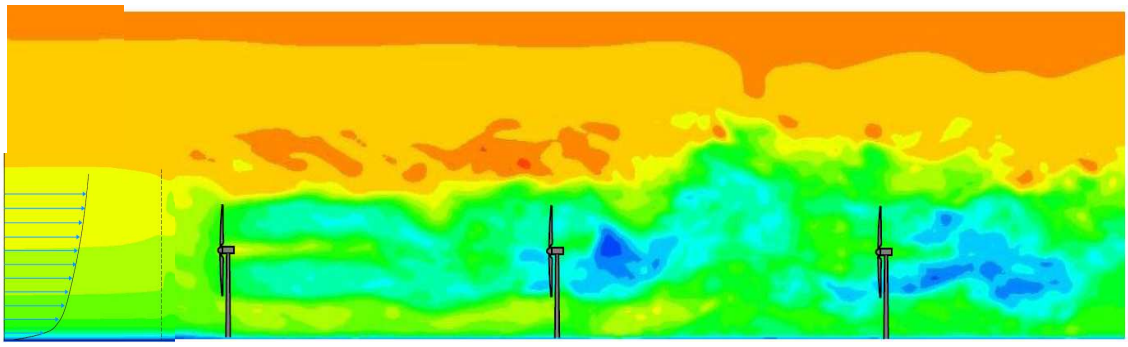

Figure 1-1. Wake effects in grouped wind turbines. Taken from [1].

As a measure to avoid the indicated wake effects within wind farms, larger distance between turbines is required. As outcome, longer cables are needed to interconnect such turbines. Nevertheless, longer cables imply more energy losses since the conductors have a limited transportation capacity as function of the cable length. It is exemplified in Figure 1-2 where the maximum current a given cable can transport is reduced when the cable length increases.

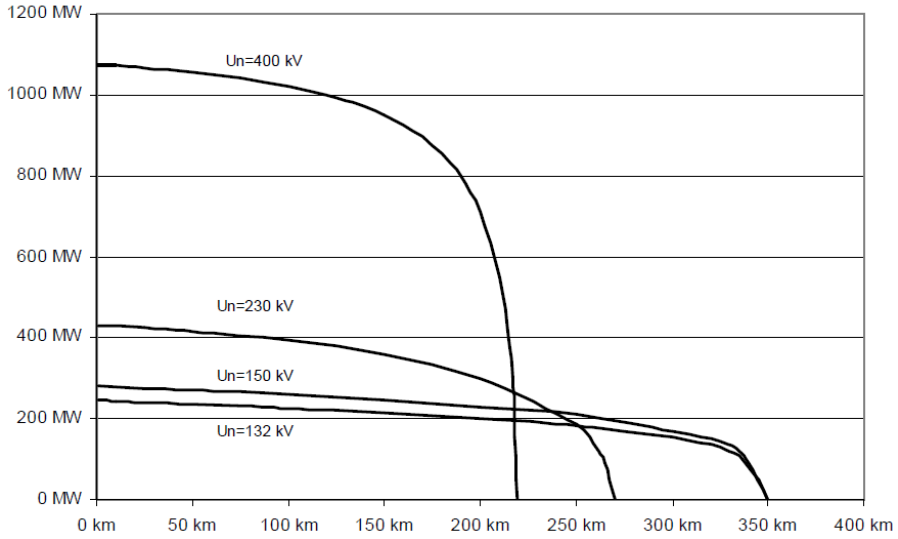

Figure 1-2. Limits of transmission capacity as function of cable length, submarine HVAC cables. Taken from [2].

In order to reduce the energy losses and avoid overheating damage to the cables, larger conductor cross section areas are required for longer cables. Consequently, thicker and longer cables imply higher costs. It is possible to understand there is a trade off between reduction of aerodynamic losses and increase of electric cable losses and costs.

Based on the previous paragraphs, two aspects are of high relevance when designing the wind farm layout: wake effects on energy caused by upwind turbines over downwind turbines and the electrical losses and costs of infield interconnection cables. These aspects become consequence of the design phase and once the farm is built, they are fixed features that will be present during the overall project lifetime. Therefore, a design tool to optimize the farm layout can improve the profitability of currently costly offshore wind farm projects.

Up to now, the few existing big wind farms have followed a symmetrical parallelogram layout, similar to the one shown in Figure 1-3.

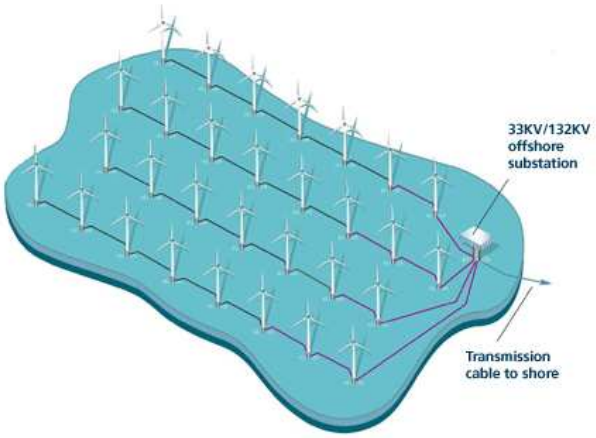

Figure 1-3. Offshore wind farm: symmetrical layout.

Hence, a tool developed to work with square layouts, which balances the gain in energy output and the increment in energy losses and costs when modifying the separation distances would be of high utility for the offshore wind farm design process.

1.2 Thesis objective

The main objective of this master thesis is to synthesize a set of knowledge related to the design of offshore wind farm layout. This knowledge can be useful to other developers when integrating this design tool into bigger framework, where a broader conceptual design tool for offshore wind farm optimization will be developed.

The tool will include simplified models to describe wake effects as well as interconnection cable properties within a wind farm. The tool performance will be measured by its ability to deliver fast and reasonable results, so it can be easily integrated into a bigger, more general tool. The calculated levelized production cost (*LPC*) and the layout dimensions are expected to be similar to existing wind farms.

Additionally, the generated knowledge will include wake effects in wind farm efficiency, wake models and their computation velocity when implemented in a computer code, influence of cable electrical losses and costs in the cost of energy, effects of wind site conditions over the layout dimensions and the tool computing cost.

1.3 Approach

In general, the project objective was pursued during the development of a tool that can be used in the wind farm design process. The tool is a computer code which aims to give an

overview of the influence of wake aerodynamic losses and collection cable electrical losses and costs over the levelized production cost.

As a preparation for the development of this project, a literature research [3] was done about wake models and electrical cable loss and cost models. Existing wake models and the validation of their effectiveness in predicting energy losses, as well as the information available about electrical cable loss and cost models were summarized. This information was used as a baseline to select the appropriate models to implement within the tool.

The first step was to develop a simplified tool version, able to find the minimum cost of energy of a wind farm composed of two turbines linked with one straight cable. After that, the number of the wind farm features to include (and therefore the tool complexity itself) was gradually increased. There were several important reasons to proceed in this way, as following indicates:

1. To get acquainted with the magnitude of the task and how long it takes to get an operational program.
2. To reduce the risk of starting developing a very complex code which at the end would not be able to work properly.
3. To estimate how much effort would be required for developing the next tool extensions. These are additional features to make the tool able to work with more realistic wind farm conditions.
4. To generate a set of useful knowledge about design process and wind farm component properties.
5. To develop a modular program structure in which additional parts can be easily added or substituted.

The theoretical base, the tool development, the verification of its performance and the explanation of the new knowledge learned during all this process are explained through the different chapters of this thesis, as indicated in the following section.

1.4 Thesis Outline

The present document is divided in seven chapters. The content of each of them is summarized as follows:

Chapter 1: Introduction to the project objective and approach followed during the design tool development.

Chapter 2: Overview of the wake and electrical cable loss and cost models described in literature that were integrated into the tool. Also, the calculation method for the *LPC* is explained.

Chapter 3: Introduction to basic concepts of the design cycle used as a helpful method for developers and the tool development approach followed during this master project.

Chapter 4: Explanation of the steps followed during the development of the first tool version. The chapter also describes the different tool expansions to include variable wind speed based on Weibull distribution, variable wind direction using a wind rose, linear and square layout, wake combination method, several wake and cable models, wind farms with more than two turbines, wake interaction within big wind farms, etc.

Chapter 5: Examples of simulations ran and results compared with data from real wind farms are presented. Also the correct functioning of the different tool extensions is checked. Moreover, here some debugging features implemented into the tool are presented.

Chapter 6: The main results from the tool development and lessons learned in the process are presented in this chapter. It includes a set of knowledge about model performance and their suitability for optimization methods. In addition, several sensitivity analyses are done. The different models integrated in the tool are compared with the aim of checking how sensitive can be the results to changes in models.

Chapter 7: The final conclusions, recommendations and future work possibilities are indicated in this chapter.

Chapter 2

Implemented models for wake, electrical infrastructure and levelized production cost

2.1 Introduction

The calculation algorithm executed by this tool uses several mathematical models found in literature. Among the most relevant models to mention are the wake models used to determine the wake wind speed deficit and wake expansion diameter behind a wind turbine. These wake models have been developed to describe the so called far wake, which is the wake portion beyond approximately two rotor diameters after the turbine. In Figure 2-1, the wind speed deficit and turbulence intensity are shown for the close and far wake subsections.

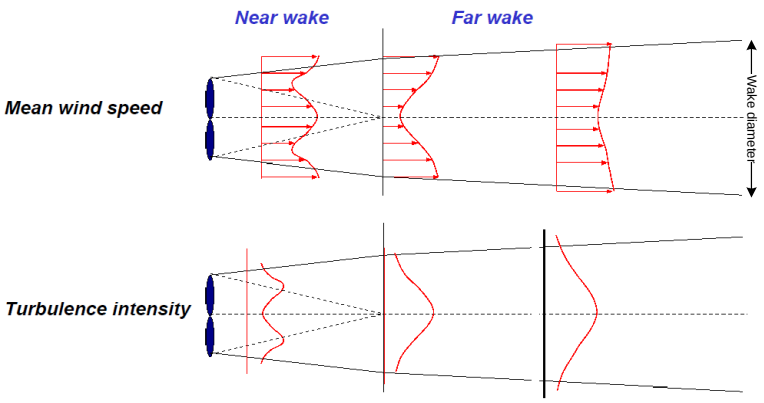

Figure 2-1. Wind turbine wake subsections. Taken from [4].

When the wind speed profile is taken into account, the wake acquires a shape like shown in Figure 2-2.

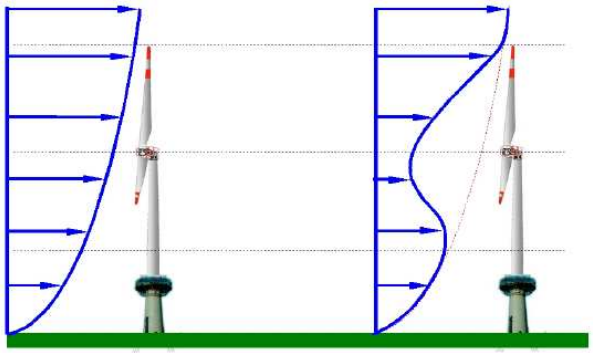

Figure 2-2. Wind speed profile and turbine wake. Taken from [4].

Regarding the electrical infrastructure, the models for the cable costs and electrical losses are also detailed in this chapter. It will be seen that these two variables will be linearly dependent on the cable length.

Finally, the model used for the calculation of the levelized production cost is explained. This model was specially proposed for wind energy applications.

2.2 Wake models

Several wake models have been found. Some of them were initially developed in the 1980's and have gone through a process of constant improvement and validation. Also,

they are found to be mainly proposed by staff from Danish research institutes. A summarized explanation of each of them is now presented.

2.2.1 Jensen model

This model was initially proposed by N.O. Jensen [5] and further developed by I. Katic [6]. It is based in the description of a single wake and considers the initial velocity reduction and a wake decay coefficient. It assumes the wind velocity to be constant inside the wake. Figure 2-3 will be used to explain the model.

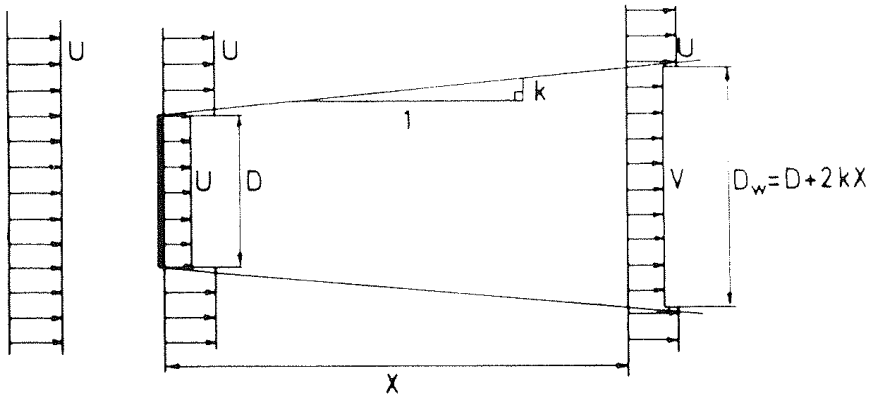

Figure 2-3. Jensen wake model. Taken from [6].

From Figure 2-3, it can be seen that Jensen's model makes some simplifications. The wake behind the turbine has an initial diameter of the same size as the rotor and it spreads linearly downwind as a function of distance. The wake velocity function gives not very accurate results at distances smaller than four diameters behind the turbine. However, in practice it is very rare to install turbines closer than this value.

A balance of momentum results in the so called *velocity deficit* of the wake at position X:

$$1-\frac{V}{U}=\frac{1-\sqrt{1-C_t}}{\left(1+\frac{2kX}{D}\right)^2} \qquad \text{eq. 2-1}$$

Or

$$\partial V = U - V = U\left(1-\sqrt{1-C_t}\right)\left(\frac{D}{D+2kX}\right)^2$$

where $\boldsymbol{C_t}$ is the thrust coefficient of the wind turbine. It is important to mention that for a given turbine, the curve for the thrust coefficient as function of the wind speed can be obtained from the manufacturer, from published data or calculating it from the turbine power curve.

Additionally, the expanding wake diameter is found to be:

$$D_w = D + 2kX \qquad \textbf{eq. 2-2}$$

where ***k*** is a constant called the decay factor. It describes the dissipation of the wake by growth of its width. It is affected by wind speed, ambient turbulence, turbine induced turbulence, and atmospheric stability. In the help section of the WAsP[1] computer program, the standard decay constants are recommended to be 0.075 for onshore conditions and 0.05 for offshore. Also an analytical expression is given by:

$$k = \frac{A}{\ln\left(\frac{h}{z_0}\right)} \qquad \textbf{eq. 2-3}$$

where:

h .....is the height.

z_0 .....is the roughness length.

A.....is a constant (≈0.5).

The result is then two equations to determine the wake width and speed deficit. There is no consideration of either wind speed profile or turbulence presence.

2.2.2 Frandsen model

The Frandsen wake model [8] is an analytical model of wind speed deficit for large offshore wind farms. It has been defined for wind farms with the following characteristics:

- Rectangular array geometry with straight rows of wind turbines.
- Equidistant spacing between turbines and rows.
- Wind flow direction parallel to rows.

The model deals with three different regimes. The next picture identifies them in a wind farm with regular array layout.

[1] WAsP is a computer program for predicting wind climates, wind resources and power productions from wind turbines and wind farms. It has been developed by the Wind Energy Department at Risø National Laboratory, Denmark.

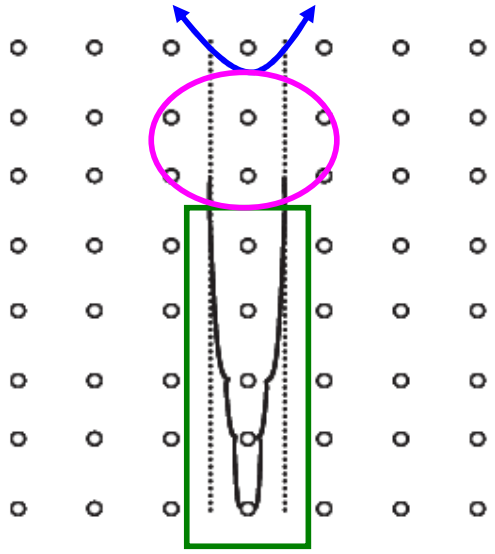

Figure 2-4. Frandsen model regimes.

The first regime is represented by the green area. It is a sector of the wind farm where turbines are exposed to multiple wake flow. An analytical relation is given for the expansion of the multiple wakes and the asymptotic flow speed deficit. The second regime belongs to the pink area, a zone where wakes from one row get in contact with neighbor wakes and horizontal expansion is not longer possible. Further more the ground is another limitation and the only available direction to expand is upwards. The third regime is indicated by the blue zone. It is located somewhere downwind in a very large wind farm. If assumed an infinitely large wind farm, the flow reaches balance with the atmospheric boundary layer.

The development of the model equations for a single wake is based on a control volume with no flow across the cylinder surface (see Figure 2-5 below). With this methodology, expressions relating turbine's thrust and power coefficients with wake's flow speed deficit are obtained.

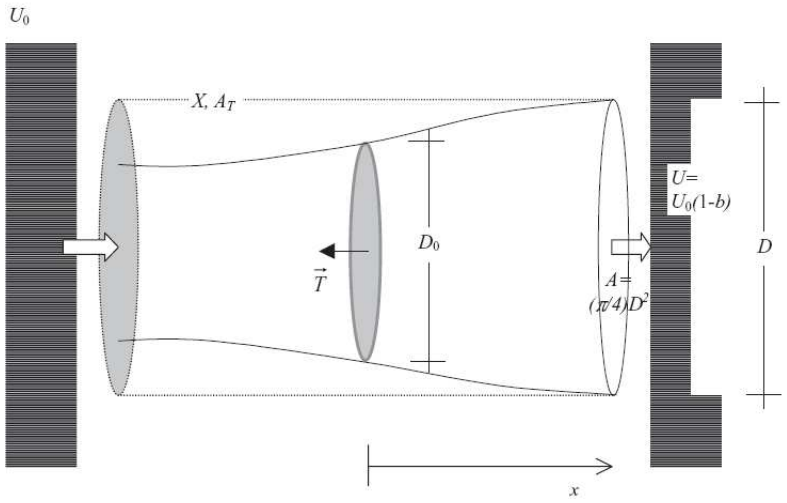

Figure 2-5. Control volume around a wind turbine rotor. Taken from [8].

The momentum equation for the flow volume X, with surface area A_T and cross-section area A is:

$$\int_X \rho \frac{\partial \vec{U}}{\partial t} dX + \int_{A_T} \rho \vec{U} \left(\vec{U} d\vec{A} \right) = -\int_{A_T} p d\vec{A} + \int_X \rho \vec{g} dX + \vec{T} \int_{A_T} \vec{\tau} dA \qquad \textbf{eq. 2-4}$$

The author considers possible to neglect the acceleration, the pressure, the gravity and the turbulent shear force terms. He also assumes the beginning and end of the cylinder separated far enough to have pressure equal to the freestream's. Any possible rotation in the flow is neglected as well and the wake is assumed axisymmetric. The equation is reduced to the form:

$$T = \int_A \rho U \left(U_0 - U \right) dA \qquad \textbf{eq. 2-5}$$

The author works out the previous formula until he obtains the final result for the flow speed ratio

$$\frac{U}{U_0} = \frac{1}{2} + \frac{1}{2} \sqrt{1 - 2 \frac{A_0}{A} C_T} \qquad \textbf{eq. 2-6}$$

and the wake diameter

$$D(x) = D_0\left(\beta^{\frac{k}{2}} + \alpha s\right)^{\frac{1}{k}} \qquad \text{eq. 2-7}$$

These two equations comprise the Frandsen model. In this case, the variable $\boldsymbol{A_0}$ represents the rotor area and $\boldsymbol{A_a}$ is the cross sectional area immediately after wake expansion. They are related as:

$$A_a = \beta A_0 \qquad \text{eq. 2-8}$$

Also, to obtain an analytical solution for the decay constant $\boldsymbol{\alpha}$, the eq. 2-7 is compared with the Jensen model to conclude it can be calculated as:

$$\alpha = \beta^{\frac{k}{2}}\left[\left(1+2\alpha_{(noj)}s\right)^k - 1\right]s^{-1} \qquad \text{eq. 2-9}$$

where $\boldsymbol{\alpha_{(noj)} \approx 0.05}$. Based on a solution given by Schlichting, a value of $\boldsymbol{k}$=3 can be assumed. Oppositely, if Frandsen solution is chosen, then $\boldsymbol{k}$=2. The other variables are given as:

$$\begin{aligned} A &= \frac{\pi}{4}[D]^2 \\ a &= \frac{1-\sqrt{1-C_T}}{2} = 1-\frac{U_a}{U_0} \\ \beta &= \frac{1-a/2}{1-a} = \frac{1}{2}\frac{1+\sqrt{1-C_T}}{\sqrt{1-C_T}} > 1 \\ s &= \frac{x}{D_0} \end{aligned} \qquad \text{eq. 2-10}$$

where $\boldsymbol{C_T < 1}$ is the thrust coefficient and $\boldsymbol{U_a}$ is the flow speed in the wake just after the initial wake expansion (slightly behind the rotor).

2.2.3 Ainslie model

The Ainslie [9] model is a wake model based on a numerical solution of the differential equations governing the wind flow. An eddy viscosity turbulence model is used, which has two contributions:

- Wake mixing due to turbulence generated within the shear layer of the wake.

- Wake mixing due to atmospheric turbulence.

These two factors are key determinants of the wake rate of recovery, it means how rapidly the wake is dissipated and the wind flow recovers its initial state. The atmospheric term is dominant in most practical situations and influences at high level the wake velocity field.

When describing wind turbine wakes, two sections are normally categorized: the near wake and the far wake. The near wake has been found to be a complex region, comprised within a distance of 2 to 4 rotor diameters downstream from the nacelle. In this region the kinetic energy extraction causes three phenomena to occur:

- A flow pressure drop at the rotor plane.
- A reduction in the centerline velocity.
- An expansion in the wake width downstream from the rotor plane.

The last two aspects are shown in Figure 2-6 where the wind speed profiles are drawn in front and behind the turbine. Note that only the upper half is presented, assuming symmetry along the horizontal axis (axisymmetric).

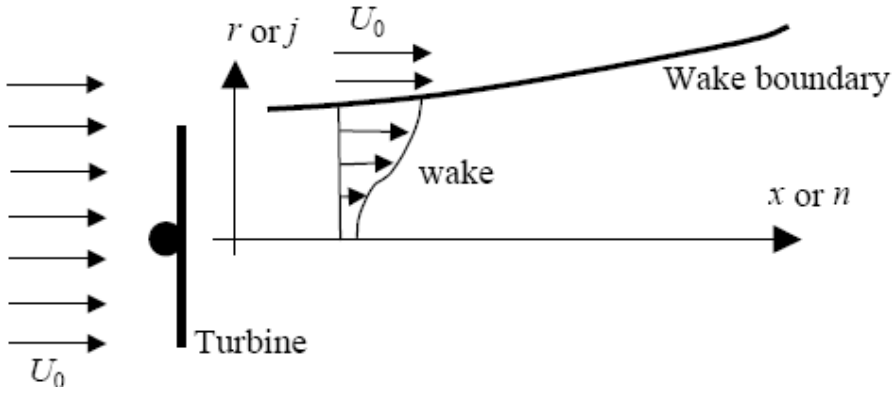

Figure 2-6. Ainslie model. Taken from [10].

The minimum centerline velocity happens between 1 and 2 diameters. Beyond this point, turbulent mixing starts to have greater influence over flow characteristics and the velocity profile becomes more similar to the initial undisturbed situation. The Ainslie model is a far wake model valid from distances of 5 diameters. There, the wake profile is taken as Gaussian and the centerline velocity deficit decays with a rate dependent on the ambient turbulence intensity. According to Ainslie, the momentum deficit in the wake is determined by the thrust coefficient of the wind turbine. Therefore it is a function of the

operating conditions like pitch angle, tip speed ratio, wind velocity, air density, turbine size, etc.

For the derivation of the descriptive equations, some assumptions are done in order to simplify the model:

- The wake is considered to be axisymmetric.
- The wake is fully turbulent.
- The wake has zero circumferential velocities.
- The wind flow field is stationary.
- The pressure gradients in the co-flowing fluid outside the wake are negligible.
- The gradients of mean quantities in the radial direction are very much greater than in the axial direction. This is taken to be true beyond the first few diameters downstream.
- The fluid is incompressible.
- The viscosity is neglected.

With such suppositions, the Navier-Stokes equation is replaced by its equivalent thin shear layer approximation, formulated in cylindrical coordinates:

$$u\frac{\partial u}{\partial x}+v\frac{\partial u}{dr}=-\frac{1}{r}\frac{\partial(r\overline{uv})}{\partial r} \qquad \textbf{eq. 2-11}$$

where:

u .....is the axial velocity.

v .....is the radial velocity.

x .....is the axial distance coordinate from the turbine.

r .....is the radial distance coordinate from the wake centerline.

The last part of the previous equation refers to the acceleration change and thus momentum transport across the flow. The term ***uv*** is the Reynolds stress which explains the interaction of neighboring fluid elements and the consequent diminution of velocity gradients.

The turbulent viscosity model is used to portray the shear stresses with an eddy viscosity described as:

$$-\overline{uv} = \in \frac{\partial U}{\partial r} \qquad \text{eq. 2-12}$$

$$\in = l_w(x) U_w(x) + \in_a \qquad \text{eq. 2-13}$$

where:

l_w .....is the "suitable length".

U_w.....is the "velocity scale".

ϵ_a .....is the ambient turbulence contribution to the eddy viscosity.

The suitable length and the velocity scale are two parameters which describe the wake shear layer. They are proportional to the wake width and to the velocity difference between the free flow and the wake across the shear layer. They depend of the downstream distance ***x*** but not of the radius ***r***.

Additionally to the previous results, Ryan [11] indicates that eq. 2-11 can be combined with the axisymmetric form of the continuity equation ($\partial/\partial\varphi=0$) in cylindrical coordinates for incompressible fluids, just like presented in eq. 2-14:

$$\frac{1}{r}\frac{\partial rv}{\partial r} + \frac{\partial u}{\partial x} = 0 \qquad \text{eq. 2-14}$$

Ryan states that these two equations form a system of differential equations used to numerically simulate the wake flow.

2.3 Electrical cable models

In relation to electrical infrastructure models, less information was available in literature. Only one detailed study was found specifically aimed to offshore wind farm applications. The main mathematical relations are presented as follows.

2.3.1 Schoenmakers cable loss model

The losses in the wind turbine interconnection cables depend on several factors as affirmed by Schoenmakers [12]. The more relevant aspects to consider are:

- Length of cables
- Infield cable voltage

- Conductor cross section
- Type of conductor
- Operating conditions

Since previous aspects are very specific for each wind farm, an approximation is done by considering the cable losses as a percentage of the total rated power output. Then the author proposes a method to calculate the infield cable losses for the operational range of the wind turbines as:

$$P_{c\text{-}loss} = \sum_{V=cut-in}^{cut-out} \left[\left(\frac{I(V)}{I_{rated}} \right)^2 \cdot LP \cdot P_{rated} \cdot f(V) \cdot \frac{Hr}{Yr} \right] \quad \textbf{eq. 2-15}$$

$$I(V) = \frac{P(V)}{\sqrt{3} \cdot V_t \cdot \frac{1}{1000}} \quad \textbf{eq. 2-16}$$

$$I_{rated} = \frac{P_{rated}}{\sqrt{3} \cdot V_t \cdot \frac{1}{1000}} \quad \textbf{eq. 2-17}$$

where:

$P_{c\text{-}loss}$ ..... are the wind turbine interconnection cable losses [W].

I(V) ..... is the total wind farm current for wind speed ***V*** [A].

I_{rated} ..... is the total rated current of the wind farm [A].

LP ..... is the wind farm loss percentage at rated power due to interconnection cables [%].

P(V) ..... is the total wind farm power for wind speed ***V*** [MW].

P_{rated} ..... is the rated power of the wind farm [MW].

f(V) ..... is the probability of occurrence of wind speed ***V*** [-].

Hr/Yr ..... are the hours per year, 8760 [-].

V_t ..... is the voltage level of the collection electrical system [kV].

In relation to the value of the loss percentage parameter, the author refers the example of the North Hoyle offshore wind farm in Wales, where it was estimated as 0.5% of the rated power.

Additionally to the previous general model, the author presents a more detailed procedure to calculate the cable losses for a certain current ***I***, based on its electrical and thermal behavior and assuming operation in moist soil. The model is specified in the following set of equations.

The cable losses are calculated as:

$$W_{total}(V) = W_d + W_{total,\Omega}\left(\frac{I(V)}{I_{rated}}\right)^2 v_\theta \qquad \textbf{eq. 2-18}$$

$$W_d = n \cdot 2 \cdot \pi \cdot f \cdot C' \cdot L \cdot \frac{V_L^2}{3} tan(\delta) \qquad \textbf{eq. 2-19}$$

$$W_{total,\Omega} = n \cdot R_{total,20} \cdot L \cdot I_{rated}^2 \left[1 + \alpha_\theta \left(\theta_{max} - 20\right)\right] \qquad \textbf{eq. 2-20}$$

where:

$W_{total}(V)$ .....are the total cable losses at certain wind speed ***V*** [W].

W_d ....are the total dielectric losses of the cable [W].

$W_{total,\Omega}$ . .....are the total Ohmic losses of the cable at rated current [W].

I(V) ....is the current distribution per phase, for wind speed ***V*** [A].

I_{rated} ....is the rated current of the cable per phase [A].

v_θ ....is the temperature coefficient [-].

n ....is the number of phases [-].

f ....is the frequency of operation (e.g. 50 or 60 Hz) [Hz].

C' ....is the capacitance per phase per unit length [F / km].

L ....is the cable length [km].

V_L ....is the RMS line voltage [V].

tan(δ) .....is the dielectric loss factor (For XLPE insulated power cables, tan(δ) = 0.0004) [-].

$R_{total,\Omega}$ .....is the total AC or DC resistance (including sheath armor losses for AC) at 20°C per unit length [Ω / km].

α_θ ..... is the temperature coefficient of conductor (i.e. for copper: αθ = 0.00393, for aluminum: αθ = 0.00403) [1 / °C].

θ_{max} .... is the maximum operating temperature of cable (90°C for an XLPE cable) [°C].

The temperature coefficient v_θ found in eq. 2-18 is calculated as:

$$v_\theta = \frac{c_1}{c_1 + c_2\left[1 - \left(\frac{I}{I_{rated}}\right)^2\right]} \quad \text{eq. 2-21}$$

$$c_1 = 1 + \alpha_\theta\left(\theta_{amb} - 20 + \Delta\theta_d\right)$$
$$c_2 = \alpha_\theta\left(\Delta\theta_{max} - \Delta\theta_d\right) \quad \text{eq. 2-22}$$

$$\Delta\theta_d = n \cdot W_d \cdot T_{total} \quad \text{eq. 2-23}$$

$$\Delta\theta_{max} = \theta_{max} - \theta_{amb} \quad \text{eq. 2-24}$$

$$T_{total} \approx \frac{\Delta\theta_{max}}{W_{total,\Omega}} \quad \text{eq. 2-25}$$

where:

c_1 , c_2 ... . are constants [-].

θ_{amb} .... is the ambient temperature of surrounding soil [°C].

$\Delta\theta_d$ .... is the temperature increase of conductor due to dielectric losses [°C].

$\Delta\theta_{max}$ .. .. is the maximum temperature difference [°C].

T_{total} .... is the total thermal resistance of a cable including its surroundings [K m/W].

Taking into account the previous information, the total losses of a cable are then calculated over the total operational range of the wind turbine in use. They are obtained by eq. 2-26:

$$P_{loss\ cable} = \sum_{V=cut\text{-}in}^{cut\text{-}out} \left(W_{total}(V) \cdot 10^{-6} \cdot \frac{Hr}{Yr} \cdot f(V) \right) \qquad \text{eq. 2-26}$$

where:

$P_{loss\ cable}$ .....is the total cable loss per cable system [MWh].

$W_{total}(V)$ .....is the total cable loss for wind speed ***V*** [W].

Hr/Yr .. ..are the hours per year, 8760 [-].

f(V) ....is the probability of occurrence of wind speed ***V*** [-].

As can be appreciated, the calculation of the total power losses in cables depends of several parameters which need to be known in order to use the previous model. These parameters are classified into two categories, one related to cables themselves and another one related to the surrounding conditions, as shown in Table 2-1 and Table 2-2.

Table 2-1. Variables of the cable surroundings needed in order to be able to perform the cable loss calculation. Taken from [12].

Variable		Unit
Burial depth	Usually 1.5 m offshore, 3.0 m near shore and 1.0 m onshore	[m]
Soil temperature	θ_{soil}	[°C]
Soil thermal resistance	T_4	[Km/W]
Presence of more cable systems	Mainly onshore issue	[-]

Table 2-2. Variables which are needed of the cable characteristics in order to be able to perform the cable loss calculation. Taken from [12].

Variable		Unit
Type of cable	AC or DC	[-]
Number of phases	1, 2 or 3	[-]
Length of Cable	L	[km]
Cable capacitance per unit length	C'	[F/km]
RMS Line voltage	V_L	[kV]
tan(δ)	0.0004 for XLPE cables	[-]
Total AC or DC resistance at 20℃ per unit length	$R_{total,20}$	[Ω/km]
Rated current	I_{rated}	[A]
Temperature coefficient of conductor	α_{20}, 0.00393 for copper, 0.00403 for aluminum	$[\frac{1}{^{o}C}]$
Maximum operating temperature	θ_{max}, 90℃ for XLPE cables	[℃]
Operating frequency	50 or 60	[Hz]
Total thermal resistance of cable incl. surroundings	T_{total}	[Km/W]

2.3.2 Schoenmakers cable cost model

The cable cost model developed by Schoenmakers is not public available since it was developed within a private company. However, he indicates that based on the cross section of the cable, it is possible to calculate the amount of conductor material per km of cable. Then, compare cable prices and aluminum, copper and lead prices for the same period of time in order to establish a percent relation of raw material and manufactured cable. Also the conversion rate Euro/Dollar has to be considered for the period of interest. With this information, it is possible to calculate the price of conductor material per km of cable. Based on this and by comparing the cost prices for the different type of cables, it is possible to calculate a trend line. As a result, a linear cost model for cables is given as:

$$P = \alpha C + \beta \qquad \text{eq. 2-27}$$

where:

- ***P*** .....is the price of single or three phase cable [M€/km].
- ***α*** .....is a constant [€/m^3].
- ***β*** .....is a constant [M€/km].
- ***C*** .....is the conductor cross section [mm^2].

The constants ***α*** and ***β*** are linked to cable characteristics, such as AC/DC type, voltage level insulation, submarine or land applications.

In relation with the installation costs, the author indicates there are far too many aspects which determine them. Therefore, it is more practical to better consider a fixed price per km. His estimations are not public available.

2.3.3 Own developed cable cost model

Based on the advice given by Shoemakers, an own model to describe the cable costs was developed. The procedure is explained as follows.

First, it is necessary to calculate the current per string of cable connecting several wind turbines, as given by eq. 2-28. The cable is assumed to have the current capacity for all the string.

$$Irs = \frac{(TP \cdot 1000000)TpS}{\sqrt{3}(V \cdot 1000)} \qquad \text{eq. 2-28}$$

where:

IrS ....is the string cable rated current [A].

TP ....is the turbine rated power [MW].

TpS..... .....is the number of turbines per string [-].

Knowing the required cable capacity, it is possible to determine the cable cross section with the help of technical data given by any cable manufacturer. In this case, data found at the ABB Power Technologies AB website was used [13]. This is summarized in Table 2-3 and Table 2-4.

Table 2-3. 10-90 kV, XLPE 3-core submarine cables armour. Taken from [13].

10-90 kV XLPE 3-core cables		
Cross section mm²	Copper conductor	Aluminium conductor
	A	A
95	300	235
120	340	265
150	375	300
185	420	335
240	480	385
300	530	430
400	590	485
500	655	540
630	715	600
800	775	660
1000	825	720

Table 2-4. 10-90 kV, XLPE single-core submarine cables, cooper conductor. Taken from [13].

Rated voltage 10-90 kV, copper conductor * Segmental conductor for 1200 mm² or more						
Cross section Cu conductor	Wide spacing			Close spacing		
	Armour resistance as % of conductor resistance			Armour resistance as % of conductor resistance		
	200%	100%	50%	200%	100%	50%
mm²	A	A	A	A	A	A
95	370	370	405	325	320	310
120	405	420	460	365	355	350
150	445	475	515	400	390	385
185	490	535	585	440	425	425
240	555	620	680	490	475	485
300	625	700	775	525	525	545
400	710	810	890	565	580	620
500	805	920	1015	610	650	700
630	915	1050	1165	660	725	795
800	1035	1195	1320	715	810	895
1000	1195	1395	1550	815	950	1065
1200*	1305	1520	1685	870	1035	1155
1400*	1420	1655	1835	935	1120	1250
1600*	1475	1700	1870	970	1155	1275
2000*	1645	1890	2070	1070	1280	1400

The next step is to calculate the cooper cost that would be necessary to produce the cable. Here, the cooper is assumed the most costly cable component and therefore is assumed as a good indicator of the cable cost. It is calculated as indicated by eq. 2-29.

$$CuC = 3 \cdot CuP \cdot CuRo \cdot Across \cdot \frac{1}{100000} \qquad \textbf{eq. 2-29}$$

where:

CuC ....is the cooper cost [Euro/km].

CuP ....is the cooper price [Euro/tonne].

CuRo ... .is the cooper density [kg/m3].

Across . .....is the conductor cross section area [mm2].

Finally, the total cable cost for the wind farm is obtained by adding up all the cable production cost plus a manufacturer profit, as given in eq. 2-30.

$$CaC = \frac{(NoS \cdot LS + LS\_c) \cdot (CuC \cdot extra \cdot profit)}{1000000} \qquad \textbf{eq. 2-30}$$

where:

CaC ....is the cable cost [MEuro].

NoS ....is the number of strings [-].

extra ....is a weighting factor = 1 if using one 3-core cable per string.

= 1.5 if using three 1-core cables per string.

profit ... .is the cable manufacturer profit per cable as % of cooper cost [%].

For the several variables described above, the values given by Table 2-5 were used.

Table 2-5. Values for some cable parameters.

Cable parameters	
Cooper density [kg/m3]	8940
Cooper price [Euro/tonne]	2782
Profit [%]	200

The value related to the cooper density is a scientific value available in chemistry books. The cooper price was found in market stock webpages. The manufacturer profit proportion was taken as an assumption.

2.4 Levelized production cost

The importance of the levelized production cost concept and its mathematical definition relies in the fact that it will be the objective function the developed tool aims to minimize. Therefore a definition expressly proposed for wind energy projects is now explained.

Based on the expression given by Hunter [14], the levelized production cost (*LPC*) is the cost of one production unit (kWh) averaged over the wind farm entire lifespan. The total utilized energy output and the total costs over the lifetime of the wind farm are both discounted to the start of operation by means of the chosen discount rate, and the *LPC* is derived as the ratio of the discounted total costs and utilized energy output. In the calculations, all costs are discounted to the present value, i. e. the first date of commercial operation of the wind farm.

If the annual utilized energy is assumed to be constant from year to year, the *LPC* can be calculated as:

$$LPC = \frac{I}{a \cdot AUE} + \frac{TOM}{AUE} \qquad \textbf{eq. 2-31}$$

where:

LPC..... ..... is the levelized production cost [Euro/kWh].

I .... is the total capital investment [Euro].

a .... is the annuity factor [-].

AUE .... is the utilized energy per year [kWh].

TOM ... . is the total levelized annual "downline costs" (all costs other than initial investment) [Euro].

For simplicity, *TOM* can be estimated as a certain percentage of the investment. Nonetheless, the formal definition is given by:

$$TOM = \frac{1}{a} \cdot \sum_{t=1}^{n} (OM_t + SC_t + RC_t)(1+r)^{-t} - SV(1+r)^{-n} \qquad \textbf{eq. 2-32}$$

where:

n .... is the economic lifetime [years].

OM_t..... ..... is the operation and maintenance cost during year ***t*** [Euro].

SC_t .... is the social cost during year ***t*** [Euro].

RC_t..... ..... is the retrofit cost during year ***t*** [Euro].

r ....is the discount rate [-].

SV ....is the salvage value after ***n*** years [Euro].

The annuity factor is given by:

$$a = \frac{1}{\sum_{t=1}^{n}(1+r)^{-t}} = \frac{(1-(1+r)^{-n})}{r} \qquad \text{eq. 2-33}$$

For the present project, the *LPC* is calculated using the formula given by eq. 2-31. As previously indicated, the *TOM* can be considered a percentage of the investment. In order to determine the adequate proportions, the *DOWEC* cost study presented by Herman [15] is considered. The main cost contributors to the *LPC* are shown in Figure 2-7.

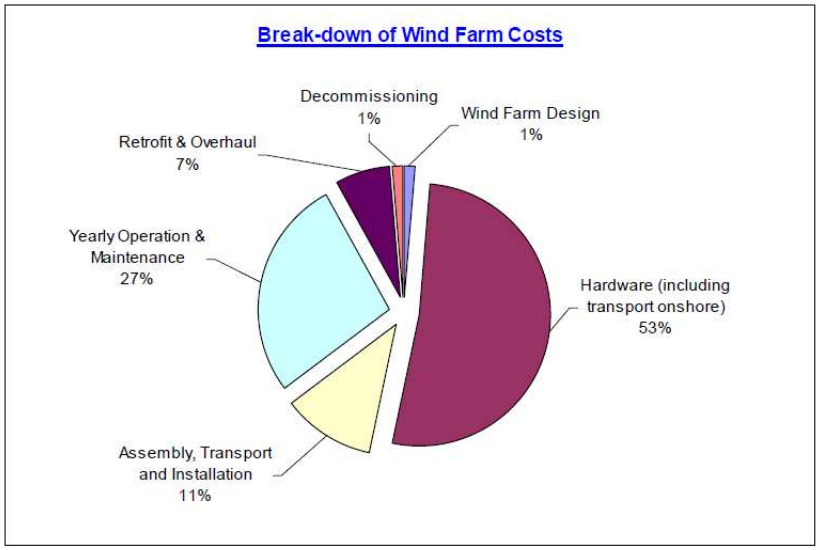

Figure 2-7. Contribution of level 1 wind farm components to the LPC cost calculation. Taken from [15].

The hardware cost contribution (53%) is taken as the reference to calculate the *LPC* since the developed tool works directly with cable lengths and the number of turbines. Thus, it is important to decompose the hardware costs into smaller subgroups. This division is given by Figure 2-8.

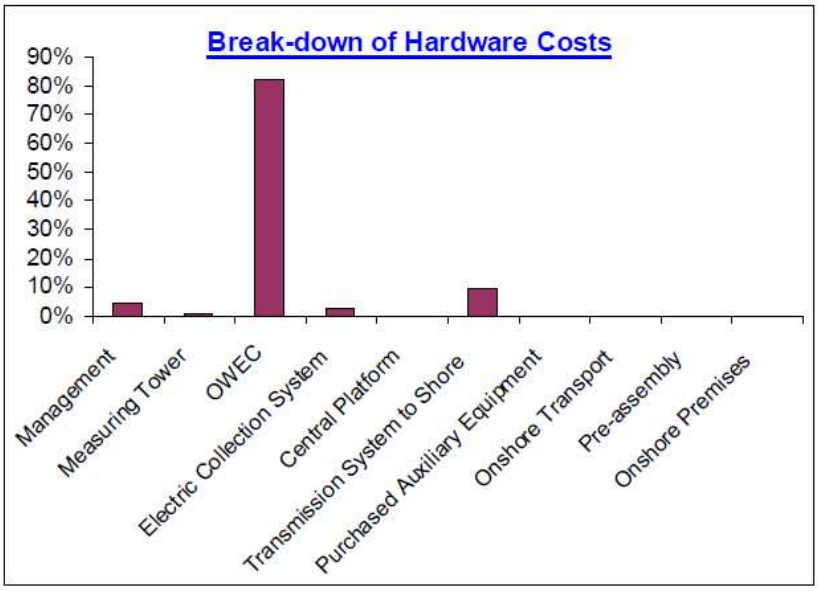

Figure 2-8. Breakdown at level 2 of Hardware costs. Taken from [15].

Using previous information, the *LPC* model implemented in the tool is defined as follows. First, the calculation of the investment costs can be separated into a fixed amount counting for every capital cost except the cable costs. The variable amount is attributed to the cable costs. This is indicated in eq. 2-34.

$$\begin{aligned} LPC &= \frac{I}{a \cdot AUE} + \frac{TOM}{AUE} \\ &= \frac{I}{a \cdot AUE} \times \frac{1}{53\%} \\ &= \frac{\left(fixed_{cost} + variable_{cost} \right)}{a \cdot AUE} \times \frac{1}{53\%} \\ &= \frac{\left(fixed_{cost} + cable_{cost} \right)}{a \cdot AUE} \times \frac{1}{53\%} \end{aligned} \qquad \textbf{eq. 2-34}$$

From Figure 2-8, the cable contribution to hardware costs is taken as 3%. To calculated the leftover 97%, the Offshore Wind Energy Converters (*OWEC*) costs contribution (80%) is used as reference value. Then, the fixed costs are calculated as:

$$fixed_{cost} = \left(OWEC_{cost} \cdot \frac{1}{80\%} \right) \cdot 97\% \qquad \textbf{eq. 2-35}$$

Combining the two previous equations, the *LPC* is obtained as:

$$LPC = \frac{\left(\left(OWEC_{cost} \cdot \frac{1}{80\%} \cdot 97\%\right) + cable_{cost}\right)}{a \cdot AUE} \times \frac{1}{53\%} \qquad \textbf{eq. 2-36}$$

Now that the main mathematical models to be integrated into the tool have been explained, it is possible to introduce the development approach followed during the tool implementation. This is described in chapter 3.

Chapter 3

Tool design and evolution approach

3.1 Introduction

Creating from scratch a tool to optimize the wind farm layout of any size can result to be a complex assignment. Without an initial experience about how to proceed solving the established project objective, the tool developer may not identify the most relevant function parameters, problem solution constraints, time consuming tasks, etc. Additionally, a code of large size is more susceptible to errors due to programming that would be difficult to identify.

Basic physical constraints and coding conditions can be perceived faster if a reduced version of the problem is used as starting point. From there, further tool expansions can be done with the advantage of having an operable code at all time. Also, the new additions can be tested separately and added to the global code once their performance is considered satisfactory.

For this reason, a stepwise tool expansion approach was followed. The aims is to start from a basic code produced to optimize a simple wind farm case and from there, continue integrating additional expansions to take into account more detailed wind and farm aspects, every time closer to real conditions.

In this chapter, the basic design cycle principles are introduced since there were used as guidance during the tool development. Furthermore, the code evolution is described in order to understand better the early tool stage and the later inclusion of the different expansions.

3.2 The design cycle as a guide for the tool development

When developing a tool with the intend to help in the optimization of wind farms, it is necessary to define at which design level the tool will work. As can be seen in Figure 3-1, the design process can be subdivided into three different levels.

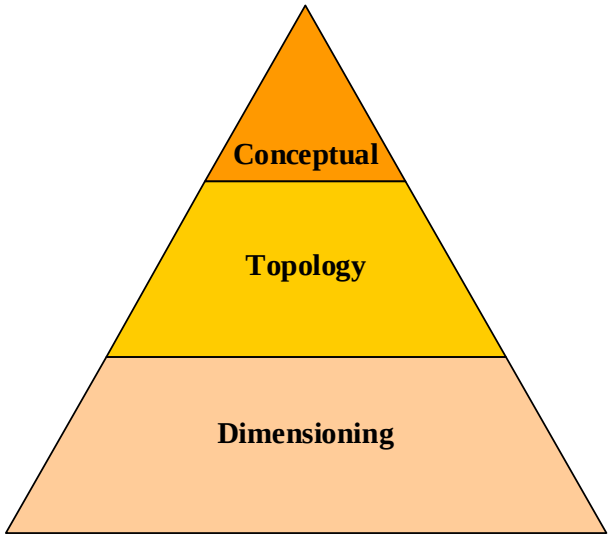

Figure 3-1. Design levels.

The conceptual design determines in this case the wind farm functions, form and the basic structure. Here belongs the definition of more general aspects like the farm power, voltage level and farm components (for instance the turbine type). It was decided that the user would introduce these options manually. The topological design involves the placement of components and how they are connected. In this level it was chosen to work with rectangular layouts and parallel cable connections as previously shown in Figure 1-3. Finally, the dimensioning aspect refers to the size and measurable variables of the object. Here, the separation distance between the turbines is the variable to modify in order to find the minimum cost of energy. Thus, at this level will be located the tool optimization function.

Based on previous wind farm projects developed in the North Sea, some knowledge based engineering (*KBE*) rules were applied during the tool development. To further clarify what a *KBE* rule is, and how it reduces the design domain, the turbine separation distance is considered as an example. The minimum separation distance should be one rotor diameter to avoid blades to crash when turbines are yawing. In addition, since the wake models used are intended to describe far wake properties, at least 2 rotor diameters should be the minimum separation distance in order to have valid results. Some additional constraints

could be added, like the minimum separation distance that environment protection studies indicate necessary to allow birds flying through the turbines without being hit. Regarding the maximum separation distance, it is rare to find in current offshore wind farms, turbines separated more than 10 rotor diameters. This value could be considered as a top reference for the layout dimensions. Considering this layout dimension domain, tool simulations can consider a limited range of turbine separation values and therefore reduce the computation cost.

Additional rules may apply to some submarine cable properties and the dominant layout configuration. With this, the tool can produce more realistic solutions and utilize a reduced input variable domain.

The development of the tool includes a design process by itself and thus, a relevant design approach was followed. There are several theories in literature on the subject of product design. One of them is known as the "Basic design cycle" [16]. In this approach, the design process can be considered as a cycle with several feedback loops. Therefore, the final design is not necessarily found in a straight forward procedure, but after several attempts. In Figure 3-2, the different phases and their inter-relation are shown.

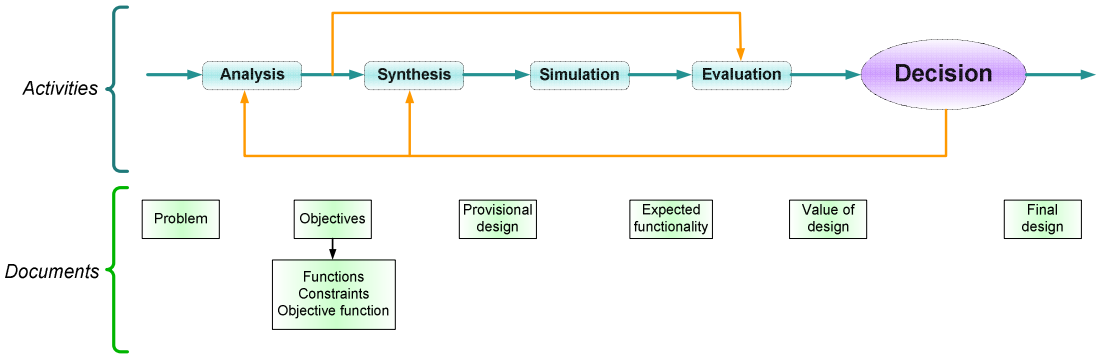

Figure 3-2. The basic design cycle.

In Figure 3-2, the upper section corresponds to activities accomplished during the development of the design tool. The lower boxes represent the documentation generated before or as product of the activities execution.

First, the problem the tool should solve was selected as the determination of an optimized layout for an offshore wind farm. The input variables, entered by the user, determine certain wind and site conditions, number and power of turbines, etc. The objective function was defined as the levelized production cost as function of the turbine separation distance.

The provisional design was a simplified tool version as explained later on in section 4.1. The expected behavior was to give a layout where the wake losses, electrical cable losses and costs are evaluated in order to produce a layout where the cost of energy is minimum. The value of the design was constantly checked by verifying the operability of the tool, as

will be detailed in chapter 5. In addition, some initial criteria the tool should meet are specified as follows:

1. The tool will have a modular structure where new or updated wake and cable models can be easily integrated.
2. The models can be based on mathematical functions or based on knowledge based engineering rules.
3. The tool should be clearly structured and widely commented in order to make it flexible to future modifications.
4. The constraints the tool may have should be clearly indicated.

The objective function for the design of the tool is to maximize the performance of the layout provided by the tool per minute of computation. Other integrated functions came from models that were proposed and already validated in previous studies. Together, these models constitute the mathematical structure of the tool which gathers all the input parameters (desires and constraints) to convert them into a solution.

The synthesis procedure combined all the separate ideas collected during the design specification, literature research and later on along the evaluation phase, into a description of the code as a whole. It was during this stage that most of the creativity and ideas came out to find a solution to the established problem.

A provisional design was formed by a modular code structure, where every part solves a specific function. It contains a main module which interconnected all the inputs and outputs of the smaller modules with specific functions. Together, these modules form the global transference function which converts the user desires into a solution.

The simulation phase in this case corresponds to the execution of the tool itself. This implies to constantly test the tool prototype. It was done after each tool extension in order check the tool behavior and properties. It helped to test the operability of the code and the suitability of the models for the desired purpose. The simulation output was compared with general results based on experience from current offshore wind farms.

3.3 Code evolution from a singular case study to a general wind farm

When deciding about what could be the best approach to follow in order to guarantee the development of an operable and reliable code, a specific-to-general methodology was chosen. It means that initially a minimalistic wind farm case formed by two turbines was the object of study. Also very basic wind conditions were considered, like single wind direction and single wind speed. The first tool version was able to calculate some basic wind farm characteristics like the energy yield and the energy cost. Afterwards, further improvements were done in order to describe in more detail the overall wind farm and site model. The different expansions can be grouped in the following main categories:

- Wind and site conditions
- Wake models
- Wake interaction
- Wind farm size
- Optimization function

Cable models have not been expanded since the implemented model, as described by Schoenmakers [12], already considers the Ohmic, dielectric and thermal losses. Therefore, in principle the model covered all the loss sources in electric cables.

It was necessary to determine what were the minimum necessary *performance parameters* or *functions* to consider. Examples of these parameters are the cable losses and turbine power output. Once they were defined, specific equations for each of them had to be determined. Some of them were based on models found in scientific literature, like the analytic wake models developed by Jensen (eq. 2-1) and Frandsen (eq. 2-6), presented in section 2.2. Initially, the models found in literature that were less difficult to implement were used. Other performance parameters were based on technical data published by manufacturers. In this group, Table 2-3 is a good example.

The *performance parameters* have an important relevance since they fix the solution for the objective function (in this case the cost of energy). Nevertheless, the designer can influence them only indirectly by assigning suitable values to a set of *design variable*. A *design variable* can be defined as any quantity or option directly under the control of the designer. For the present project, they include the voltage level, lifespan of the wind farm, number of turbines, model of turbines, etc.

Once a first tool version was achieved, it served as baseline for further step by step expansions to include more detailed characteristic of wind properties, turbine response to variable wind conditions, wake models and wake interaction. A description of the work done at this stage is described in the afterward chapter.

Chapter 4

Tool development

4.1 Introduction

Initially, a basic tool was developed in order to have an initial understanding of the main wind farm analysis variables. With this first experience, further expansions were added in order to make it useful for more general purposes. It means, the tool was able to include more details about the wind and wake characteristics and their interaction within wind farms. In this chapter, the development of the initial reduced tool and the subsequent additions are explained. The tool expansions have been cataloged in three main groups. The first group includes all the expansions related to wind characteristic and site conditions. The second group describes the main consequences of grouping wind turbines, like the wake interaction and impact over downstream turbines. At the end of the chapter, the different simulation modes are described. It will be seen that the tool has two main operating modes. One mode allows the user to have a comprehensive visualization of the levelized production cost as function of the wind farm layout dimensions. The second mode can be used to find the optimum layout dimensions at a shorter computation time.

4.2 Initial tool implementation for a reduced wind farm

Based on the state of art in offshore wind farms, the conceptual design level was predetermined to medium voltage alternating current (MVAC) interconnection cables at 33kV. Turbines were considered in fixed positions and the lifespan of the wind farm was taken as 20 years. Moreover, the wind speed was fixed at one single value and one single direction paralleled to the two turbines.

Only the dimensioning level was affected during the optimization routine. The separation distance between turbines was gradually modified back and forth. At some point, the reduction of wake losses (therefore increase of energy yield) compensated for the increase in cable losses and costs. Nonetheless, there were some initial constraints to take into account. For instance, the separation distance should not be shorter than 2 rotor diameters (***D***). There are two main reasons for previous constraint. First, the turbine yawing may cause the blades of different turbines to crash each other if separation is lower that 1 ***D***. In second place, the wake models used have been developed for the far wake region (2 ***D*** and beyond).

4.2.1 Prototype description

During the first phase of the design tool, one of the main interests was to get acquainted with the difficulty level of developing a working code, able to calculate the cost of energy and to optimize the layout dimensions for the case of a wind farm composed of two turbines. This simple initial problem helped to omit the consequences of different wind speeds, directions and the selection of wake combination methods.

The structure of the program is elaborated as detailed in Figure 4-1.

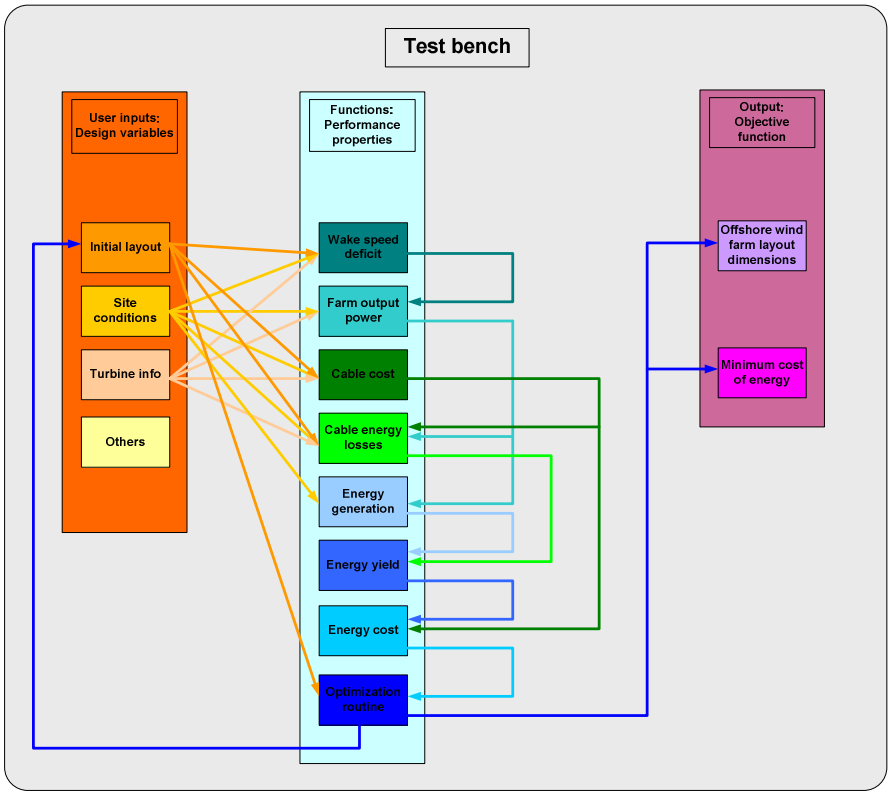

Figure 4-1. Design tool: modular scheme.

The “Test bench” is the module that acquires the user inputs, interconnects the other modules and displays the solution. The other modules are specific functions like the wake models or contain tabulated information like the turbine and cable properties.

The design tool uses existing models for the wake and cable losses and for the cable and other component costs. The optimization routine was implemented as numerical optimization of the objective function. Therefore, a trial and error approach was followed as explained later on in section 4.2.3.

The tool output is a function of parameters given by the user like the turbine power and some constraints like the maximum turbine separation (consequently the maximum wind farm area). These parameters constitute the design variables and are grouped inside the orange box in Figure 4-1. As can be appreciated, changes in them can result in different layout solutions. Further more, there are some parameters corresponding to outputs produced by the internal functions, like the cable losses and power output. They are grouped in the center light-blue box in Figure 4-1. These parameters are called performance properties and their values are function of the design variables.

The performance properties can set some constraints like the minimum cable cross section diameter. Additionally, the performance properties offer the chance to evaluate some important indexes when two or more properties are related in a proportion. For instance: the energy yield to losses ratio, the wind speed deficit to separation distance ratio, etc. The objective function can be derived as a combination of one or more of these performance indexes. For the present project, it has been selected the levelized production cost.

In order to further clarify how these parameters are categorized, the scheme of Figure 4-2 shows the wind farm components and their respective parameters. Here, the case of a cable has been described in more detail as an example.

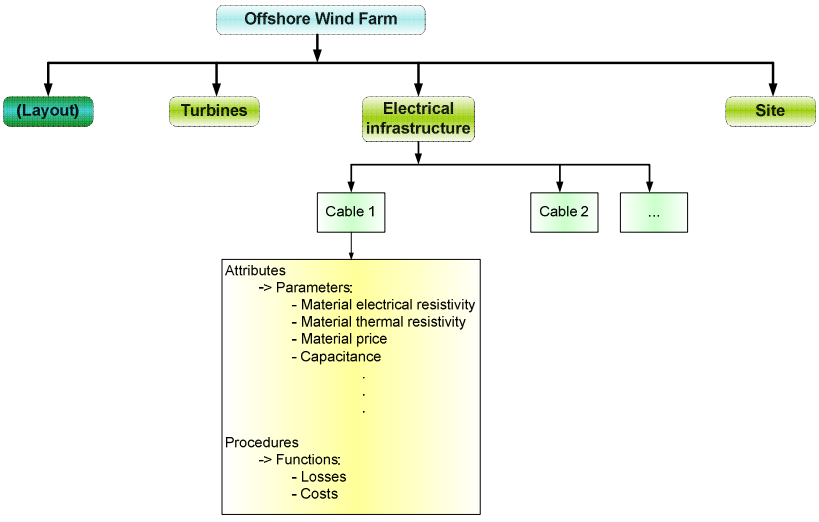

Figure 4-2. Wind farm component break-down.

The wind farm can be divided into several components (objects), which at the same time can be divided into further subcomponents. Each component has a set of attributes and procedures that determine their characteristics and the function they fulfil within the wind farm. The layout is a particular case since in one hand it is a property of the wind farm itself but in the other hand it can be seen as a component formed by all the wind turbines interconnected in a defined configuration.

4.2.2 Implemented wake, cable and LPC models

For the calculation of the wind speed deficit in a turbine wake, as well as the wake expansion diameter, the Jensen wake model described in section 2.2.1 was implemented. In regard to the electrical infrastructure, the cable cost and loss models presented in section 2.3 were integrated into the tool. Moreover, for the *LPC* calculation, the model described in section 2.4 was included.

4.2.3 Optimization routine

The execution of the tool is a sequential computation of functions in order to calculate the objective function (cost of energy). The optimization routine includes a feedback loop which modifies only one parameter of the layout properties in order to recalculate the cost of energy. The two results are compared and the procedure repeats itself until a minimum cost of energy is found. The output is the minimum cost of energy and the corresponding separation distance between aligned turbines with respect to the wind direction.

For a wind farm of two turbines as shown in Figure 4-3, the optimization routine extends or reduces the separation distance ***sr*** until reaches an optimum point were the cost of energy is minimum. It is done by taking into account the energy production, wake losses, electrical cable losses, fixed farm costs and variable cables costs.

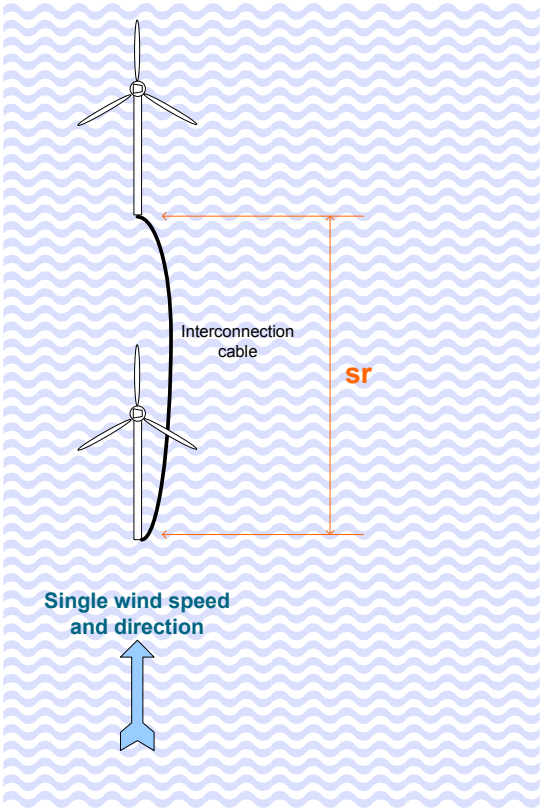

Figure 4-3. Offshore wind farm sketch.

The optimization routine is in charge of finding the minimum value for the cost of energy given a set of input variables. The logical functioning is summarized in the flow chart presented in Figure 4-4.

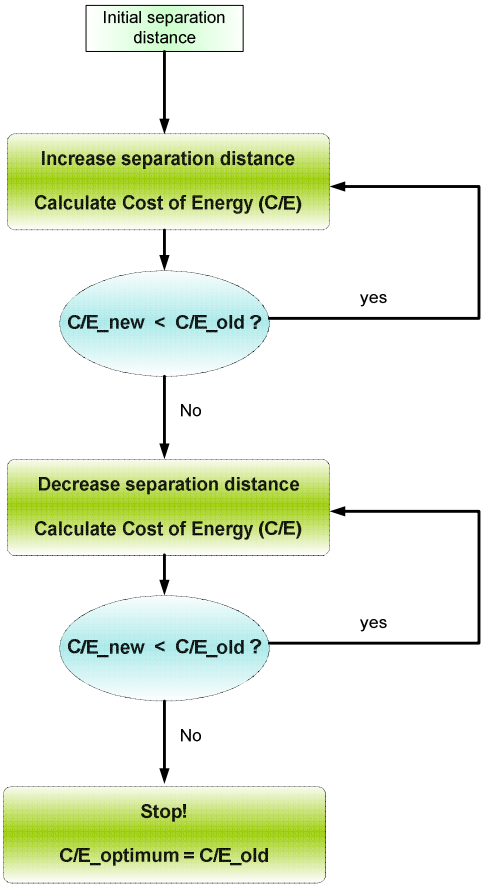

Figure 4-4. Optimization routine flow chart.

The logical operation of the optimization routine exposed above is based on the supposition that there exists only one minimum point in the curve cost of energy versus separation distance. A graphical view in Figure 4-5 helps to further clarify this reasoning.

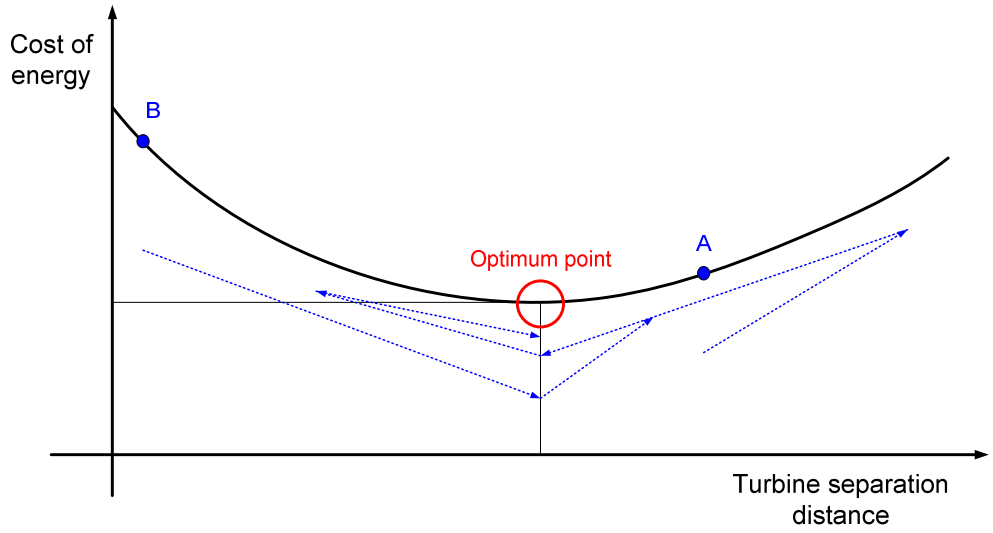

Figure 4-5. Cost of energy as function of turbine separation distance.

The initial separation distance (selected by the user) may result to be located before or after the optimum value. The cost of energy is calculated for this first point to conform the blue dot on the curve indicated by either ***A*** or ***B***. The optimization routine starts incrementing the separation distance by a determined step size and recalculates the new cost of energy. From point ***A***, since the new cost will be higher, the separation distance is consequently decreased in the next step and the process is repeated several times as long as the cost of energy is being reduced. Once the cost becomes higher again, it indicates the minimum point has been crossed and therefore returns back one step. This path is indicated by the doted blue lines. If the starting point is ***B***, after the first cycle the cost of energy is found to be smaller; then the distance is increase continuously until it becomes higher at some point. That is the point where the two blue lines join together. The rest of the routine is executed as explained previously for the ***A*** case.

4.2.4 Code functioning and result displaying

This first tool version is a Matlab code divided in different M-files. Each file contains a function which corresponds to the different modules of the project. The tool includes the option to run in TEST mode which means that no optimization routine is used but instead a sweep of row separation distance is executed. The user can select the minimum and maximum separation limits as well as the incremental step size. In each iteration, the program memorizes several parameters (including the cost of energy). During the execution, the program is able to plot and display several intermediate results. Also, at the sweep end the program can graph the overall behavior of several curves as a function of the separation distance. Some examples of the variables to plot are:

1) Annual energy generation (includes aerodynamic losses but not electric losses)

2) Total cable losses
3) Annual energy yield = 1) – 2)
4) Total cable costs
5) Levelized production cost

By inspecting the resultant plots and display messages, it is feasible to understand better the code functioning. For example, it is possible to see in which order are calculated the different variables, what is the execution sequence of the different internal loops and when and how often the different modules are called. Also, the curve shapes indicate the variable behavior. For instance, the cable costs depend of its length; therefore it is expected to see the curve "Cable Cost" as function of the cable length with a constant positive slope. Moreover, the plots help to verify the results against possible errors by comparing the graphs with expected results based on engineering knowledge. Some of these features are further detailed in section 4.6.

4.3 Wind and site related tool extensions

Once the development of the first tool version was satisfactorily achieved, the original assumptions started to be gradually modified. Firstly, characteristics related to the wind properties were improved in order to reflect more realistic environmental conditions for the wind farm location.

For the initial improvement about wind condition properties, the simple case of a two turbine wind farm was still used. Initially, the Weibull wind speed distribution was included replacing the single wind speed assumption. After that, a wind rose was also integrated allowing multiple wind direction. As a consequence of this last expansion, the calculation of partial wake incidence also started to be accounted.

4.3.1 Weibull distribution

The first extension allows the description of site properties by a Weibull wind speed-frequency distribution. For this, the user has to introduce the global shape and scale parameters. The tool is then able to calculate the wind farm annual energy yield based on the site conditions. Figure 4-6 illustrates the idea of this tool extension.

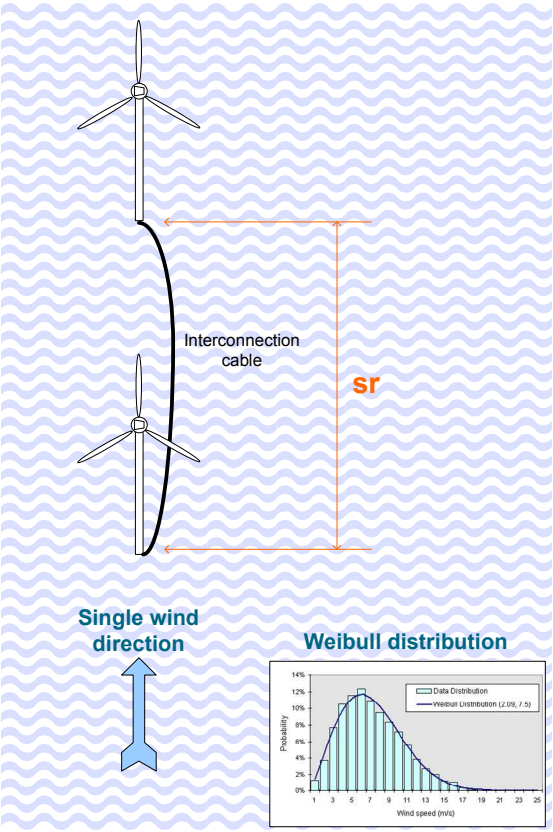

Figure 4-6. Characterization of wind speed by a Weibull distribution.

Since not a unique wind speed is considered anymore, the influence of low wind speeds and high wind speeds on the deficit behind the first turbine affects in opposite directions over the optimum separation distance ***sr***. Therefore, a different value is expected from the previous case when a unique wind speed was considered.

4.3.2 Wind rose

The next extension of the design tool was the inclusion of a wind rose to characterize a given site. The user can select the number of sectors in which the wind rose is divided (i.e. 4, 8, 16… up to 40 sectors). The characterization of each sector is independent and can be defined by different Weibull distribution shape and scale parameters. With this approach, the tool allows the use of detailed wind site data. Figure 4-7 shows the concept of this tool extension.

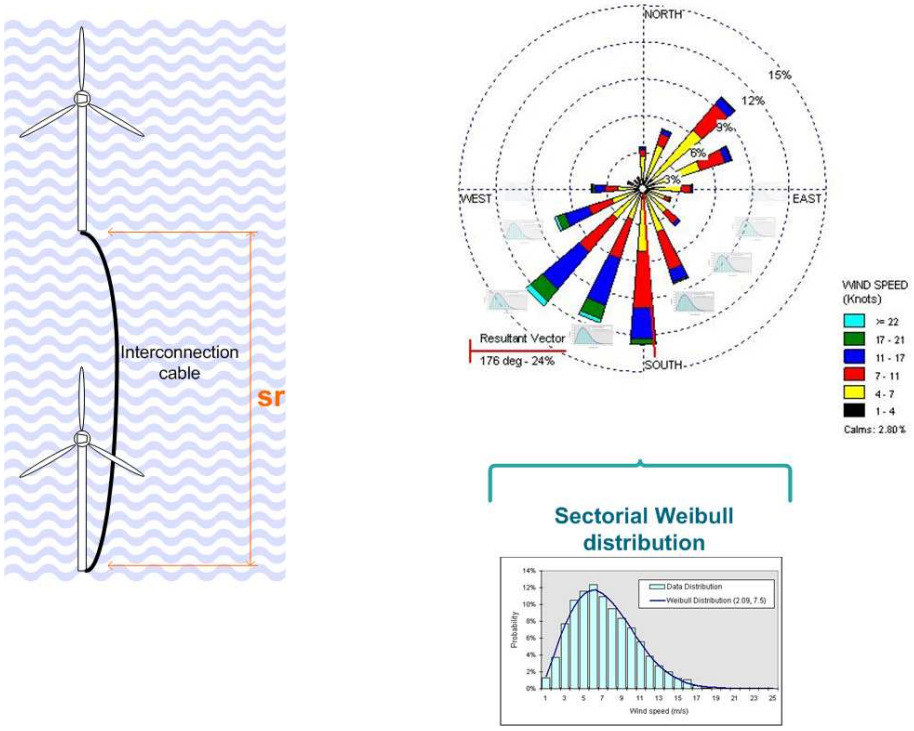

Figure 4-7. Characterization of wind speed by a wind rose and sectorial Weibull distribution.

The effect of considering different wind directions influences again the optimum separation distance. Now the wind is not always aligned with the column of turbines. Therefore, the wake of one turbine does not reach the other turbine all the time. Actually there can be cases of total, partial or null wake incidence as will be explained in section 4.3.3.

Additionally, depending on the wind rose distribution, the predominant wind direction as well as the highest wind speeds may or may not be align with the turbine column. Consequently, different optimum values for ***sr*** may be obtained from different site conditions.

4.3.3 Effect of variable wind direction over wake incidence

When variable wind direction is considered, upstream wakes can affect partially or totally over downstream turbines. It depends on several wind farm properties like the number for turbines, the layout and the separation distance between turbines. Since wind can come from any direction, there is always this kind of interaction and thus it is fundamental to consider it within the tool. Figure 4-8 shows the distinction when wake incidence is total, partial or null.

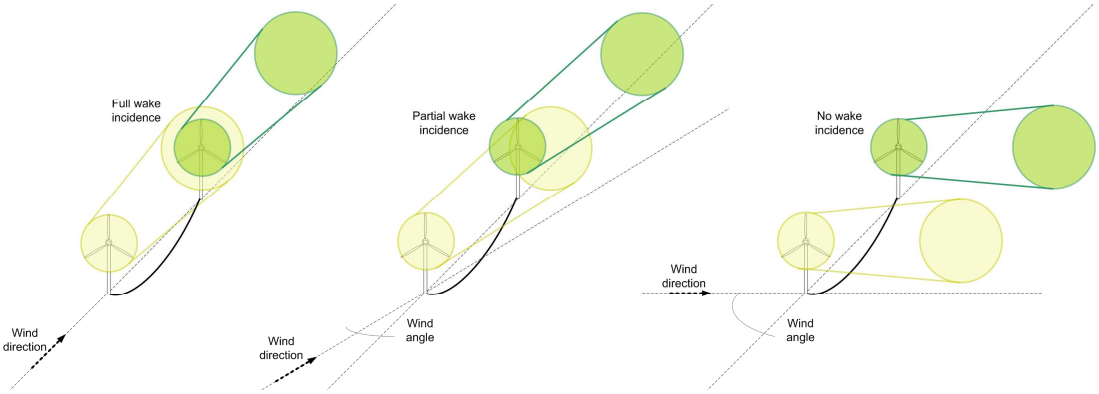

a) Full wake incidence **b) Partial incidence** **c) Null wake incidence**

Figure 4-8. Wake incidence over turbine rotor plane.

When there is null wake incidence, the wind speed reaching the turbine at the hub height is taken as the free flow wind speed:

$$U_T = U_0 \qquad \text{eq. 4-1}$$

where:

U_T.....is the average wind speed impacting the turbine at hub height.

U_0.....is the average free flow wind speed at hub height.

In the case a wind turbine experiences full wake incidence from an upstream turbine, the wind speed is taken as the free flow wind speed minus the wind speed deficit produced by the first turbine. The value of this deficit will depend on the selected wake model:

$$\begin{aligned} U_{T2} &= U_{T1} - dV_1 \\ &= U_0 - dV_1 \end{aligned} \qquad \text{eq. 4-2}$$

where:

U_{T2}.....is the average wind speed impacting the turbine-2 at hub height.

U_{T1}.....is the average wind speed impacting the turbine-1 at hub height.

dV_1 .....is the average wake wind speed deficit produced by turbine-1.

Based on the work presented by Attias [17], when there is partial wake incidence, the wind speed at the rotor plane is calculated as a weighted average of the free flow wind speed and the upstream turbine's wake wind speed:

$$U_{T2} = (U_{T1} - dV_1)\frac{A_{T2\_wake}}{A_{T2\_total}} + U_0\frac{A_{T2\_free}}{A_{T2\_total}} \qquad \text{eq. 4-3}$$

where:

A_{T2_wake} .....is the turbine-2 rotor area with incidence from turbine-1 wake.

A_{T2_free}.....is the turbine-2 rotor area without incidence from turbine-1 wake.

A_{T2_total} .....is the total turbine-2 rotor area.

The weighting factors are the proportion of the rotor area with and without wake incidence, as shown in Figure 4-9.

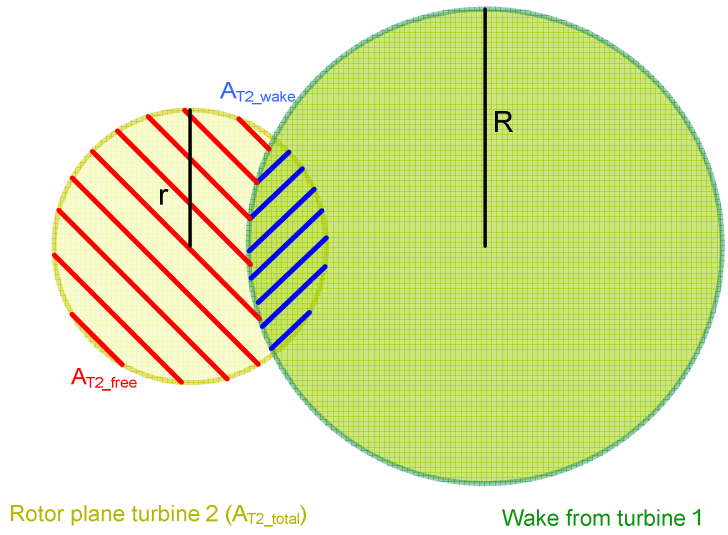

Figure 4-9. Partial wake incidence.

When two or more wakes interact and impact another turbine, it is necessary to select a wake combination method as will be explained in section 4.4.4.

4.3.4 Additional wake models

Since the interaction turbine-wake is a fundamental aspect of the aerodynamic efficiency of the wind farm, it is fundamental for the present tool to count with optional models to calculate the wake wind speed deficit and wake expansion diameter.

From the wake models found in the literature, the ones more commonly used that also have been validated in several published studies, were implemented into the code. They are:

1) Jensen wake model (already included in the firs tool version)
2) Frandsen wake model
3) Ainslie wake model

With this feature, the tool has the capacity to calculate the wind speed deficit and wake expansion behind each turbine using a wake model selected by the user. In addition, the user can select to plot a wake model benchmark in order to compare the output of these different models.

4.4 Layout related tool extensions

4.4.1 Multiple number of turbines in a line

After completing the implementation of most of the features possible for the simplest case of a two turbine wind farm and achieving satisfactory performance, the tool was extended to work with any number of wind turbines equal or higher than two. As a first step, a layout configuration of single row has been considered. The turbine location is shown in Figure 4-10.

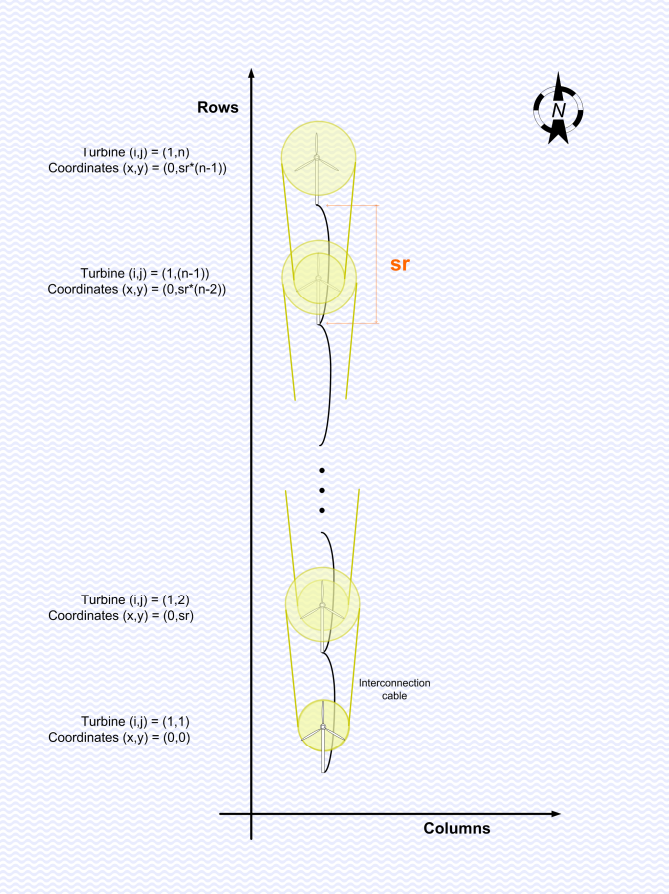

Figure 4-10. Unique column layout for *n* turbines. Wakes shown when wind coming from south.

The most important consequence of this tool extension was the necessity to include a method for wake wind speed deficit combination. From Figure 4-10, it is possible to see the northern turbine is affected by all the turbine wakes when wind is coming from south direction. In section 4.4.2, the method to analyze these cases is explained.

4.4.2 Computation method for combined wind speed deficits

In wind farms, turbines are close to each other and therefore it is very likely that wakes from two or more turbines overlap. The number of wakes interacting depends on the layout configuration and the wind direction. Figure 4-11 shows an example of ***n*** wind turbines aligned parallel to the wind direction.

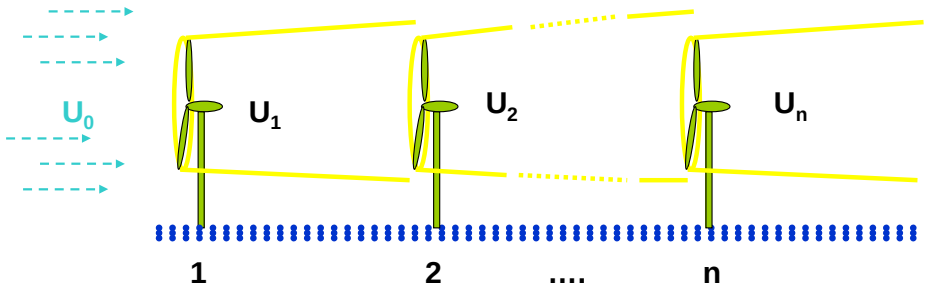

Figure 4-11. Turbine wakes overlapping.

When two or more wakes overlap, Katic [6] indicates the kinetic energy deficit of a mixed wake is assumed to be equal to the sum of the energy deficits for each wake at the calculated downwind position. In the simple case of two overlapping wakes, the velocity deficit behind the second turbine is found to be:

$$\left(1-\frac{V}{U}\right)^2=\left(1-\frac{V_1}{U}\right)^2+\left(1-\frac{V_2}{U}\right)^2 \qquad \text{eq. 4-4}$$

Here, V_1 and V_2 are the original wake velocities. The velocity deficits are squared and then the total velocity deficit in the wake from a line of turbines will quickly reach an equilibrium level, usually after 3 to 4 turbines. The equilibrium velocity depends on the turbine thrust coefficient, which at the same time depends on the wind speed. For this reason, the equilibrium velocity is conditioned by the free flow wind speed. A scheme of the two turbine case from eq. 4-4 is presented in Figure 4-12.

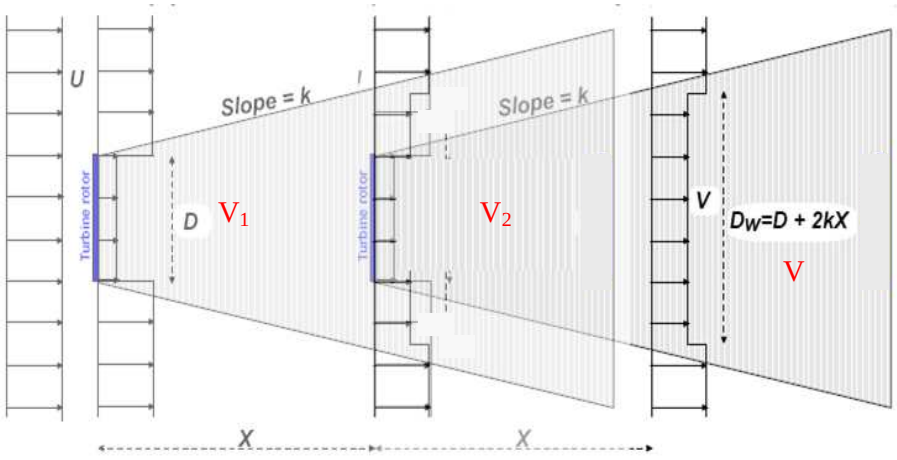

Figure 4-12. Wake superposition. Modified image, based on [6].

Apart from the free flow wind speed, the equilibrium wind speed for aligned turbines is linked to the turbine separation distance by the following formula deduced by Jensen:

$$\frac{V_\infty}{U} = 1 - \frac{2x}{1-x} \quad ; \quad x \equiv \frac{1}{3}\left(\frac{r_0}{r_0 + kx_0}\right)^2 \qquad \textbf{eq. 4-5}$$

When the separation distance (equal from turbine to turbine) is for example 7 rotor diameters, and $\boldsymbol{k}$ is taken as 0.04 for offshore conditions, the result is that $\boldsymbol{V}_\infty = \boldsymbol{U} * 0.68$.

Larsen [7] gives an expression for the asymptotic, relative flow speed behind several turbines whose wakes are superimposed. This is the result of his *Regime 1* analysis. Some important parameters are identified in Figure 4-13 which details two given wind turbines belonging to a long wind turbine row inside a wind farm.

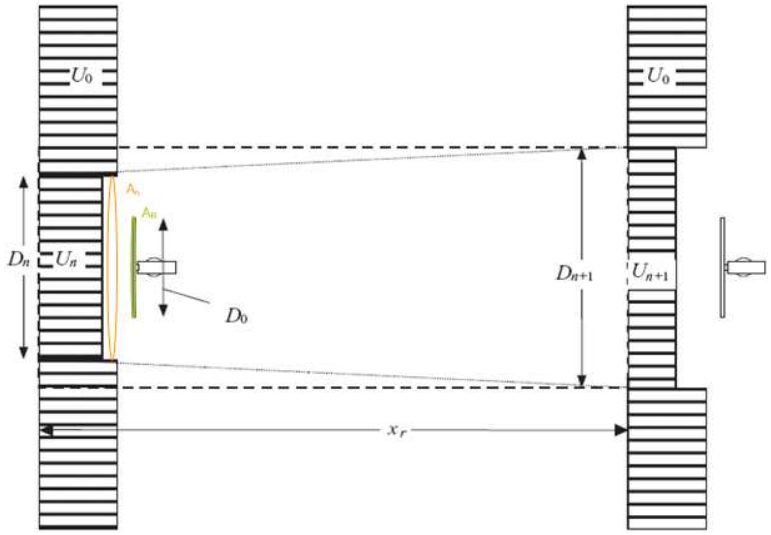

Figure 4-13. Flow between two wind turbines.

The wind speed ratio $\boldsymbol{c = U/U_0}$ is obtained for turbine $\boldsymbol{n+1}$ located after turbine $\boldsymbol{n}$. The result is given by:

$$c_{n+1} = 1 - \left(\frac{A_n}{A_{n+1}}(1 - c_n) + \frac{1}{2}\frac{A_R}{A_{n+1}} C_T c_n\right) \qquad \textbf{eq. 4-6}$$

where:

$\boldsymbol{A_n}$ .....is the area of the incoming wake with diameter $\boldsymbol{D_n}$, in front of each unit.

$\boldsymbol{A_R}$ .....is the rotor area.

C_T .....is the initial wake deficit (from first turbine in the undisturbed wind).

The author assumes that for an infinitely large number of wind turbines, there must be an asymptotic non-zero wake flow speed c_w. The result obtained is expressed by next relation:

$$c_w = \frac{\alpha}{\alpha + \frac{1}{2}\frac{C_T}{s_r}} \qquad \text{eq. 4-7}$$

where:

α .....is the decay constant.

s_r.....is the separation distance between turbines as multiple of rotor diameters.

In addition, Mosetti [18] also points out that the kinetic energy deficit of a mixed wake is equal to the sum of the individual energy deficits. Based on Mosetti, Grady [19] gives an expression to calculate the wind speed behind ***n*** wind turbines:

$$U_n = U_0\left[1 - \sqrt{\sum_{i=1}^{n}\left(1 - \frac{U_i}{U_0}\right)^2}\right] \qquad \text{eq. 4-8}$$

where:

U_n.....is the wind speed behind the ***n*** wind turbine.

U_0.....is the free flow wind speed.

U_i.....is the wind speed behind the ***i*** wind turbine.

An explanation of this relation can be done using the same example of Figure 4-11, turbine-1 produces wind speed deficit over turbines 2, 3, 4…n. Then, the velocity faced by turbine-2 is the free flow velocity minus the deficit of turbine-1. At the same time, turbine-2 produces a wind speed deficit over turbines 3, 4…n. Then turbine-3 faces a wind velocity equal to the free flow velocity minus the root of the sum of squares of velocity deficits produced by turbine-1 and turbine-2, at the location of turbine-3. The process repeats in the same way for the rest of turbines.

The model presented in eq. 4-8 is the combination method implemented in the tool. However, an additional modification is still necessary, as will be explained in section 4.4.4. In chapter 5, results from a test are presented to verify and further clarify the functioning of this model.

4.4.3 Multiple number of turbine lines in a farm

The next step in the tool development was to expand the capacity to analyze wind farms with turbines distributed in multiple rows and columns in a rectangular layout, being the square layouts a particular case. An example of a rectangular layout and the scheme to number the turbines is shown in Figure 4-14.

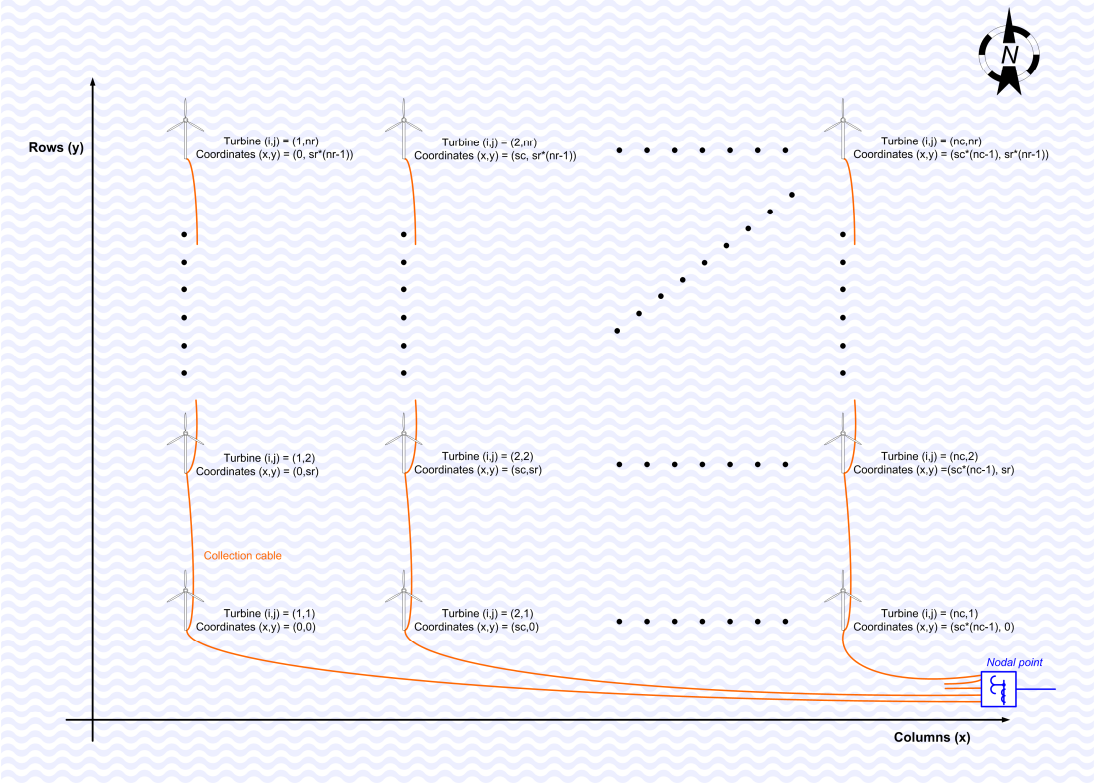

Figure 4-14. Wind turbine coordinates. nc (nr) = number column (row), sc (sr) = column (row) separation.

Now that layouts are two dimensional, wakes coming from different turbines can overlap and impact other turbines downstream. The number of wakes interacting and the incidence magnitude depend on the wind direction and layout dimensions. It was therefore necessary to include a method to calculate this multiple wake interaction. It is presented in section 4.4.4.

4.4.4 Wake and turbine interaction within the wind farm

With this new extension, the tool became able to analyze the wake interaction between all turbines for every wind direction indicated by the wind rose module. This means it searches for the wake incidence over all the possible turbines downstream and calculates

the (partial) wake incidence affecting each turbine. As an example, in Figure 4-15 a 3x3 wind farm is shown in order to illustrate that for a determined wind direction, the wake produced by the first turbine have partial incidence over three turbines downstream. The same analysis is done for every turbine at every wind direction.

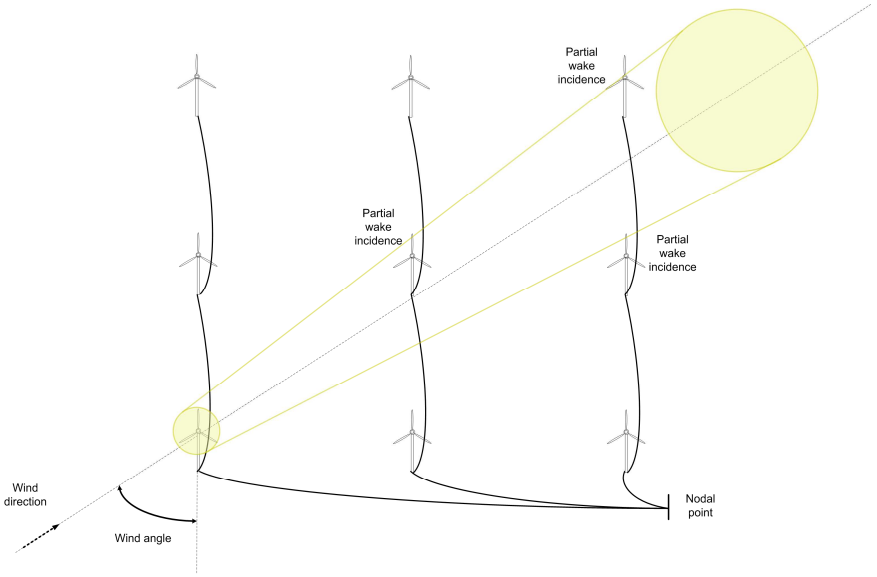

Figure 4-15. Determination of wake incidence over all downstream turbines.

The previous feature is very important since the wake incidence changes constantly depending on the farm dimensions. Also the interaction between wakes is affected by the turbine positioning, as shown in Figure 4-16.

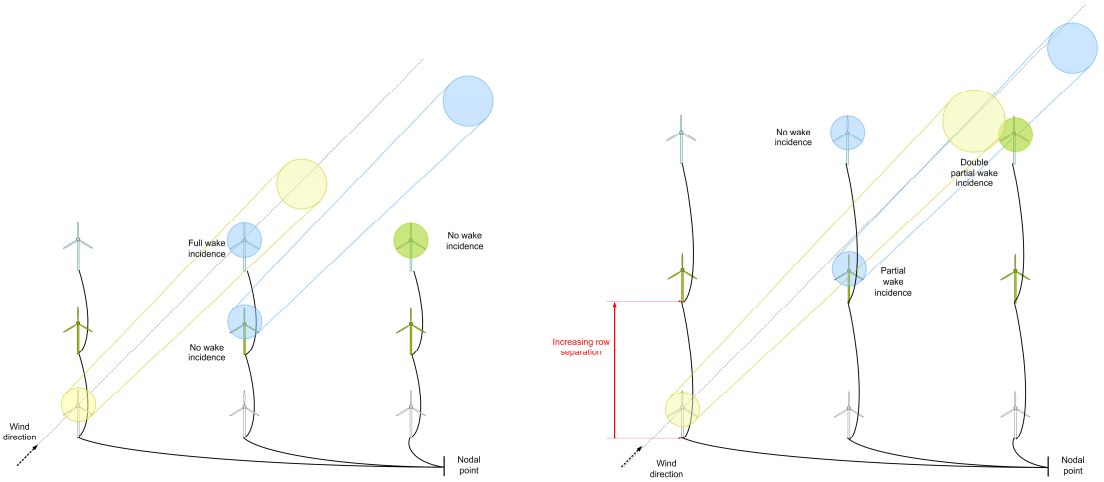

a) Initial dimensions **b) Increasing row separation distance**

Figure 4-16. Wake incidence and interaction over all downstream turbines.

Now that the effects of partial wake incidence and the wake combination method have been explained, it is necessary to define how to combine both when analyzing the wake interaction in a large wind farms.

For every turbine, it is determine the wake incidence and the wake speed deficit over every turbine located downstream according to a given wind direction. This data is recorded into a memory. Then, when calculating the effective wind at each wind turbine, the previous (full, partial, null) wake incidences from all the ***n*** upstream turbines are acquired from the memory and used to calculated the effective wind speed using eq. 4-9.

$$U_n = U_0 \left[1 - \sqrt{\sum_{i=1}^{n} \left(\left(1 - \frac{U_i}{U_0} \right) \cdot \frac{A_{T\_wake\_i}}{A_{T\_total}} \right)^2} \right] \qquad \textbf{eq. 4-9}$$

where:

$\boldsymbol{U_n}$ .....is the effective wind speed seen by the current turbine.

$\boldsymbol{A_{T\_wake\_i}}$.....is the current turbine rotor area with incidence from turbine-***i*** wake.

$\boldsymbol{A_{T\_total}}$ .....is the current turbine total rotor area.

With the aim to illustrate effect of the combination method, a test was run for four V80 turbines in a row, separated 7 rotor diameters, with wind parallel to them at speed of 7 m/s. The result is shown in Figure 4-17.

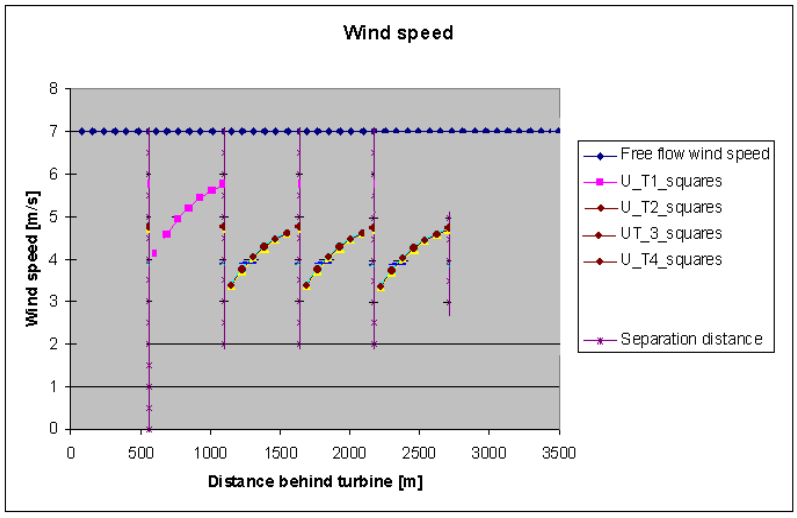

Figure 4-17. Wake combination (root of the sum of squares). Test of four turbines in a row.

Figure 4-17 shows that by using the root of squares combination method, the deficit for the second and other downstream turbines have the same magnitude and the lower and upper limits do not change.

4.5 Simulation modes

The tool has two modes to run wind farm simulations. One is the separation sweep mode and the second is the optimization mode. Their main characteristics are described in section 4.5.1 and section 4.5.2.

4.5.1 Separation distance sweep mode

The tool includes the option to run in separation distance sweep mode which means that no optimization routine is used but instead a sweep of column and row separation distance is executed. The user can select the minimum and maximum separation limits as well as the incremental step size. At the sweep end, it is possible to graph the overall behavior of several curves as a function of the separation distance.

Since computing time plays an important role when using a tool to support the wind farm design process, the user is allowed to adjust some variables in order to modify the precision and velocity of the calculations. They are:

- Initial separation distance [D]: Since some constraints can be based on user knowledge or physical limitations, a minimum separation distance between the turbines can be selected. Units in rotor diameters.
- Delta [D]: It is the size of incremental steps of the separation distance when performing the simulation sweep. Units in rotor diameters.
- Final separation distance [D]: It is the maximum separation distance possible between turbines. With this feature it is possible to delimit the maximum area to be covered by the wind farm. Units in rotor diameters.
- Resolution [m/s]: It is the incremental steps of wind speed when using a Weibull distribution and the turbine power curve to calculated the produced annual energy yield. Units in meter per second.

4.5.2 Optimization mode

Despite an optimization routine was developed for the first tool version as explained in section 4.2.3, it is not the purpose of this project to implement a more elaborated optimization routine for the final tool version. Instead, the optimization mode means that an optimization function included in Matlab is used to find the minimum *LPC*. Optimization methodologies can be themselves a topic for a thesis work. Table 4-1 details the optimization tools included in Matlab and a brief description.

Table 4-1. Optimization tools included in Matlab.

Minimization functions	Description
bintprog	Solve binary integer programming problems
fgoalattain	Solve multiobjective goal attainment problems
fminbnd	Find minimum of single-variable function on fixed interval
fmincon	Find minimum of constrained nonlinear multivariable function
fminimax	Solve minimax constraint problem
fminsearch	Find minimum of unconstrained multivariable function using derivative-free method
fminunc	Find minimum of unconstrained multivariable function
fseminf	Find minimum of semi-infinitely constrained multivariable nonlinear function
ktrlink	Find minimum of constrained or unconstrained nonlinear multivariable function using KNITRO third-party libraries
linprog	Solve linear programming problems
quadprog	Solve quadratic programming problems

From the list above, the only two suitable functions are *fmincon* and *ktrlink*. From these two, *fmincon* has been selected since it adapts to the problem requirements listed as follows:

- The optimization aim is to find the minimum value of the objective function.
- The objective function output is a scalar which is the *LPC*.
- The objective function is not linear.
- The objective function has a vector input, composed by the column and row separation distances. These are the design variables.
- The design variables have constraints (minimum and maximum separation distance).
- Additional parameters should be possible to be passed to the objective function (number of turbines, voltage level, etc.).

The function *fmincon* finds the minimum value of constrained nonlinear multivariable objective function. According to Matlab help manual [20], it finds the minimum of a problem specified by:

$$\min_x f(x) \text{ such that } \begin{cases} c(x) \le 0 \\ ceq(x) = 0 \\ A \cdot x \le b \\ Aeq \cdot x = beq \\ lb \le x \le ub, \end{cases} \qquad \textbf{eq. 4-10}$$

where:

x .....is the design variable vector.

lb, ub .....are vectors containing the design variable lower and upper limits.

A, Aeq .....are matrices used to establish the linear constraints.

b, beq .....are vectors.

c(x) .....is the inequality constraint nonlinear function that returns a vector.

ceq(x) .....is the equality constraint nonlinear function that returns a vector.

f(x) .....is a nonlinear function that returns a scalar.

Depending on the objective and constraint function definitions, one or several optimization algorithms can be used. *Fmincon* automatically selects one of three possible algorithms: Trust-region-reflective, Active-set or Interior-point. It is out of scope for this thesis to describe the algorithms in more detail. Whether more information is of interest

for the reader, it is advisable to look into the Matlab help [20]. Extensive explanation for these algorithms is included.

With the implementation of the capacities described in this chapter, the tool is able to analyze wind farms of any size in rectangular layouts. It is important then to verify the correct tool functioning. This work is presented in Chapter 5.

During the tool development and functionality verification, several important lessons were learnt. Some of them can be of interest for general designers and some others are more focused on wind energy aspects. They are further described in Chapter 5.

4.6 Analysis and debugging features

With the purpose to facilitate the user the result visualization, the tool allows plotting additional figures. Some of these features are presented in following subsections.

4.6.1 LPC distribution

It is important to have a general overview of the *LPC* dependency on the layout dimensions. In Figure 4-18 a) is combined the levelized production cost surface with a black triangle which indicates the location of the row and column separation combination that gives the minimum *LPC*. Also, the user can choose to view a two dimensional representation of the *LPC* as shown in Figure 4-18 b).

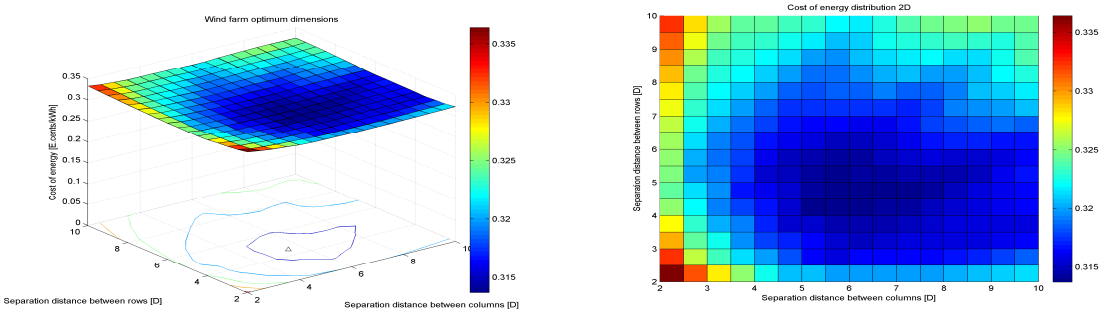

a) Optimum dimensions indicated by a black triangle at floor plane **b) Cost of energy in a 2-D view**

Figure 4-18. LPC representations.

Previous figure describe the overall wind farm. Nevertheless, individual turbine contribution to the annual energy yield can also be displayed as shown in next section.

4.6.2 Turbine energy yield

Because the turbines face different wake incidence depending of where they are located within the layout, it is also important to have a view of the annual energy contribution per turbine. In Figure 4-19, an example of 9 turbines in rectangular layout is shown.

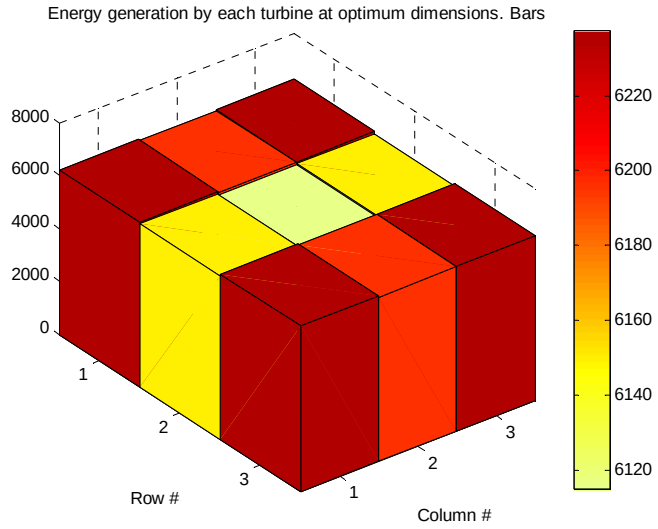

Figure 4-19. Annual energy generation per turbine.

In previous figure, soft colors represent lower energy contribution while darker color indicates higher energy contribution. It is important to notice that peripheral turbines contribute with more energy because they have less wakes incidence, with null incidence at certain wind directions. Inner turbines have wake incidence from several wind directions.

4.6.3 Layout aerial view

Layout plotting is a feature integrated in the tool that allows observing a wind farm "aerial view". Before running the simulation, the user can select an initial guess of what could be the optimum layout dimensions. This is a necessary input if the tool is running in optimization mode, as is explained ahead in section 4.5. Once the optimum dimensions have been calculated, the final result is plotted together wit the initial guess. An example for a rectangular wind farm of 9 turbines is shown in Figure 4-20.

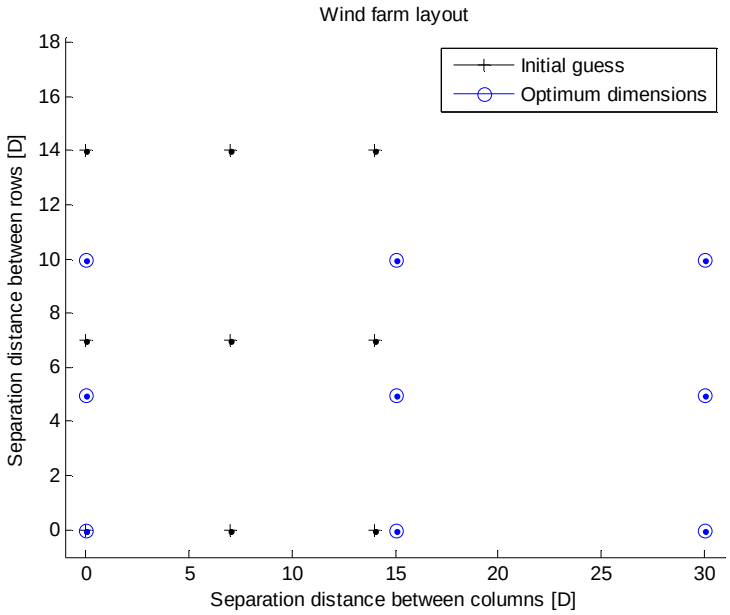

Figure 4-20. Wind farm layout aerial view.

Previous graph helps the user to compare a possible knowledge based presumption with the software calculated optimum dimensions.

4.6.4 Wind speed distribution and wind rose

As explained in Chapter 3, the tool progressed from considering very simple wind conditions to more detailed wind properties. At its final stage, the tool can consider site conditions given by a wind rose of any number of sectors in a succession of four (i.e. 4, 8, 12, 16…). An example is given for the Horns Rev site conditions given by Bot [26]. Table 4-2 indicates the Weibull distribution scale and shape parameters for each of the 12 sectors in which the wind rose has been divided. Also the wind direction frequency is included.

Table 4-2. Wind site conditions at Horns Rev. Based on [26].

Angle [°]	Frequency [%]	A	k
0	4.7	8.84	1.97
30	3.6	6.98	1.93
60	8.8	7.88	1.99
90	7.1	8.63	2.26
120	6.1	8.88	2.25
150	11.1	8.38	2.1
180	5.9	9.54	1.94
210	5.9	10.04	2.08
240	15.7	10.39	2.19
270	9.4	10.79	2.17
300	6.7	11.09	2.23
330	14.8	10.99	2.2

Using the information from Table 4-2, the tool offers the option to plot the wind conditions in a Weibull speed distribution graph divided by the number of sectors, as shown in Figure 4-21.

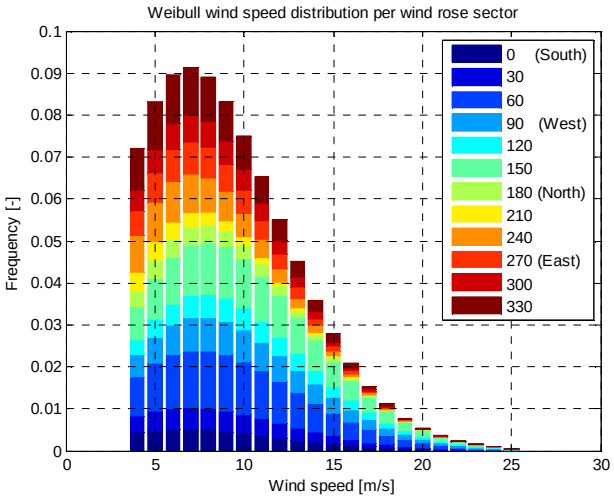

Figure 4-21. Cumulative frequency over all sectors.

Another manner to visualize the wind information displayed previously is to plot a sectorial graph as shown in Figure 4-22. Here, wind direction frequency is indicated by the length of the bars. The wind speed for each sector is divided in ranges. The length of each range indicates its frequency. The wind rose formed offers an easy way to visualize the general wind conditions at the selected site.

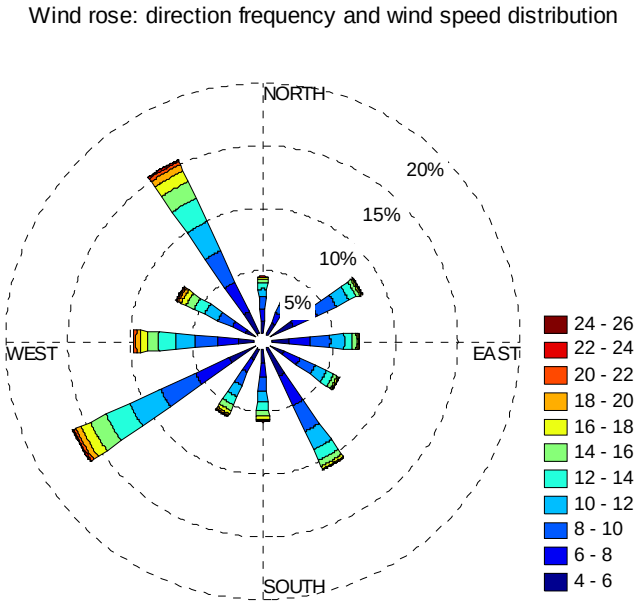

Figure 4-22. Wind rose: direction frequency and wind speed distribution.

Optionally, the sectorial wind direction frequency can be plotted separately as in Figure 4-23.

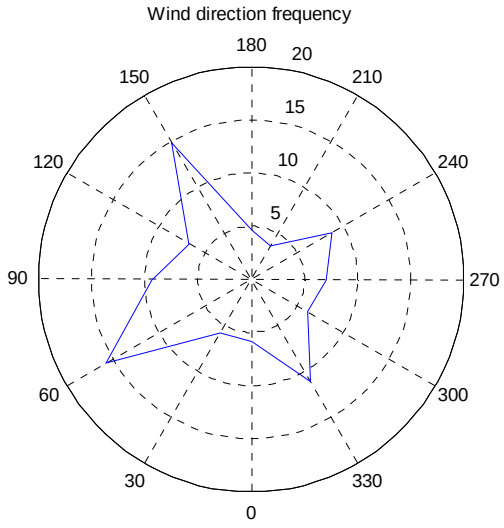

Figure 4-23. Wind direction frequency.

Some other general and code debugging features are explained in section 4.6.5.

4.6.5 Other features

The tool presents a summary of the results in the command screen as shown by Figure 4-24. Some of the basic information displayed includes the energy generation, cable losses, energy yield, fixed farm costs, *LPC*, and the turbine separation distance at the optimum point. Also the time required to run the simulation is displayed.

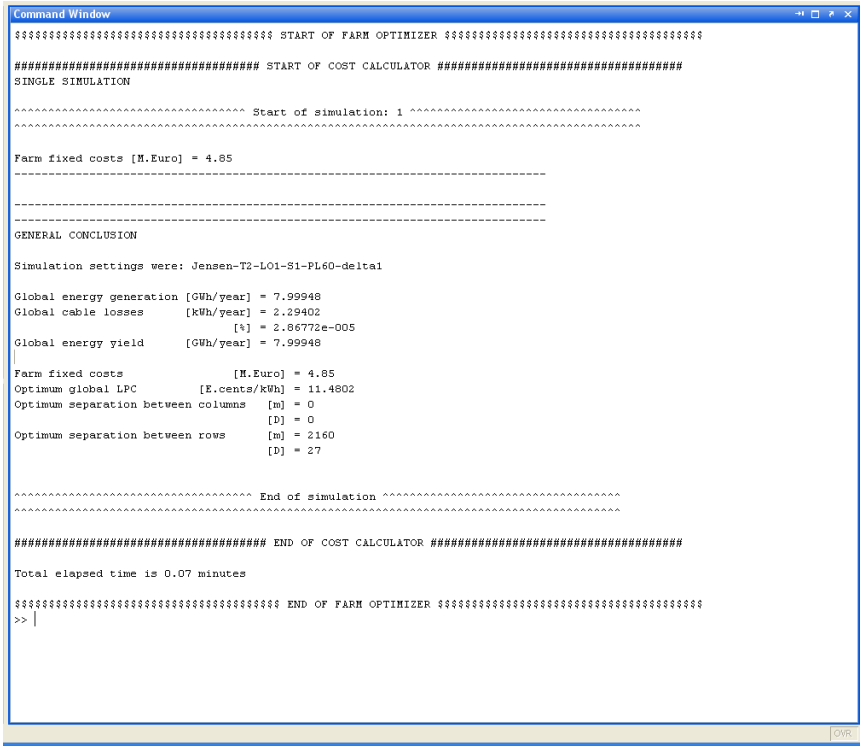

Figure 4-24. Display of results on command screen.

Several other debugging plots can be done in order to observe the behavior of the tool and assure proper results and inputs. For instance, some intermediate calculation values like the turbine power and thrust coefficient curves, the Weibull wind speed distribution for every sector (and global), the percentage of wake incidence, the wake diameter and speed deficit for selected turbines can be plotted.

Besides, the tool can show on the command screen up to seven different hierarchy levels of result displays. This means, during the computation process, from general overall results, to much more detailed step by step calculation results can be displayed. The user can select the number of display levels to use, since as trade off, they slow down

considerably the computation velocity. If desired, all the displayed information can be saved in a text file for logging and debugging purposes.

The user can choose to save the plotted pictures in separate image files. In order to avoid confusions, a standard name system has been adopted. As example, the name of one of previous figures is given below:

August-20-2009_ 1-02AM Turbine_power_deficit Jensen-T8-LO1-S32-PL7-delta0.5- ST1.png

The date and time when the simulation started is included. This helps to avoid identical names for different simulations. Next is the plot name and the wake model used; T8 means (8) turbines; LO1 means (1) rotor diameters as lower separation limit between turbines; S32 means (32) sectors in the wind rose, PL7 means (7) rotor diameters as maximum plot limit, delta0.5 means (0.5) rotor diameters as incremental steps in turbine separation; ST1 means a simulation time of (1) minute was required.

Chapter 5

Verification of tool component functioning and development stages

5.1 Introduction

During the tool development, the program functioning was constantly checked in order to guarantee coherent performance at each stage. It means the results given by the code were within expected ranges based on engineering knowledge. The inspection was done by running several tests and verifying how the results were sound and logical. In this chapter, the workability of the different tool features is verified. First, it is explained why it was difficult to validate the results given by the cable models. Next, the wake speed deficit computed by the different models is compared with published data. A similar procedure is done for the wake combination method. The effects of the Weibull wind speed distribution and wind rose are verified when energy yield calculation results for a real wind farm are compared with results from another commercial tool.

5.2 Electrical cable models

The verification of the cable models was difficult since it was found very few data regarding cable losses and costs models and real measurements from offshore wind farms. Also, most of the information available was related to high voltage transition systems, but not to medium voltage collection systems.

In a recent publication, Martinez [21] gives a model for submarine cable costs for HVAC systems. He indicates that three core XLPE cable (132kV) cost can be estimated as:

$$C_{132} = 1.5 MEuro / km \qquad \text{eq. 5-1}$$

In another study done by Green et. al. [22], it is indicated that submarine power cables are custom manufactured to meet the requirements of each unique project; as a result, extensive electrical and cost data on specific cable sizes and types are not readily available. The authors found that performance and cost data are highly variable between manufacturers. For instance, when price data was requested to several companies, one manufacturer provided cable prices about twice as high as the other two.

Additionally, the authors indicate that two manufacturers provided performance data for their cables. However, in addition to an inconsistency in these variables, they had too little information about the cables themselves to calculate losses from first principles. Instead, the authors refer to the following table in order to obtain information about cable costs.

Table 5-1. Costs for cables with specific conductor sizes from two companies. Highlighted costs were extrapolated from known costs. Taken from [22].

Conductor Size mm^2	Company A	Company B
	Cost ($/m)	Cost ($/m)
Collection System		
95	152	455
150	228	494
400	381	609
630	571	635
800	600	731
Transmission System		
630	755	860

In regard to the cable losses, the author refers to the following figure.

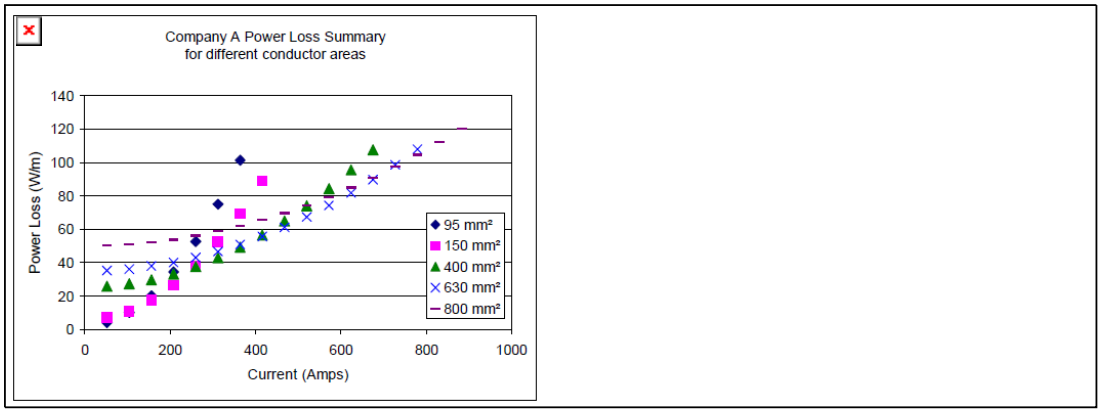

Figure 5-1. Loss results for two company cables at various currents and conductor sizes. Taken from [22].

With previous information, it could be possible to evaluate the results of the implemented models. Still, it is important to keep in mind that commodity prices are about one third of the cable costs and variations in cooper price. As indicated by Green, the price of copper increased significantly between 2003 and the summer of 2006, at one time by more than 300%.

As conclusion, previous data can be used as a reference point to compare the tool results, but not necessarily can completely verify or reject the performance of the implemented cable models.

5.3 Wake models

The different wake models produce the same output which is the wind speed deficit and wake diameter expansion as function of the distance behind the rotor plane. In a validation study of wake models with data from the Vindeby offshore wind farm; done by Rados [23] for the Efficient Development of Offshore Wind Farms (*ENDOW*) project, the performance of the Ainslie model is assessed. This study allows comparing the Ainslie model integrated into the design tool, with the results from those models integrated into other commercial software.

A single wake case study was developed with data from Vindeby turbine 6E. Figure 5-2 details its location within the farm.

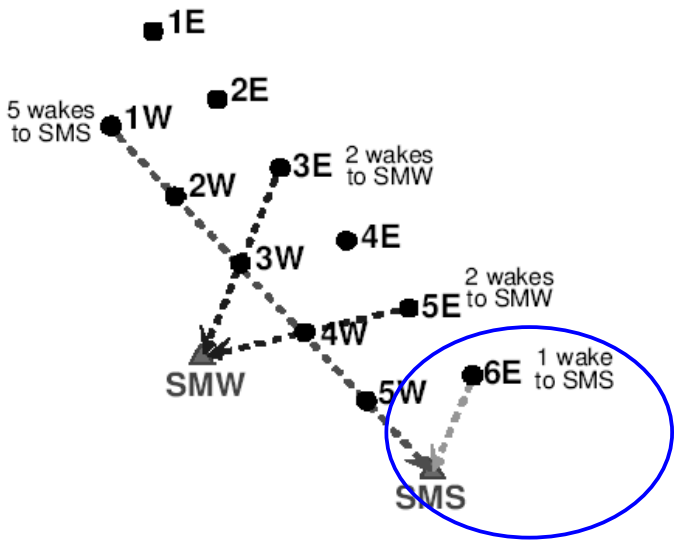

Figure 5-2. Layout of the wind farm at Vindeby (● shows each of the eleven wind turbines and ▲ the two sea masts). Taken from [23].

The most relevant site and turbine conditions from the experiment that were emulated into the tool are the following:

- Free flow wind speed of 7.5 m/s
- Turbine power of 450 kW
- Turbine diameter of 35 m
- Hub height of 38 m
- Thrust coefficient of 0.76

The velocity profiles are calculated at five different distances behind the wind turbine 6E, using the following tools:

Table 5-2. Wake models and tools

Abbreviation	Partner (tool)	Wake model
Riso	Risø National Laboratory	CFD code and semi-analytical engineering model
MIUU	Uppsala University	Taylor hypothesis
GH	Garrad Hassan	Ainslie
RGU	Robert Gordon University	CFD code
UO	University of Oldenburg	Ainslie
ECN	ECN	CFD code

The results are shown in Figure 4-17. For the distance of 9.6 rotor diameters (D), these values are compared with the meteorological mast measurements. The dotted line

represents the turbine hub height (38m) and the single solid line represents the undisturbed variables obtained by Monin-Obukhov similarity theory applied to atmospheric surface layer.

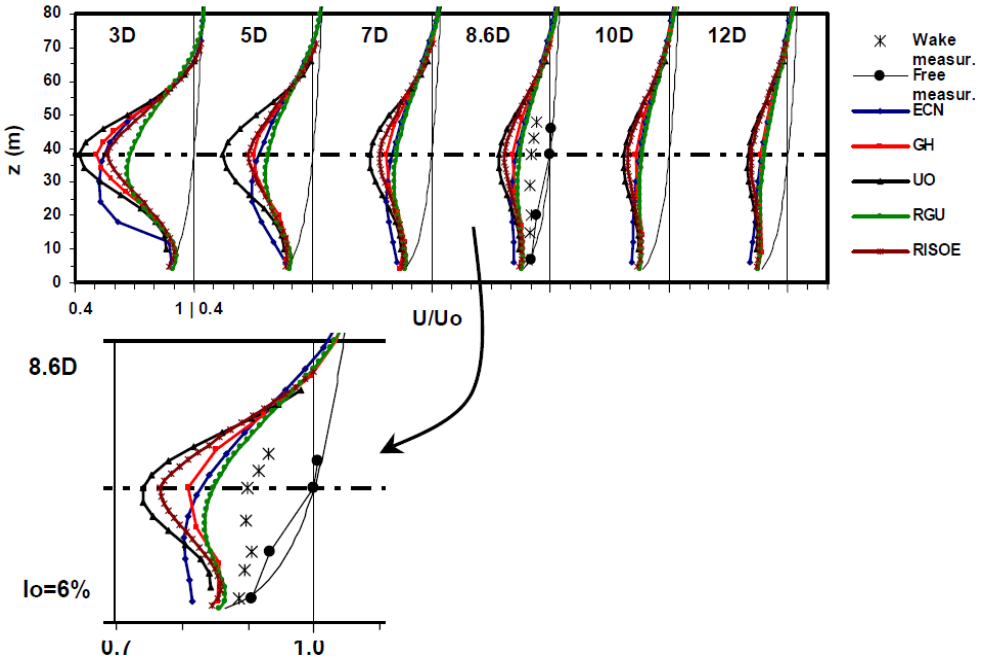

Figure 5-3. Velocity profiles normalized with the undisturbed wind speed at hub height on the vertical centre plane downstream of the 6E wind turbine for ambient turbulence intensity 6%. Free wind speed at hub height, Uo = 7.5 m/ s, thrust coefficient, C_T = 0.76, Monin-Obukhov length, L = -10000m. Taken from [23].

From Figure 5-3, the wind speed deficits given by the different wake model implementations, including the Ainslie, are obtained. The deficits are plotted in Figure 5-4 together with the computation results given by the developed design tool.

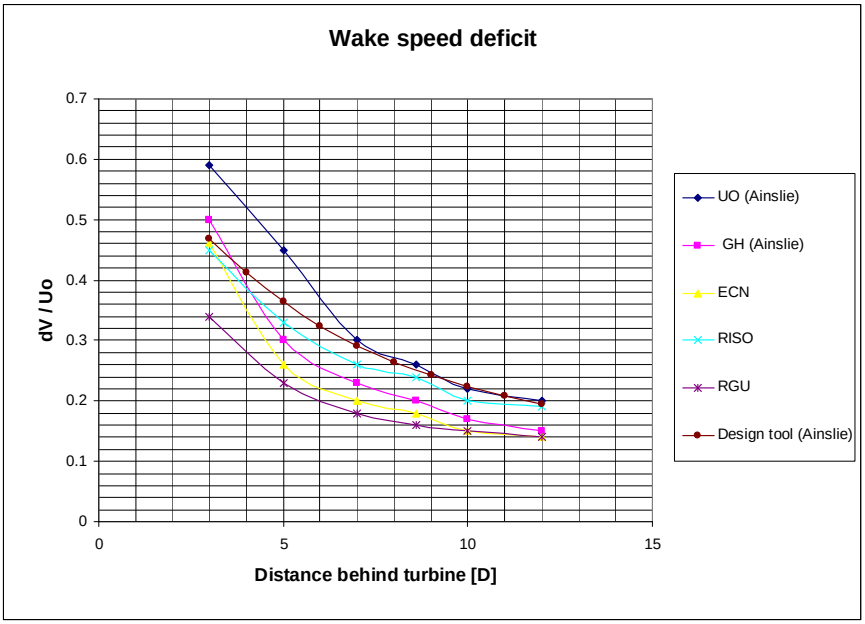

Figure 5-4. Ainslie wake model: wake speed deficit.

Comparing the different curves, the behaviour of the tool results is very similar to the validation study. The result from the implementation done by the University of Oldenburg (implementation of Ainslie wake model) is almost identical to the design tool result after 7 rotor diameters. The differences at shorter distances could be due to the turbine thrust coefficient curve used by the *UO* software.

Luna [24], worked developing a two-dimensional wake model. He compared his model results with the Jensen and the Frandsen models. The main inputs he used for the simulation are the next:

- Wind speed of 10 m/s
- Thrust coefficient of 0.7
- Surface roughness of 0.05 m

Luna's results are compared with the design tool output in Figure 5-5.

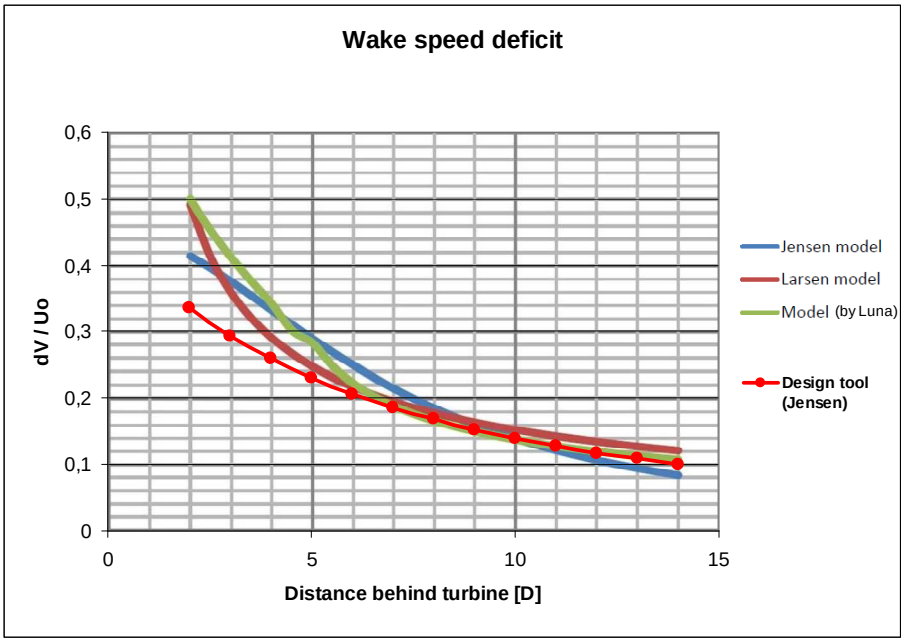

Figure 5-5. Jensen wake model: wake speed deficit.

The Jensen wake model implemented in the tool has shown lower deficit output at close distances behind the rotor plane. Nevertheless, at separation distances of 8 rotor diameters and beyond, the results are more similar to those presented by Luna.

Frandsen proposed an analytical model of wind speed deficit in large offshore wind farms [8]. He compared his model with the Jensen model in Figure 5-6 using the following parameters:

- C_T = 0.7, $\alpha_{(noj)}$ = 0.05
- U_noj is the Jensen model
- U_(1/2) is the Frandsen model with linearization of momentum equation, k=2
- U_(1/3) is the Frandsen model with linearization of momentum equation, k=3
- U_base is the Frandsen model with no linearization of momentum equation, k=3

The tool output for the Jensen and Frandsen models implemented in the design tool are integrated in the same graph.

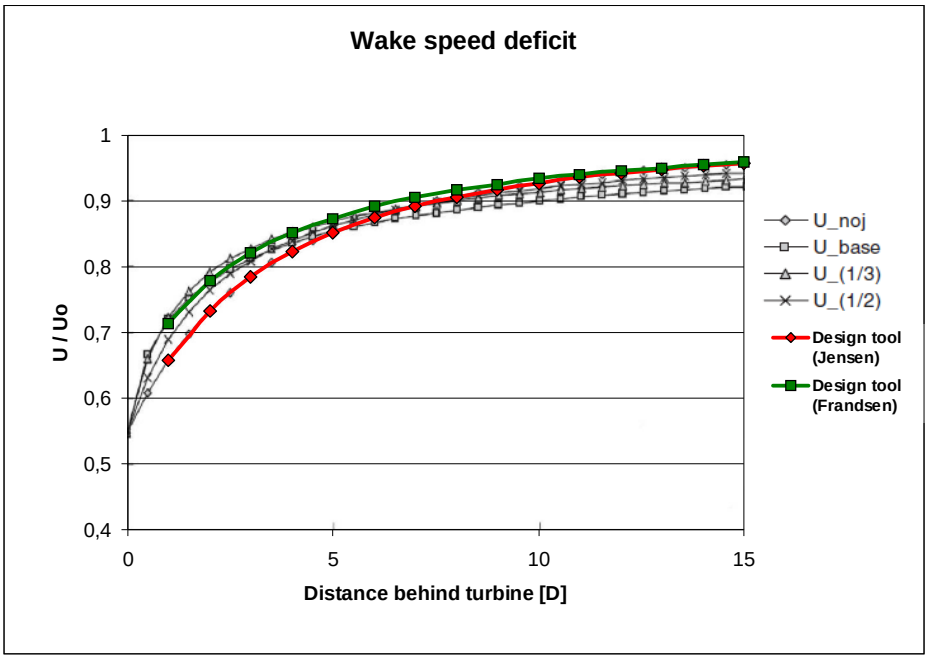

Figure 5-6. Comparison of single wake models.

Notice the very close results for the Jensen wake model in this case. The line matches almost perfectly the one presented in the Frandsen study, named U_noj. On the other hand, the Frandsen model implemented in the tool have similar values at short distances rather than long distances when compared with its equivalent U_base in Figure 5-6.

It can be concluded that the implemented Ainslie, Frandsen and Jensen wake models have very similar performance to equivalent implementations done by other authors with results found in literature. Therefore, for the goal pursued in the present project, the wake models performance can be considered satisfactory.

Now that wake model has been verified, it is necessary to proceed with the wake combination method to be used when several turbines are aligned with the wind direction. This is done in section 5.4.

5.4 Wake wind speed deficit combination method

The most straight forward method to combine the effect of overlapping wakes would be the linear superposition of speed deficits. Nevertheless, empirical studies have shown that the speed deficit is overestimated with this method. Instead, the use of the root sum of squares of velocity deficits has proved to be a better approach when compared with measurements from real wind farms.

With the aim to verify the method to calculate the wind speed deficit when two or more wakes overlap and impact over another turbine, a test was set up trying to emulate the conditions found in the Horns Rev offshore wind farm, in a study done by Barthelmie [25]. The case to analyze included eight Vestas-V80 turbines separated 7 rotor diameters and several wind speeds coming from west direction.

For different wake models, power losses were compared with the validation study mentioned above. The results are shown in Figure 5-7.

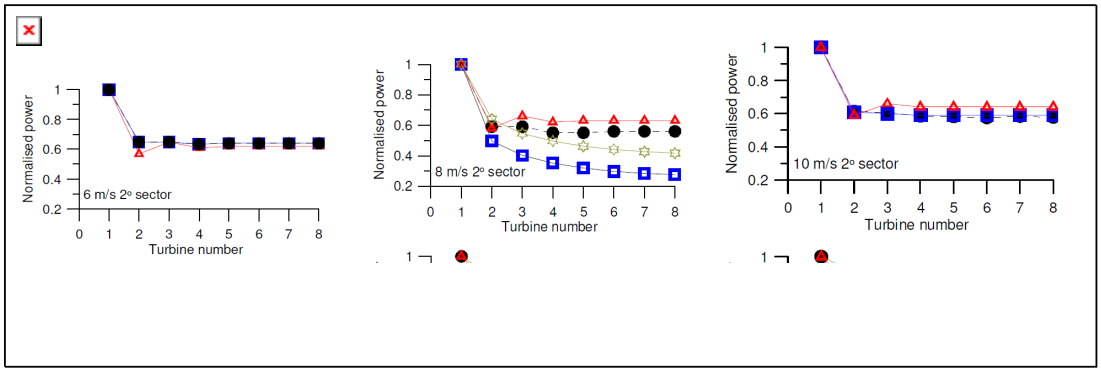

a) Wake model prediction and real measurements at Horns Rev. Models not specified. Taken from [25].

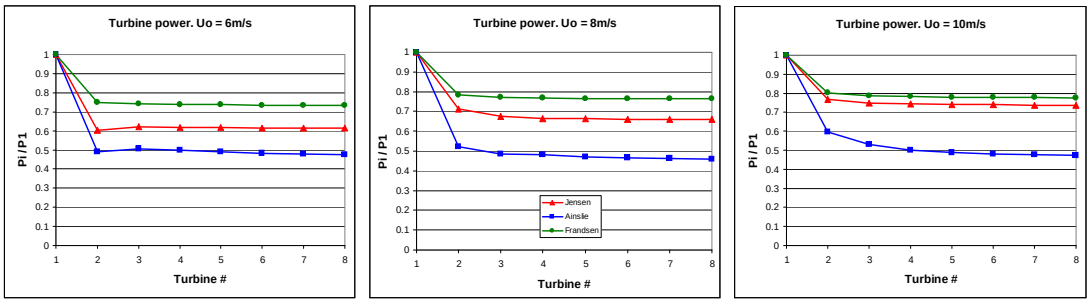

b) Implemented models.

Figure 5-7. Normalized power for 8 turbines aligned with westerly wind direction at several speeds.

The first detail to consider when analyzing Figure 5-7 is the deficit at the second turbine. At wind speed of 6m/s, the Jensen wake model matches the best the power deficit. For the case of 8m/s, there is more discrepancy in the results. The same happens with the models simulated in the study done by Barthelmie. In the 10 m/s case, the Ainslie wake model matches better the power drop at second turbine. The rest of the points in the curves are mainly dependent on the wake combination method implemented in the tool. The general behavior of maintaining a straight line is properly emulated by the tool results.

Through several tests, it was found the likely reason of the discrepancies relies on the turbine thrust coefficient curve used for the calculations. Since it is not publicly available, the source of information (manufacturer or on-site measurements) may result on different curves from the one used in the case study and the curve used for this project, as shown in Figure 5-8.

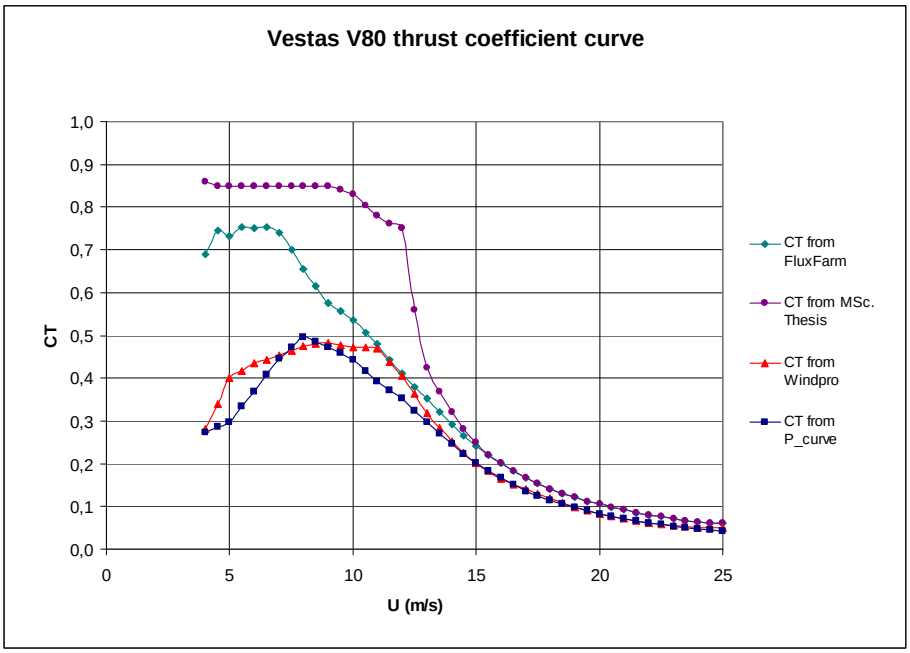

Figure 5-8. Thrust coefficient curve for the V80 wind turbine; from several data sources.

The difference of using different thrust curves can be noticed in Figure 5-9. There, the case of $\boldsymbol{U}$=6 m/s, using Jensen wake model is shown for each of the four thrust curves from Figure 5-8. As can be seen, a higher thrust coefficient curve implies larger wind speed deficit and therefore larger power deficit for downstream turbines.

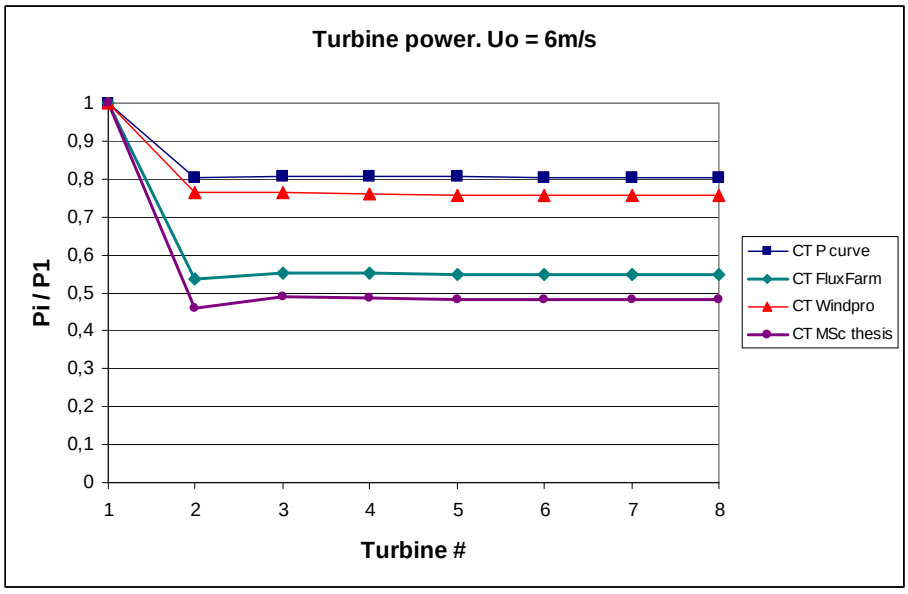

Figure 5-9. Power deficit: using Jensen wake model and several thrust coefficient curves for V80 turbine.

From previous figures, it can be concluded that the implemented combination method shows results in accordance with the data found in literature when similar simulation conditions are used.

Once individual components have been tested, the global tool functionality is verified. In section 0, the results for the levelized production cost calculation are described.

5.5 Energy production calculation

The energy production algorithm is compared with the results of FluxFarm program developed by ECN. For the Horns Rev study case, the same wind and site conditions, turbine power curve and turbine thrust curve were emulated as reported by Bot [26]. The annual energy yield results are compared in Table 5-3.

Table 5-3. Annual energy yield calculations for Horns Rev wind farm.

	Flux Farm	Design tool		
Wake model used	Wind tunnel measurements (z0 = 0.001)	Jensen	Ainslie	Frandsen
Annual energy yield [GWh]	600.973	539.610	513.157	555.728
Wind farm efficiency [%]	0.942	0.919	0.874	0.947
Annual energy yield (without wake losses) [GWh]	637.976	586.879	586.879	586.879
LPC [Eurocent / kWh]	-	6.70	7.05	6.51
Simulation time [minutes]	-	2.19	34.35	2.19

In Figure 5-10, the Horns Rev layout (reproduced by the design tool) is presented.

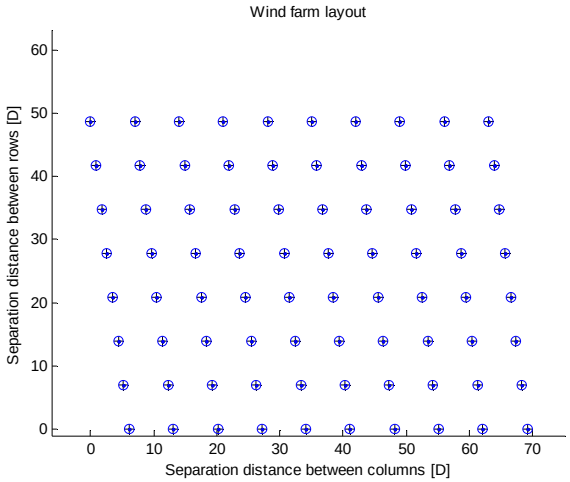

Figure 5-10. Horns Rev layout.

Using the design tool with the Frandsen wake model delivers closer results when compared to the FluxFarm software. It is important to notice there is a difference in the energy yield output even if no wake losses were considered. The design tool calculates a yield equivalent to 92% of that one calculated by FluxFarm. This is a relevant result that helps to verify the performance of the energy production calculation routine.

The difference in results can be due to, for instance, reported wind speed measurements were taken at a different height from the turbine hub. On the other hand, the farm efficiency differences can result from using different wake models and also from the wake combination methodology implemented.

The results presented in Table 5-3 provide a verification of all the aerodynamic aspects together (Weibull distribution, wind rose, wake models, wake combination method, energy calculation). This is a very valuable overall verification.

Chapter 6

Results and new knowledge

6.1 Introduction

During the development of the design tool, valuable knowledge was generated. Some of it is attainable to designers in general; while some other is mainly of interest for people involved in the wind energy industry. For the several development stages, the main lessons learnt are described with more detail in this chapter.

Firstly, some experienced during the tool development is appointed. Later on, the main results from the implementation of the different wake models are described. A similar description is done for the implementation of the wind rose and the introduction of multiple turbine row layouts.

An important outcome from the comparison of the two operation modes is presented. There, the dependency of the starting point for the optimization mode will be discussed. Finally, the sensibility of the optimum *LPC* to the different wake models is presented.

6.2 Development approach: from simple to complex

The tool development approach resulted to be a very proper manner to create a functional code able to optimize the wind farm layout. With the development of the first tool version, several basic components were developed and tested, like the wake and cable models. They continued serving during the rest of the project and better understanding of their properties and limitations was acquired.

As the tool eventually became bigger and more complex; it was more difficult to evaluate individually the code subsections. An important lesson learned during the first part was the development of a modular code requires testing of individual components and assurance of their correct operability, in terms of functionality and consistent results, before integrating them into the main code structure. Otherwise debugging would become a difficult task.

The implementation of an optimization routine was one of the parts that consumed more time per line of code. However, it was important to program it in order to have a better perception of the complexity of the optimization process.

6.3 Wake models

The output of all the wake models included in the tool can be compared by running a wake model benchmark. The wake characteristics are plotted for a selected turbine, indicated by giving its number in accordance to the scheme presented in Figure 4-14.

An example for the turbine in positions (1,1) is shown in Figure 6-1. In this case, the plot has been drawn for free flow wind speed of 7 m/s, turbine type is V80 (2MW).

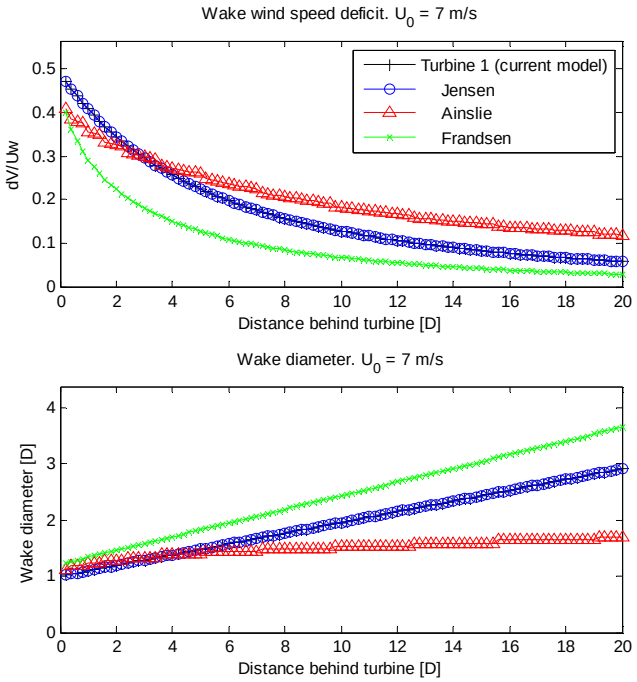

Figure 6-1. Wake model benchmark: wake wind speed deficit and diameter. U_o = 7 m/s; C_T = 0.75; z_o = 0.002.

The distance behind the turbine and the wake expansion is divided by the rotor diameter to make them dimensionless. Also the wind speed deficit is divided by the wind speed reaching the turbine. Therefore the wind speed deficit can be seen as a fraction. For example, in Figure 6-1 the maximum speed deficit at close distance behind the rotor is around 48%, given by the Jensen model.

As can be seen in Figure 6-1, the Jensen model presents the maximum wind speed deficit at short distances behind the rotor plane. However, after 3 ***D*** behind and longer distances, the Jensen deficit becomes smaller than the Ainslie deficit. The Frandsen model always results in lower wind speed deficits when compared to the other models.

In regard to the wake diameter, the Jensen and Frandsen models present similar linear expansion behavior, being the Frandsen the largest of all. The Ainslie model presents the smaller wake diameter and it is not linear. Actually after some large distance behind the rotor plane, it starts to contract as can be seen in Figure 6-2. This is the only wake model that presents this behavior. The wake boundary was defined as the wake region where the wind speed is 99% of the free flow wind speed (or in general the speed of wind arriving to the turbine location).

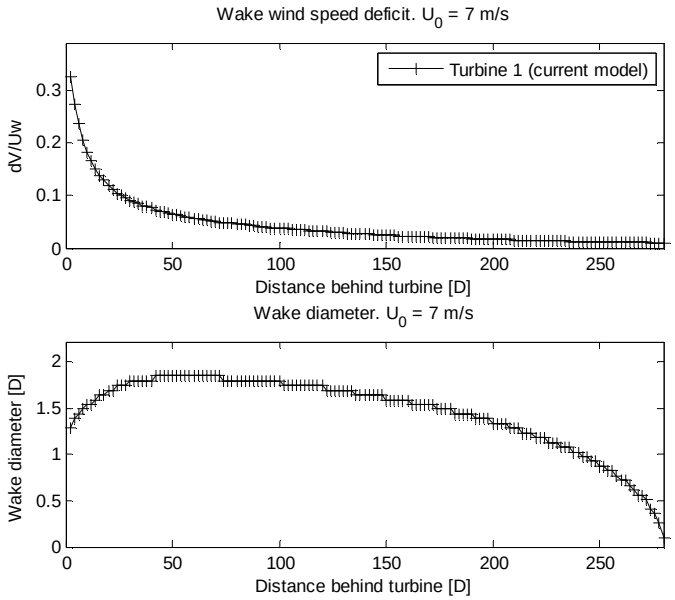

Figure 6-2. Wake speed deficit and diameter for Ainslie wake model.

The Ainslie wake diameter contraction is a delicate feature to consider when analyzing large wind farms with long separation distances between turbines. A consequence is that, even if the wake is completely aligned with downstream turbines, at some point the incidence is partial and not total over downstream turbine rotor planes.

Other relevant deduction when comparing the wake model characteristics is that despite computing the lowest wind speed deficit, Frandsen model gives the wider wake expansion. Therefore there is more probability to hit turbines downstream. The opposite happens with the Ainslie model which gives the highest speed deficit, but also the thinner (and even contracting) wake diameter. Consequently the chances to reach other turbines downstream are lower. Based on previous relations, it is not possible to anticipate which model would result in lower or higher *LPC* calculations for large wind farm cases.

In order to evidence the effect of using different wake models when calculating the cost of energy, a simple simulation was done. This case assumed 2 wind turbines and static wind conditions:

- Unique wind direction parallel to turbine column.
- Wind speed fixed to 5 m/s.
- Offshore conditions → z_0 = 0.002

By selecting these conditions, there is only one variable that affects the *LPC*: the turbine separation distance. Resultant *LPC* as function of the separation distance can be appreciated in Figure 6-3.

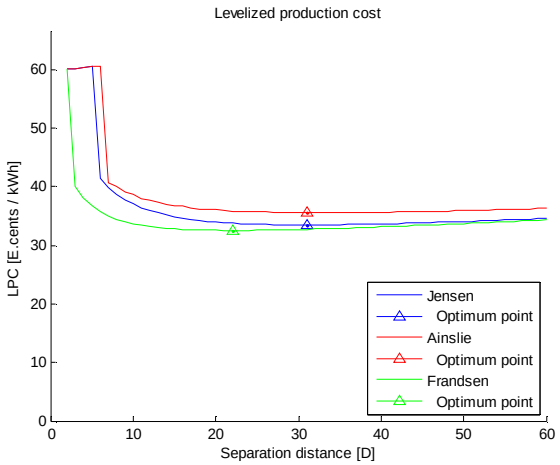

Figure 6-3. Wake model benchmark: LPC for 2 turbines, fixed wind speed and direction.

Curves above show a peculiar shape when turbines are very close each other. The reason of the step is that for very close separation distances, the second turbine behind is turned off due to high wind speed deficit coming from first turbine. Once the separation distance increases and the speed deficit is reduced thanks to air mixing between the exterior and interior of the wake, the second wind turbine starts when the mean wind speed velocity in

the wake is higher than $\boldsymbol{V_{cut\text{-}in}}$. Since more energy is suddenly produced, the *LPC* is sharply reduced.

As can be appreciated, the optimum separation distance differs when using different wake models. After a certain distance (around 20 ***D*** in this case), the *LPC* calculated with all the models reaches similar values (around 35 E.cents/kWh). For the Jensen and Ainslie models, especially at short separation distances, the calculated wind speed deficit is higher when compared with the Frandsen model calculations. Therefore the second turbine is working at lower power, producing less energy and thus the *LPC* is higher.

For each model, the minimum cost of energy is indicated by the dot on the curve. As can be seen, the optimum separation distances differ as indicated:

- Jensen wake model = 31 ***D***
- Ainslie wake model = 31 ***D***
- Frandsen wake model = 22 ***D***

Under the simulation conditions, the Jensen and Ainslie model produce the same optimum separation distance, higher than the Frandsen model. In case the roughness length were changed to onshore conditions ($\boldsymbol{z_0}$ = 0.075), the results would be as shown in Figure 6-4.

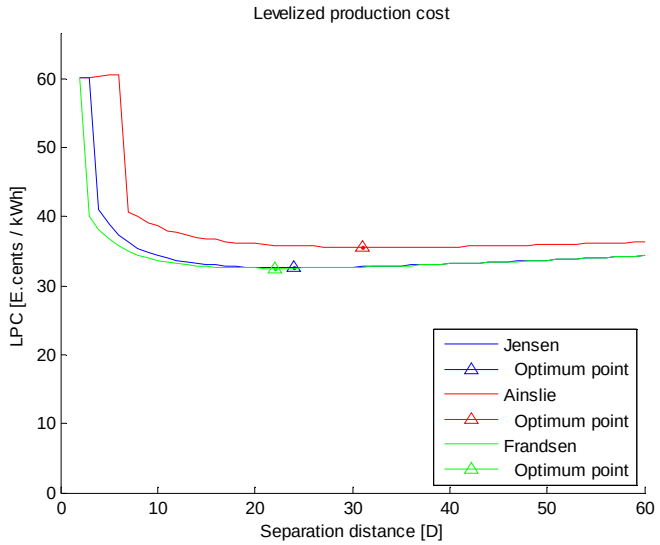

Figure 6-4. Same as Figure 6-3, but z_0 = 0.075

Now the Jensen output is more similar to the Frandsen model since it depends on the surface roughness. This is an indicator that site conditions affect the results of layout dimensions obtained by using the different wake models.

If not static wind conditions are used, but instead a wind rose of 36 sectors with homogenous sectorial Weibull distribution and even direction probability, the resultant *LPC* curves, as well as optimum layout dimensions are more similar as shown in Figure 6-5.

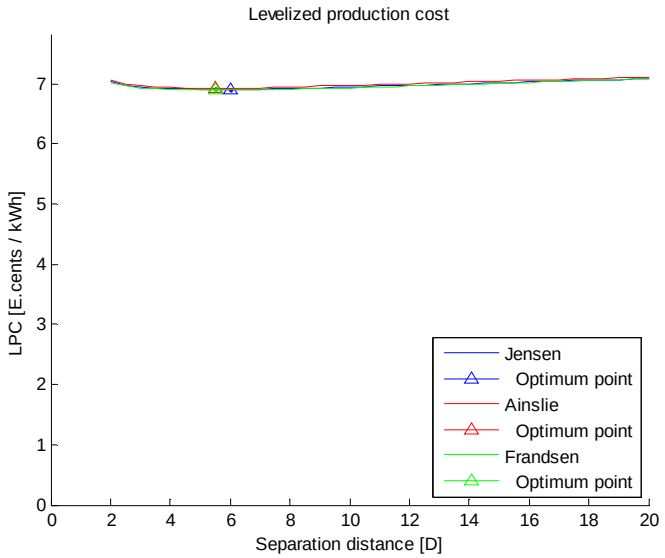

Figure 6-5. Wake model benchmark: LPC for 2 turbines, 36 sector wind rose, Weibull speed distribution.

Changing the wind conditions, the new optimum separation distances are shown as follows. The simulation time is also indicated:

- Jensen wake model = 6 ***D***; 0.31 minutes.
- Ainslie wake model = 5.5 ***D***; 0.94 minutes.
- Frandsen wake model = 5.5 ***D***; 0.27 minutes.

Based on previous results, it is advisable to use the Jensen wake model since the optimum cost of energy it gives is relatively similar to the others models, the computational cost is cheaper than the Ainslie model and it has been validated in several case studies available in literature.

6.4 Wind rose

It is important to make evident the effects of using simple or detailed wind conditions. With this purpose, Figure 6-6 makes possible to compare the effects of three simulation

cases for a wind farm composed by four Vestas V80 wind turbines (rated power of 2MW) in square layout. The following simulation settings were used:

- Fixed wind speed of 7 m/s; fixed wind direction (from south)
- Weibull wind speed distribution; fixed wind direction (from south)
- Weibull wind speed distribution; wind rose of 36 sectors (equal frequency)

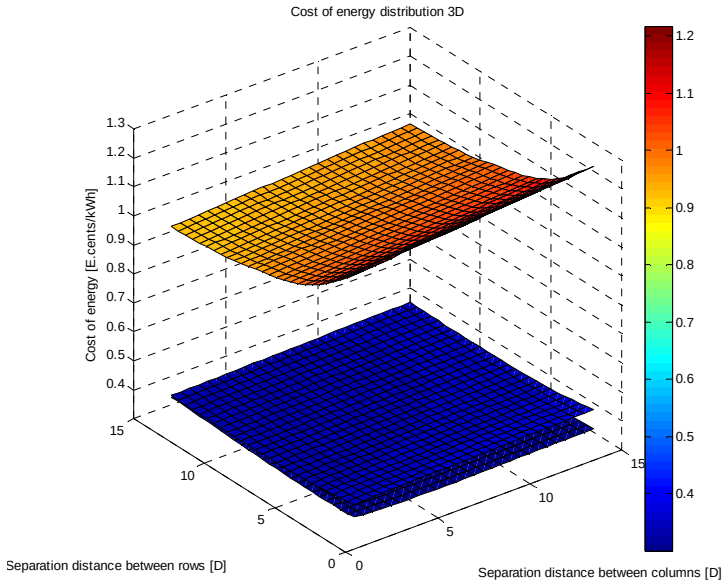

Figure 6-6. Multiple simulation output, from top to bottom: Fixed wind speed and direction; Weibull wind speed distribution / fixed wind direction; Weibull wind speed distribution / 36 sector wind rose.

By considering a Weibull wind speed distribution, the cost of energy is much lower when compared to a fixed wind speed value, than can be for instance the local average wind speed. Additionally, the inclusion of a wind rose reduces further the cost of energy since now there is not wake incidence over turbines all the time.

The resultant optimum layout dimensions are also affected. The inclusion of Weibull wind speed distribution reduces the row separation because wind speeds higher than 7 m/s up to 25 m/s are also taken into account and more energy is generated in that range. Besides, the inclusion of the wind rose divided in 36 sectors with even wind direction probability was assumed. As an effect, the wind direction is not always aligned with two given turbines causing less wake-turbine interaction, reflected in higher energy production and consequently lower general cost of energy. It results in the reduction of the row separation distance. On the other hand, the column separation is augmented even longer than the row separation because there are fewer cables in that direction and therefore it is less expensive to increase such distance.

After the tool was extended to consider wind farms with more than two turbines, in rectangular layouts, the *LPC* became a dependent of two variables: the column separation distance (***sc***) and row separation distance (***sr***). When running a simple case composed of four turbines in rectangular layout, it was found the number of wind rose sectors affects the shape of the *LPC* surface as function of ***sc*** and ***sr***. Figure 6-7 shows the example of using 4, 8, and 32 sectors. The separation distance was increase in steps of 1 rotor diameter and the Jensen wake model was used.

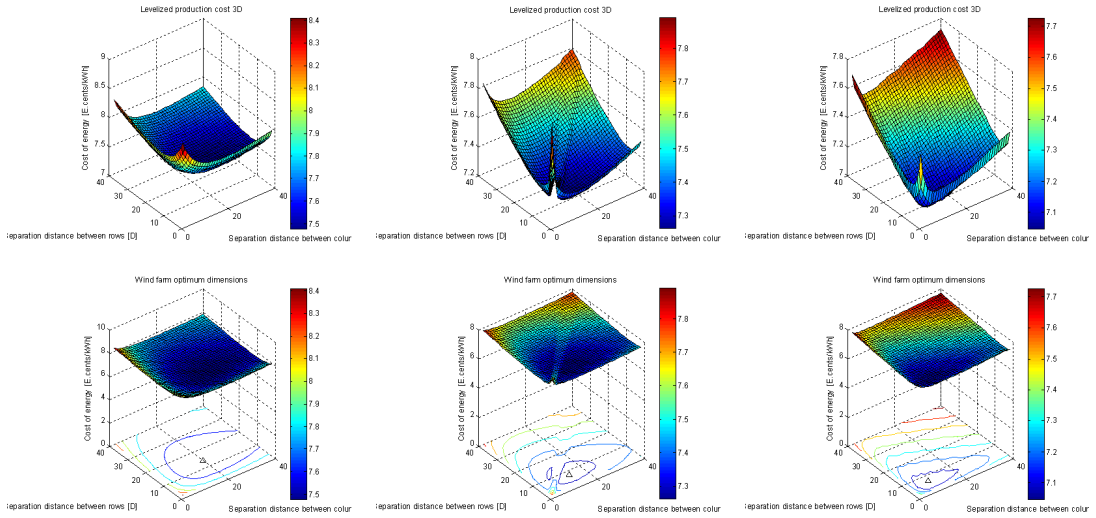

a) 4 sectors **b) 8 sectors** **d) 32 sectors**

Figure 6-7. LPC as function of column and row separation. Wind farm of 4 turbines in rectangular layout.

In Figure 6-7, it is possible to notice how the number of wind rose sectors influences the *LPC* computation. For the a) case, where four sectors were used (one for each cardinal orientation), the output is a smooth valley surface. However, increasing to 8 sectors to include diagonal wind directions like in the b) scenario, the cost of energy is influenced by additional wake interaction and a ridge shape is formed.

Smoothness of the *LPC* surface affects the optimum layout dimensions. The number of wind rose sectors is a discretization of a continuous variable, which is the wind direction. In reality wind can come from any given direction and therefore, it is necessary to further increment the number of sectors in order to approach a more realistic scenario. The effect of this can be noticed in the c) case where 32 sectors were used. When compared with the a) case, the *LPC* becomes higher and the optimum turbine separation distances are reduced.

It is then advisable to use the maximum number of wind rose sectors to assure even more precise results. However in practical terms, this option would not be very convenient since other factors like the simulation time can be a constraint to this approach. Here appears a significant tradeoff between precision and computational time. For example, when using 4 sectors the total computational time was 3.65 minutes, while for the 32 sector example, the simulation needed 28.92 minutes to run.

Having a better understanding of the relation between the number of wind rose sectors, the *LPC*, the optimum dimensions and the computation time would be of great usefulness when selecting these parameters before running a big wind farm simulation. For this reason, a set of tests was run in order to identify these relations.

A case of 4 wind turbine wind farm was chosen and the separation incremental step was set to 2 in order to reduce the computation time of each simulation. The wake model used was Jensen. Table 6-1 summarizes all test results at the optimum wind farm dimensions (i.e. when minimum cost of energy occurs).

Table 6-1. Influence of wind rose sector number over several variables.

Sectors		4	8	12	16	20	24	32	36	64
Global energy generation	[GWh/year] =	24.3946	24.6244	24.8514	24.7384	24.9373	25.0769	25.0796	25.1424	25.1076
Global cable losses	[kWh/year] =	17.0308	9.85937	7.48591	4.97029	5.0219	7.5875	7.58788	7.60647	7.5916
	[%] =	6.98E-05	4.00E-05	3.01E-05	2.01E-05	2.01E-05	3.03E-05	3.03E-05	3.03E-05	3.02E-05
Global energy yield	[GWh/year] =	24.3946	24.6243	24.8513	24.7384	24.9373	25.0769	25.0796	25.1424	25.1076
Farm fixed costs	[M.Euro] =	9.7	9.7	9.7	9.7	9.7	9.7	9.7	9.7	9.7
Optimum global LPC	[E.cents/kWh] =	7.4795	7.26195	7.16308	7.09774	7.05734	7.05028	7.04953	7.04801	7.05778
Optimum separation between columns	[m] =	1600	1120	1120	480	640	640	640	800	800
	[D] =	20	14	14	6	8	8	8	10	10
Optimum separation between rows	[m] =	1120	640	480	320	320	480	480	480	480
	[D] =	14	8	6	4	4	6	6	6	6
Total elapsed time	[minutes] =	0.53	0.93	1.35	1.82	2.24	2.64	3.5	3.91	6.98

In Figure 6-8 is presented a visualization of how the number of wind rose sectors affects the levelized production cost surface as function of the turbine separation distance. When the number of sectors increases, the surface becomes smoother and the existence of local minimum points is reduced. By doing this, it is easier to identify a global minimum point. This is an important feature when running the optimization algorithm since it will be more likely to find the global minimum *LPC* value.

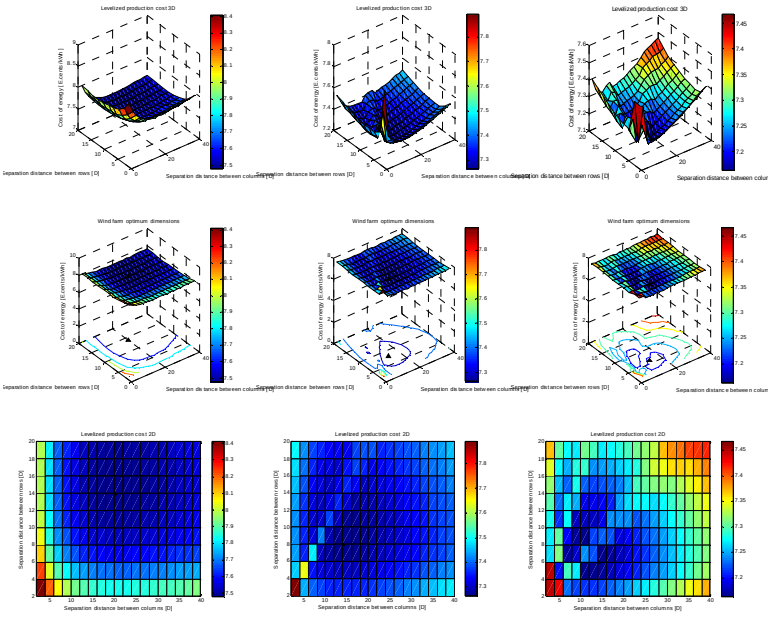

a) From left to right: 4, 8, 12 wind rose sectors.

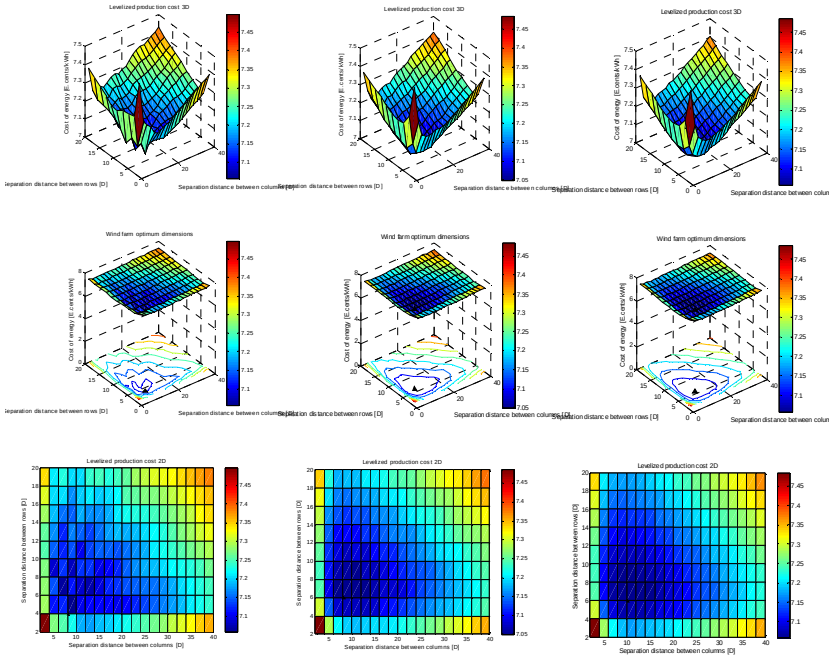

b) From left to right: 20, 32, 64 wind rose sectors.

Figure 6-8. LPC as function of the column/row separation distance.

One of the main interests is to determine the relation of the computation time as function of the number of wind rose sectors. Figure 6-9 shows a plot of these two variables.

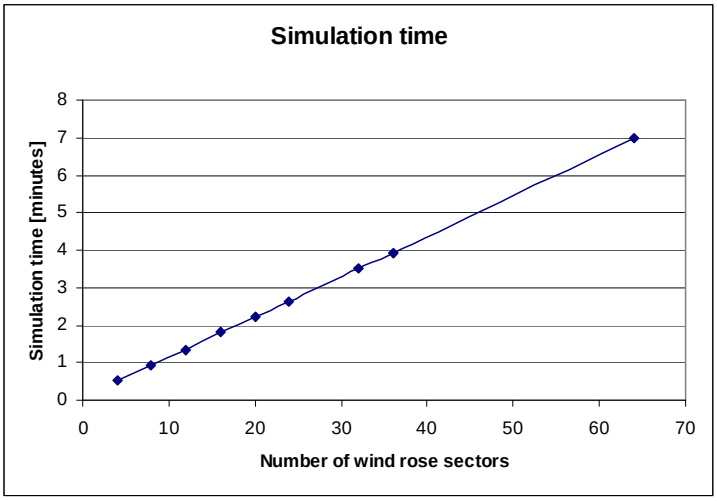

Figure 6-9. Simulation time as function of wind rose sector number.

As can be seen in previous graph, there is a linear relation between the number of wind rose sectors and the simulation time for a wind farm of 4 turbines. It is still necessary more information in order to have better criteria about what is a proper number of wind rose sectors to chose. Figure 6-10 shows the relation of the *LPC* as function of sector number.

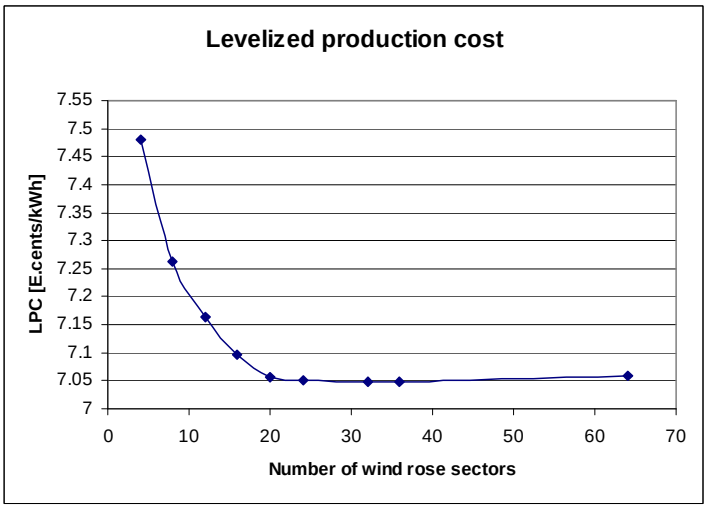

Figure 6-10. Levelized production cost as function of wind rose sector number (for optimum layout).

As seen in Figure 6-10, the value of the *LPC* stabilizes after a value of 24 sectors. Nevertheless, for 64 sectors, the *LPC* slightly increases due to a correspondent increment in the column separation distance, as seen in Figure 6-11. This increment implies more cable losses and costs, therefore affecting the energy cost.

A last aspect to consider is the behavior of the optimum layout dimensions as function of the number of sectors. This can be appreciated in Figure 6-11.

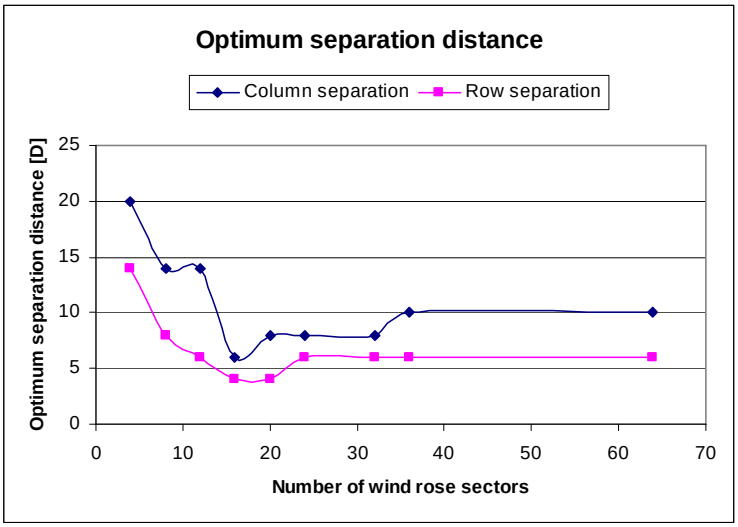

Figure 6-11. Optimum separation distance as function of wind rose sector number.

The optimum dimensions for the column and row separation distance seem to reach stable values after using 36 wind rose sectors. Just the column separation distance presents an increase when using more wind rose sectors. The reason is that increasing the number of sectors improves the smoothness of the *LPC* curve. Then, the more precise definition of optimum point will be more sensitive to variations in the column separation distance. Increasing the column separation distance is cheaper that increasing the row separation distance where more cables interconnect the turbines.

Based on previous results, it is recommended to use a total of 36 wind rose sectors when using this tool for layout optimizations of offshore wind farms.

6.5 Number of turbines

Similarly to the analysis done for the wind rose sector variable, the turbine number influence over several parameters is overviewed. Despite it was previously recommended to use a minimum of 36 sectors when looking forward to precise results; for this test purpose, 12 sectors were used. The aim was to scale down the simulation time for each

test, in special when large number of turbines was used. The separation incremental step was set to 2 in order to further reduce the computation time of each simulation. The wake model used was Jensen. Table 6-2 summarizes all test results at the optimum wind farm dimensions (i.e. when minimum cost of energy occurs).

Table 6-2. Influence of the number of turbines over several variables.

Turbines		4	9	16	25	36	49	64	81	100	121
Global energy generation	[GWh/year] =	24.7738	55.2757	97.4748	151.607	219.818	298.447	389.012	491.507	605.934	713.996
Global cable losses	[kWh/year] =	8.70561	51.7816	185.051	482.897	1766.28	3364.07	5853.56	9510.69	14661.2	12519.8
	[%] =	3.51E-05	9.37E-05	1.90E-04	3.19E-04	8.04E-04	1.13E-03	1.50E-03	1.94E-03	2.42E-03	1.75E-03
Global energy yield	[GWh/year] =	24.7738	55.2756	97.4746	151.607	219.817	298.444	389.006	491.498	605.92	713.983
Farm fixed costs	[M.Euro] =	9.7	21.825	38.8	60.625	87.3	118.825	155.2	196.425	242.5	293.425
Optimum global LPC	[E.cents/kWh] =	7.16102	7.31731	7.4128	7.49523	7.54218	7.5746	7.60024	7.75343	7.93356	8.10745
Optimum separation between columns	[m] =	720	1120	1120	1280	1120	1120	1120	1120	1120	1120
	[D] =	9	14	14	16	14	14	14	14	14	14
Optimum separation between rows	[m] =	560	480	480	480	800	800	800	800	800	480
	[D] =	7	6	6	7	10	10	10	10	10	6
Total elapsed time	[minutes] =	1.32	4.46	13.16	31.28	65.45	119.69	201.47	344.43	524.14	730.8

Firstly, the impact over the *LPC* surface is shown in Figure 6-12. The wind direction frequency is equal for every wind direction. Square layouts have been used in all cases to avoid differences due to asymmetries. The simulations used the Jensen wake model.

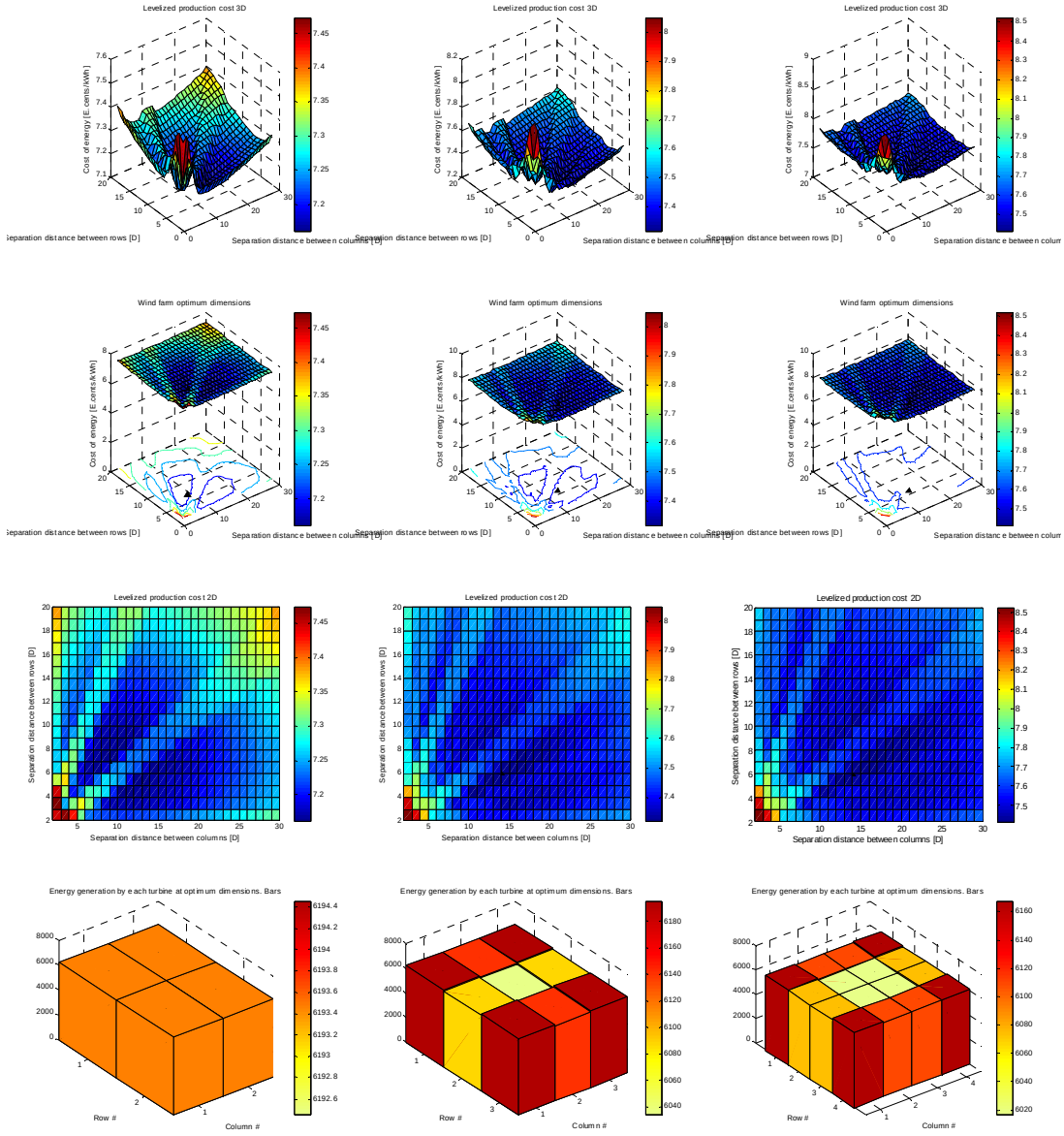

a) From left to right: 4, 9, 16 turbines.

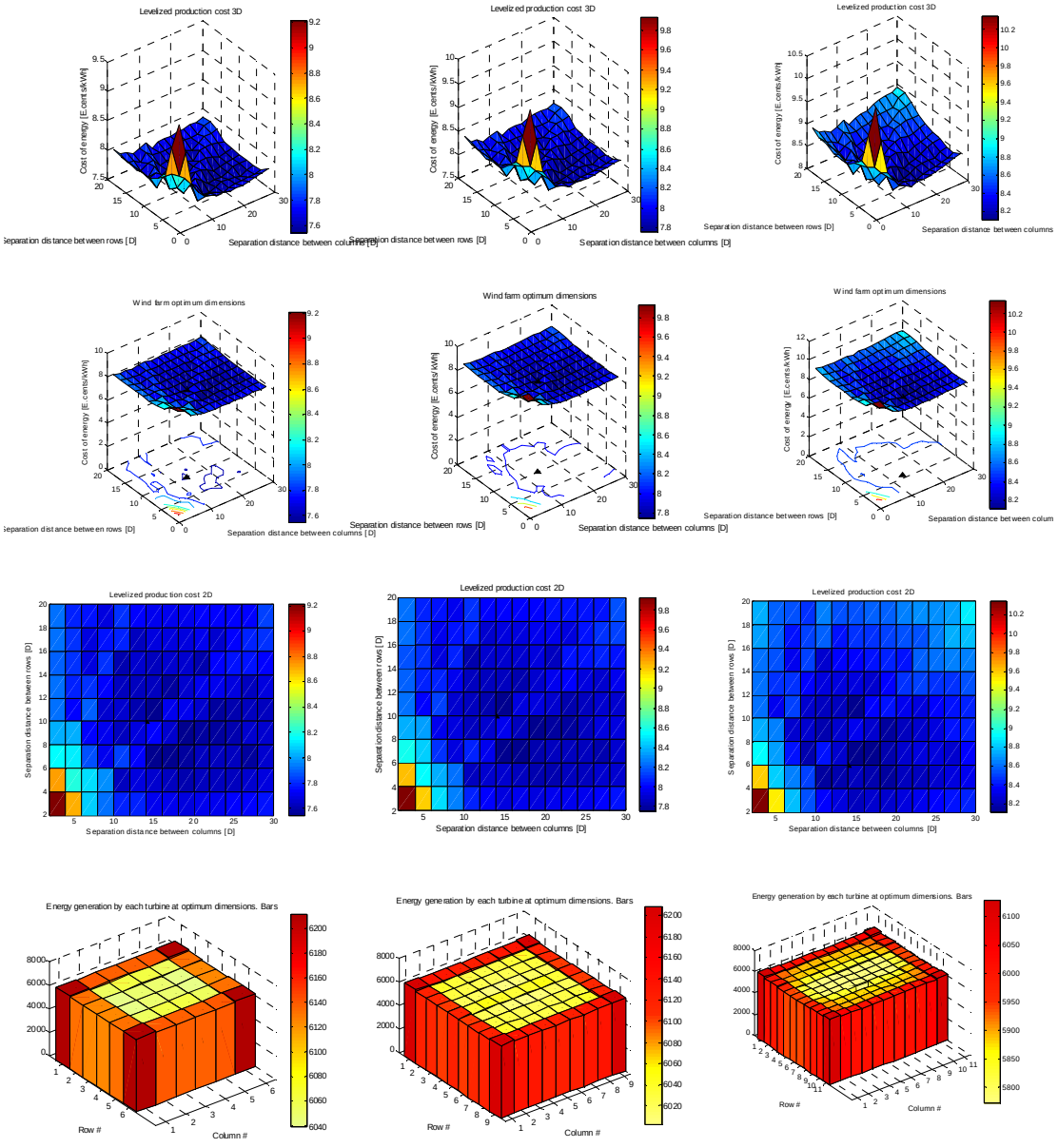

b) From left to right: 36, 81, 121 turbines.

Figure 6-12. Levelized production cost as function of the column/row separation distances.

First impression is that *LPC* surface becomes flatter when more turbines are included in the wind farm. Behavior of the optimum *LPC* at each case will be shown latter on in this section. The lower row of graphs in Figure 6-13 shows the annual energy contribution for each turbine. As was expected, outer turbines produce more energy since they are less

susceptible to wake interference. The corner turbines indicated as light green have 270 degrees of free wind incidence. The other external turbines indicated by dark green have some less than 180 degrees of free wind incidence. Notice in the case of big wind farms, like the example of 81 turbines; how the middle turbine of external rows shows even lower energy production. This is due to the impact of several wakes in a row when wind comes from parallel directions. In all the examples, the inner turbines (blue color) produce approximately the same amount of energy. This is explained by the phenomenon detailed previously in section 5.4. The wind speed deficit is maximum after the first turbine facing wind but keeps approximately constant for other turbines downstream.

Different from the wind rose sector case, simulation time does not have a linear relation with the turbine number, but instead it resembles a polynomial curve as shown in Figure 6-13.

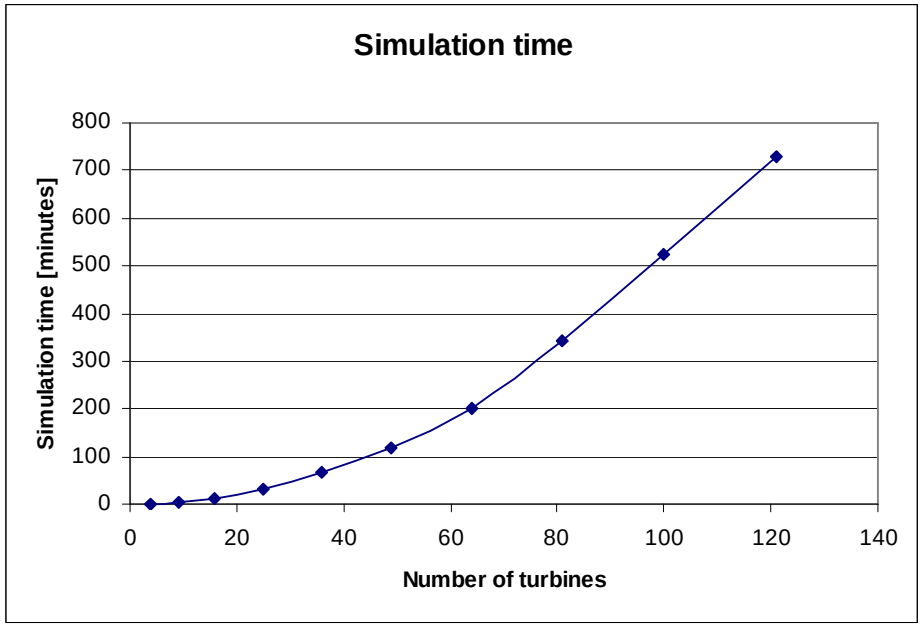

Figure 6-13. Simulation time as function of number of turbines.

For a wind farm with similar number of turbines as Horns Rev, the simulation time is around 11 hours. In addition, it is important to see how the *LPC* depends on the turbine number. Figure 6-14 shows that *LPC* increases at different rates when more turbines are added to the wind farm.

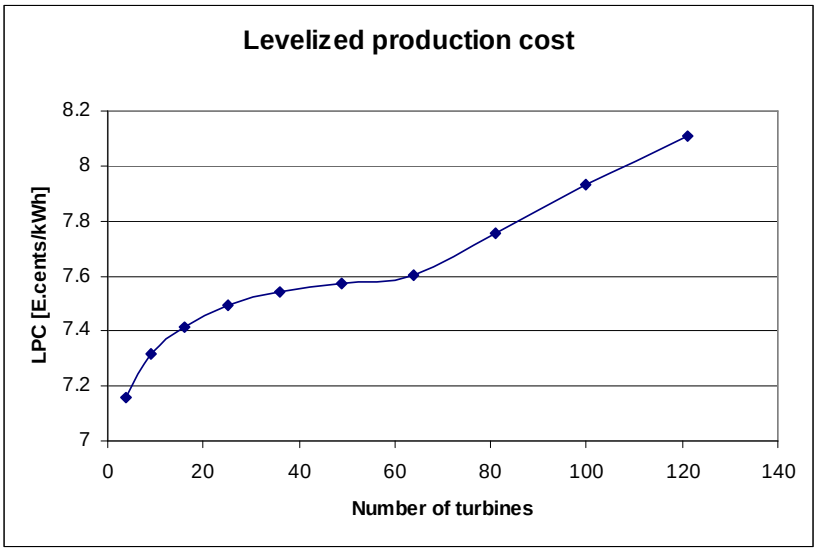

Figure 6-14. Levelized production cost as function of number of turbines (for optimum layout).

In regard to the optimum separation distance, the column and row curves show stabilization after the simulation case where 25 turbines were used. The column separation distance is higher than the row one since less cables are used to connect the columns than to connect all the turbines in each column, following the scheme presented previously in Figure 4-14.

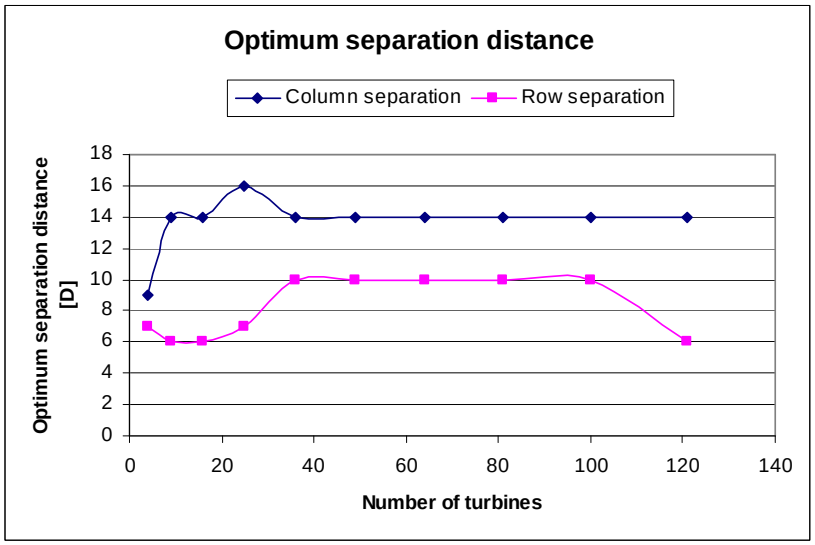

Figure 6-15. Optimum separation distance as function of number of turbines.

In rectangular layouts, the column and row distances are varied independently. Like it was indicated above in Figure 6-15, the column separation tends to be larger than row separation due to the collection cable connection scheme.

The sharp reduction of the row separation distance for the case of 121 turbines is because the minimum point *LPC* point is crossing from one side to the other over the ridge in the *LPC* surface. This can be seen when comparing last two cases in Figure 6-12. If the surface were smother, the change might be smaller.

6.6 Optimization function

The optimization algorithm included in Matlab presented some limitations when finding the global minimum *LPC*. Final results were found to be dependent on the initial starting point (initial guess) given by the user. Using a wind farm of 4 turbines and a wind rose with 12 sectors, three simulations were run in order to exemplify this situation. First, the *LPC* surface for the simulation conditions is shown in Figure 6-16. There, it is possible to appreciate the formation of two ridges due to the number of wind rose sectors: 12 sectors imply two diagonals. The reason of these formations was previously explained in section 6.4.

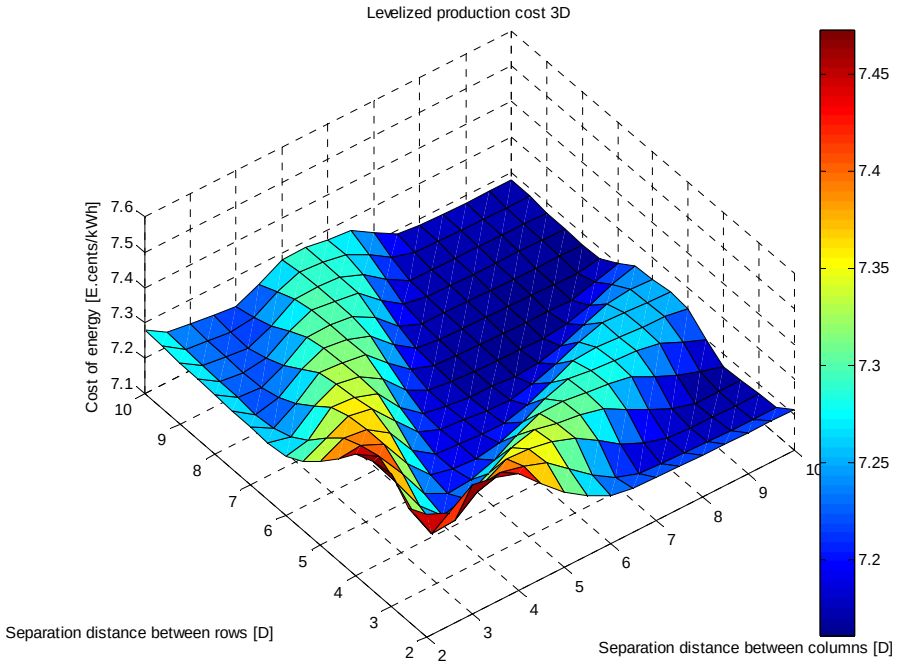

Figure 6-16. Levelized cost of energy surface showing two ridges.

Location of the minimum global *LCP* is indicated by a dark triangle in Figure 6-17. It was calculated running a separation distance sweep which also helped to plot the complete *LPC* surface. Then, the optimization routine was run three times, but using different starting points (initial guess). Each iteration result is indicated by a red dot in the graph, except the starting point which was indicated with a green dot.

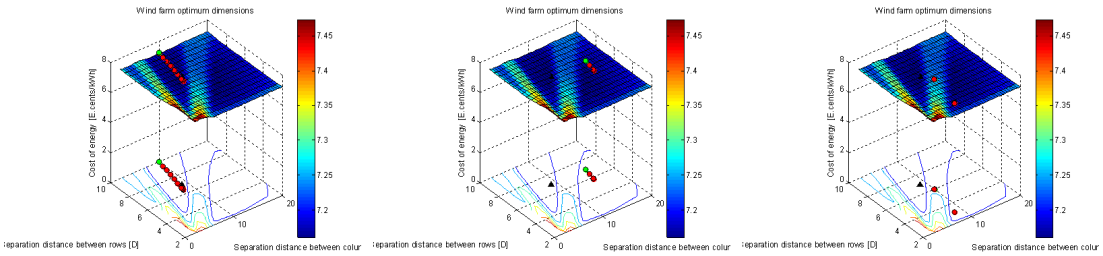

a) Starting point: (10,10) **b) Starting point: (16,7)** **c) Starting point: (10,6)**

Figure 6-17. Optimization routine results.

As can be seen, the local optimum found by the optimization routine is different for each case. When starting using layout dimensions (column,row) = (10,10), the local minimum found coincides with the global minimum point. Nevertheless, when starting on the other side of the ridge at point (16,7), the local minimum found differs from the global minimum. An additional test was run starting at some point on the ridge top, in this case (10,6). The result is that the optimization routine tried to find a local minimum close to the starting point. Since it found difficult to obtain a local minimum point, it made a big jump and continued looking for a local minimum. The final result is indicated at some location around (9,3).

Simulation times for each of the simulation modes are compared as follows:

- Simulation time using separation distance sweep = 4.22 minutes.
- Simulation time using optimization routine = 1.42 minutes.

Based on previous results, wind farm designers are advised to start running a separation distance sweep to have an initial overview of the *LPC* surface. Then, it is possible to start with a smarter initial guess when running additional tests. This helps to big changes in the simulation conditions. Then, the optimization routine can be used with more confidence on its results. By following this procedure, there is the advantage of saving considerable computation time.

6.7 Layout dimensions and LPC sensitivity to wake models

When calculating the *LPC* for a wind farm, differences in the results can appear from using one wake model to another one. A simulation test has been run under same conditions, except of the wake model used. In this case a square wind farm of 9 turbines was used. Figure 6-18 shows the variation of the cost of energy as a function of the separation distance between rows and columns. A wind rose of 36 sectors was used.

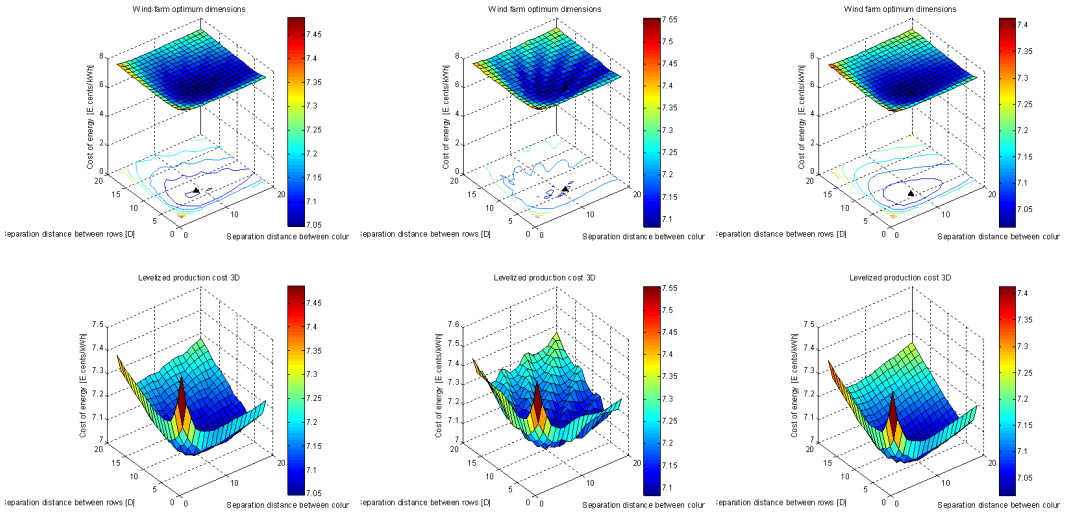

a) Jensen = 7.047 **b) Ainslie = 7.082** **c) Frandsen = 7.017**

Figure 6-18. Minimum LPC [E.cents/kWh] for 9 turbines in rectangular layout.

As can be appreciated, the smoothness of the *LPC* surface is affected by the wake model used. For the Ainslie model, the surface is more irregular when compared with the Jensen and Frandsen model, being the latest the one which presents the smoothest surface. As a consequence, different layout dimensions are obtained when using different wake models. The optimum dimensions show slight differences from using one model to another, nevertheless the computational time is less for Jensen and Frandsen models when compared to the Ainslie model.

Chapter 7

Conclusions, Recommendations and Future Work

From the realization of the present thesis work, the main conclusions in regard to the tool development itself and about knowledge acquired related to the design process, are summarized as follows.

7.1 Conclusions

Having general knowledge of the design process helped to follow a working path were at each stage, the tasks were easier to define and the results easier to evaluate. Also, documenting the results was structured and straight forward.

The tool development approach allowed having an operating code at all time and understand the tool functioning when new expansions were included.

During the research of suitable models to describe the main wind farm components, it was found more information about wake models rather than about electrical infrastructure models, specifically related to the wind energy applications.

There are two main categories of far wake models. The first includes the analytical models, which calculate the wind speed deficit at certain distance behind the turbine based on the turbine thrust coefficient. The second group is base in solutions to differential equations

describing the wind flow properties behind the turbine. This group includes numerical solvers to Navier-Stokes equations.

The implemented analytical Jensen and Frandsen wake models have shown faster computation times still with similar results to those given by the Ainslie wake model, which is implemented by a numerical solver.

The implemented wake models have shown similar outputs when compared to results published in literature.

The developing of the design tool revealed that modeling the behavior of a real wind farm is a complex task since many variables are interacting. Especially, the multiple wake interaction resulted to be a difficult task to describe and compute.

In regard to wind direction properties, it is advisable to consider wind roses with at least 36 sectors in order to have a smoother description of the levelized production cost as function of the column and row separation distances.

In general, the design tool can be useful for its later integration into a bigger wind farm optimization tool where additional wind turbine, layout properties and construction costs will be considered. Also, the lessons learnt during the tool development can be useful for later developers of a bigger wind farm optimization tool.

7.2 Recommendations

When developing a program to compute the levelized cost of energy for a wind farm design, it is recommended to start form a simple case of two turbines and simple wind conditions. Once a working code is developed, new improvements can be done gradually to describe more detailed component behavior. By following this approach, better understanding of the mathematical models and the complexity of the problem is acquired in a gradual way that facilitates the learning process.

If the developed tool is to be used for designing the layout of an offshore wind farm, it is advisable to start using the separation distance sweep mode with rough computation conditions. It means to sacrifice precision in order to reduce computation time. Once having a general visualization of the *LPC* surface, it is possible to delimit better the input domain for simulations and also to use the optimization function with more confidence.

The computation time can be affected by the selection of certain parameters defined by the user like the wind speed resolution, number of wind rose sectors, selection of wake model,

etc. It is then recommendable for the user to try these different parameters in order to understand how it affects the computation process. Moreover, it is recommendable to use different wind and site conditions parameters, as well as the different wake models in order to verify how sensitive the tool output is to these conditions.

Since the optimization function was sensitive to the starting point and therefore it was not always able to find the global minimum *LPC*, it is recommended to double check the results with a separation sweep before giving a final optimum layout.

Regarding the cable cost and loss models, it is recommended to look for further literature about submarine cable performance in order to validate the models implemented in the design tool. Also, it is recommended to look for alternative cable models and integrate them into the tool.

7.3 Future work

Future work can embrace the development of a tool that includes more detailed wind farm conditions and design constraints. Between them it is possible to mention:

- Include additional wake models like the Larsen wake model or another type of numerical solver.
- Include another type of cable models and compare it to the one already implemented.
- Implement another optimization function or develop a new one. Once a new optimization function confident results, it is possible to extend the design variables to include not only the separation distances, but for instance the turbine number, turbine power, different layouts, etc. With a bigger domain, it would not be possible to plot the *LPC* as function of all this variables and therefore an optimizer would be of great value to reduce computation time.
- Expand the tool to handle the inclusion of more wind farm area restrictions and shapes.
- Expand the tool to handle different layout topologies apart from rectangular layouts.
- Expand the tool to handle different cable interconnection topologies apart from parallel strings.

References

[1] Ivanell, S. et al. Three dimensional actuator disc modelling of wind farm wake interaction. Proceedings of the 2008 European Wind Energy Conference. Brussels, Belgium, March 2008

[2] Bjørnstad, B. Presentation: Cable Power cables and umbilicals - experience and challenges for longer distances. Nexans Norway AS. Intsok Oil & Gas Seminar. Veracruz, March 2009

[3] Borbon, F. SIP-2 report: Overview of models and design tools for offshore wind farms, relating to wake effects and electrical infrastructure. Delft University of Technology, 2009

[4] Trujillo, J. Presentation: Wake induced loading of wind turbines. EAWE 2nd PhD Seminar on Wind Energy. Roskilde, October 2006

[5] Jensen, N.O. A note on wind generator interaction. Risø National Laboratory. Denmark, 1983

[6] Katic, I. et al. A simple model for cluster efficiency. Proceedings of the 1986 European Wind Energy Conference. Rome, Italy, October 1986, p. 407-409

[7] Larsen, G. A simple wake calculation procedure. Risø National Laboratory. Denmark, 1988

[8] Frandsen, S. et al. Analytical modelling of wind speed deficit in large offshore wind farms. Wind Energy. 2006; 9: p. 39-53

[9] Ainslie, J.F. Calculating the flow field in the wake of wind turbines. Journal of Wind Engineering and Industrial Aerodynamics. 1988; 27: p. 213-224

[10] Sørensen, T. et al. Adapting and calibration of existing wake models to meet the conditions inside offshore wind farms. EMD International A/S. Aalborg, 2008

[11] Ryan, D. Investigation of observed and modeled wake effects at Horns Rev using WindPRO; Masters Degree Thesis. Technical University of Denmark, 2006

[12] Schoenmakers, D. Optimization of the coupled grid connection of offshore wind farms; Graduation project at Evelop Netherlands BV. Technical University of Eindhoven, December 2008

[13] XLPE Submarine Cable Systems. Attachment to XLPE Cable Systems - User´s guide. ABB Power Technologies.

[14] Hunter, R. et al. Recommended practices for wind turbine testing and evaluation. 2. Estimation of cost of energy from wind energy conversion systems. 2nd ed. International Energy Agency, 1994

[15] Herman, S.A. DOWEC Cost Model. DOWEC-068. The Netherlands, 2003

[16] Roozenburg N. et al. Product Design: Fundamentals and Methods. Wiley, Chichester, 2nd ed. 1998

[17] Attias, K. et al. Optimal economic layout of turbines on windfarms. Journal of Wind Engineering. 2006; vol. 30, no. 2: p. 141-151

[18] Mosetti, G. et al. Optimization of wind turbine positioning in large windfarms by means of a genetic algorithm. Journal of Wind Engineering and Industrial Aerodynamics. 1994; vol. 51, p. 105-116

[19] Grady, S. et al. Placement of wind turbines using genetic algorithms. Renewable Energy. 2005; vol. 30, p. 259-270

[20] Matlab help. Fmincon function. Also available online at [last access: October 2009]:

http://www.mathworks.com/access/helpdesk/help/toolbox/optim/index.html?/access/helpdesk/help/toolbox/optim/ug/fmincon.html

[21] Martinez, I. et. al. Transmission alternatives for offshore electrical power. Renewable and Sustainable Energy Reviews. 2009; vol. 13, p. 1027-1038

[22] Green, J. et. al. Electrical collection and transmission systems for offshore wind power. Offshore Technology Conference. Houston, April 2007

[23] Rados, K. et al. Comparison of wake models with data for offshore windfarms. Journal of Wind Engineering. 2001; vol. 25, no. 5: p. 271-280

[24] Luna, D. Modeling of wakes behind wind turbines, M.Sc. Thesis. Technical University of Denmark, March 2008

[25] Barthelmie, R. et al. Modelling and measurements of wakes in large wind farms. The Science of Making Torque from Wind, Journal of Physics: Conference Series 75 (2007) 012049

[26] Bot, E. FluxFarm: A program to determine energy yield of wind turbines in a wind farm. ECN-C--06-029

Additional consulted bibliography

[27] Barthelmie, R. et al. Modelling and Measurements of Power Losses and Turbulence Intensity in Wind Turbine Wakes at Middelgrunden Offshore Wind Farm. Journal of Wind Energy. 2007; 10: p. 517-528

[28] Barthelmie, R. et al. Analytical modelling of large wind farm clusters. Risø National Laboratory. Denmark, 2003

[29] Bulder, B. et al. Dutch Offshore Wind Energy Converter; Task 12: Cost comparison of the selected concepts; ECNC--01-080. ECN. Petten, The Netherlands, 2000

[30] Cerda Salzmann, D. Offshore Wind Farm Design (OE5662) lecture presentation. TUDelft, The Netherlands, February 2009

[31] Corten, G. et al. Heat Flux: Increase of wind farm production by reduction of the axial induction. Proceedings of the European Wind Energy Conference. Madrid, Spain, June 2003

[32] Elkinton, C. Offshore wind farm layout optimization; Doctor of Philosophy dissertation. University of Massachusetts Amherst, September 2007

[33] Elkinton, C. Offshore wind farm layout optimization (OWFLO) project: preliminary results. University of Massachusetts Amherst, 2006

[34] Greenpeace. North Sea offshore wind – A power house for Europe. Hamburg, 2000

[35] Gunther, C. Optimization of grid connection of offshore wind farms; Diploma Thesis. Delft University of Technology, April 1997

[36] Habenicht, G. Comparison of different wake combination methods to model offshore wakes. Renewable Energy System presentation, 2008

http://www.dffv.dk/VindKraftNet%20Wake%20day%2016%20sept%202008/Habenicht%20Comparison%20of%20different%20wake%20combination%20methods%20to%20model%20Offshore%20wakes.pdf

(last access: [February 2009])

[37] Kooijman, H. et al. Cost and Potential of Offshore Wind Energy on the Dutch part of the North Sea. ECN. Petten, The Netherlands, 2001

[38] Mechali, M. et al. Wake effects at Horns Rev and their influence on energy production. Report based on the "Large wind farms shadow: measurements and data analyses" project.

[39] Pierik, J. et al. Steady state electrical design, power performance and economic modelling of offshore wind farms. ECN, [unknown date]

[40] Pierik, J. et al. Electrical and control aspects of offshore wind farms II (Erao II). Volume 2: Offshore wind farm case studies. ECN-C- -04-051, March 2004

[41] Pierik, J. et al. Dowec WP1 Task 7: Electrical System, baseline design. DOWEC 045 rev. 2, February 2002

[42] Rathmann, O. Wind farm Wake-effect model in WAsP8. VEA / Wind Power Meteorology presentation.

http://www.risoe.dk/vea/storpark/presentations/WAsP8%20Wake-effect%20model.pdf

[43] Schachner, J. Power connections for offshore wind farms; Diploma Thesis. Delft University of Technology, Section Wind Energy, January 2004

[44] Schepers, G. Modelling of wake aerodynamics + new wind farm control strategies. ECN presentation. Dutch Wind Workshop. October 2006

http://www.ecn.nl/fileadmin/windworkshops/doc/Gerard_Schepers_Wake_and_farm_modelling.pdf

[45] Tempel, J. et al. Interconnectors, the power of cables. The world wind energy conference and exhibition. Berlin, 2002

[46] Thomsen, K et al. Fatigue loads for wind turbines operating in wakes. Journal of Wind Engineering and Industrial Aerodynamics. 1999; 80: p. 121–136

[47] Troldborg, N et al. Numerical Simulations of Wakes of Wind Turbines in Wind Farms. Technical University of Denmark, 2006

[48] Tronæs, S. Turbulence and turbulence-generated structural loading in wind turbine clusters; PhD. dissertation. Technical University of Denmark, 2007

[49] Wright, S. Transmission options for offshore wind farms in the United States. Proceedings of the WINDPOWER 2002 Conference and Exhibition. American Wind Energy Association. Portland, OR, 2002

[50] Fluxfarm software website. (last access: [November 2008])

http://www.ecn.nl/en/wind/products-services/services/software/fluxfarm/

[51] UPPSALA UNIVERSITET website. (last access: [January 2009])

http://www.geo.uu.se/luva/default.aspx?pageid=1312&lan=1

Appendix 1

Tool user interface

The main tool menu is contained in the m-file called Farm_Optimizer. From there, the user can specify the component parameters and the tool operation mode. Also, the user is allowed to select the number of variables to plot and the amount of information to be displayed during the when computation process. Each parameter is clearly commented to facilitate the understanding. An example of this menu is presented as follows:

```
%_____________________________________________________________________
% Simulation settings                                                \
%
% ---- Simulation aspects ----
multiple_simulation_wind = 0;               % 1 = runs multiple
simulation and compare results for:
                                                                     % a)
assuming fixed single wind speed
                                                                     % b)
assuming global Weibull distribution
                                                                     % c)
assuming sectorial Weibull distribution
multiple_simulation_wake = 0;               % 1 = runs multiple
simulation and compare results for:
                                                                     % a) Jensen
wake model
                                                                     % b) Ainslie
wake model
                                                                     % c)
Frandsen wake model
```

```
                                                                % d) Larsen
wake model
multiple_simulation_turbine = 0;            % 1 = runs multiple
simulation and compare results for:
                                                                % a) 2
turbines
                                                                % b) 3
turbines .... until total turbine number
%
%
separation_distance_sweep = 10;              % control variable: 1 = run
in test mode
                                                                      %
plots all variables for a separation distance going from
                                                                      %
"initial_distance_sweep" to "final_distance_sweep" in "delta" steps ->
to get
                                                                      % a
general overview of the cost of energy behaviour.
                                                                   % 0 = run
in optimization mode
%
% ---- Wind aspects ----
resolution = 1;                             % Weibull wind speed curve
resolution [m/s] -> incremental steps for energy yield calculation
(Wind_pdf x TurbinePower)
%
fixed_speed = 0;                            % 1 = considers one unique
wind speed and direction (south) for all calculations
                                                % This avoids effects of
Weibull distribution and sectorial wind rose
    V_fixed = 7;                            % fixed wind speed velocity
for testing purposes:
                                                                % a) fixed
speed test
                                                                % b) wake
model benchmark
Weibull_global = 0;                         % 1 = use global wind speed
distribution instead of per sector. Consider worst case assuming unique
                                            % wind direction paralell to
turbine columns (maximum wake shadowing)
%
% ---- Plotting aspects ----
plot_result_figures = 10 * separation_distance_sweep;       % 1 &
separation_distance_sweep = plots final result figures
    print_figures = 0 * separation_distance_sweep;          % 1 &
separation_distance_sweep = saves previously plotted figures as
individual emf files
%
plot_layout = 0;                            % 1 = plots optimum wind
farm layout at each column separation
%
plot_wind_rose = 0;                         % 1 = plots wind rose
%
```

```
plot_power_curve = 0;                          % 1 = plots turbine power
curve
%
plot_power_deficit = 0;                        % 1 = plots power deficit of
a turbine column
%
plot_wakes = 0;                                % 1 = plots results for
wakes calculations
wake_models_benchmark = 0;                     % 1 = plots wake
characterization by each of the wakes models.
    turbines_to_compare = 1;                   % Number of turbines to
compare (1 or 2)
    % Coordinates of first turbine (number of row, number of column)
    nr_benchmark_1 = 1;
    nc_benchmark_1 = 1;
    % Coordinates of second turbine (number of row, number of column).
(Optional)
    nr_benchmark_2 = 2;
    nc_benchmark_2 = 1;
%
% ---- Debuging aspects ----
debuging_plot_results_level_1 = 0;             % 1 = plots results for
debuging purposes
debuging_plot_results_level_2 = 0;
debuging_plot_results_level_3 = 0;
debuging_plot_results_level_4 = 0;
debuging_plot_results_level_5 = 0;
debuging_plot_results_level_6 = 0;
%
debuging_display_results_level_1 = 10;          % 1 = displays results on
command screen for debuging purposes
debuging_display_results_level_2 = 10;
debuging_display_results_level_3 = 0;
debuging_display_results_level_4 = 0;
debuging_display_results_level_5 = 0;
debuging_display_results_level_6 = 0;
debuging_display_results_level_7 = 0;
%
save_to_text = 0;                              % 1 = save command screen
output into a text file
%                                              Simulation settings
%_____________________________________________________________________/
%
%
%_____________________________________________________________________
% Design variable definition                                          \
%
location = 'Horns Rev';                         % location of wind farm:
'Holland' / 'Horns Rev' / 'experimental' /
wind_rose_sectors = 12;                        % number of subdivisions of
the wind rose: 4, 8, 12 (a must for Horns Rev location), 16 ... up to 40
Tmodel = 'V80';                                % turbine model: 'V80' /
'experimental' /
```

```
V = 33;                                     % turbine interconnection
voltage [kV]
fc = 50;                                    % voltage frequency [Hz]
lifetime = 20;                              % project liftetime. Usually
20 [years]
discount_rate = 0.07;                       % discount rate
%
owecs = 80;                                 % number of turbines: min =
2, max = 100. Number must assure that array will have complete columns
and rows. (80 is a must for Horns Rev layout)
type = 3;                                   % type of layout:
                                                % 1 = then it puts all
the turbines in one single column. Helps to test wake effects
                                                % 2 = square array
                                                % 3 = Horns Rev
%
wake_model = 'Ainslie';                      % to select wake model:
'Jensen' / 'Ainslie' / 'Frandsen' / 'Larsen'
wake_losses = 1;                            % 1 = consider wake losses
(use strictly 1 or 0 since it is a multiplier)
%
fixed_cost_method = 2;                      % method to calculate fixed
wind farm costs:
                                                % 1 = collection cables
represent 3% of total capital investment costs
                                                % 2 = wind turbines
represent 80% of total capital investment costs. Assumption 1MW =
1M.Euro
%
% ---- Dimensioning aspects ----
% Columns
initial_distance_sweep_column  =  2;        % initial distance to start
the separation distance sweep. Also lower limit for the optimization
routine. Multiple of rotor diameters [D]
optimum_dimension_guess_column =  7;        % initial guess of optimum
dimension: starting point for optimization routine. Multiple of rotor
diameters [D]
final_distance_sweep_column    = 15;        % final distance to end the
separation distance sweep. Also upper limit for the optimization routine.
Multiple of rotor diameters [D]
% Rows
initial_distance_sweep_row     =  2;
optimum_dimension_guess_row    =  7;
final_distance_sweep_row       = 15;
%
delta = 1;                                  % incremental steps in
separation distance between columns and rows. Used for iterations in the
separation distance sweep. Multiple of rotor diameters [D]
%_____________________________________________________________________/
```